UNIVERSITÄT ZU LÜBECK

From the Institute for Endocrinology & Diabetes
of the University of Lübeck
Directors: Prof. Dr. rer. nat. Jens Mittag
and Prof. Dr. med. Sebastian Schmid

"The good, the bad and the ugly – Identification and characterisation of thyroid hormone-dependent biomarkers"

Dissertation for Fulfilment of Requirements
for the Doctoral Degree
of the University of Lübeck

from the Department of Natural Sciences

Submitted by

Sebastian Nock
from Anklam, Germany

Lübeck, 2020

First referee: Prof. Dr. rer. nat. Jens Mittag
Second referee: Prof. Dr. med. Markus Schwaninger
Date of oral examination: March 31, 2020
Approved for printing: Lübeck, April 1, 2020

Eigenständigkeitserklärung

Ich versichere, dass ich die vorliegende Dissertation ohne fremde Hilfe angefertigt und keine anderen als die angegebenen Hilfsmittel verwendet habe. Weder vorher noch gleichzeitig habe ich andernorts einen Zulassungsantrag gestellt oder diese Dissertation vorgelegt. Ich habe mich bisher noch keinem Promotionsverfahren unterzogen.

_____

Sebastian Nock

Lübeck, den 06.01.2020

Zusammenfassung

Die Schilddrüsenhormone (SDHs) T_4 und T_3 spielen eine entscheidende Rolle in der Entwicklung und Homöostase der meisten Säugetiere, weshalb ihre Sekretion durch das hypothalamische Hormon TRH und das hypophysäre Hormon TSH reguliert wird. Aufgrund ihrer peripheren Sekretion in den Blutkreislauf und der robusten und spezifischen verfügbaren Detektionstests, stellen TSH und freies T_4 (fT_4) die wichtigsten klinischen Parameter zur Evaluation des SDH-Status dar. Jedoch spiegeln diese Parameter ausschließlich den allgemeinen Status an SDH wider ohne jedoch gewebsspezifische Unterschiede zu berücksichtigen. Diese Diskrepanzen entstehen durch verschiedene Proteine im SDH-Metabolismus und den zwei SDH-Rezeptorisoformen TRα und TRβ. Demzufolge sind, unter bestimmten klinischen Bedingungen, TSH und/oder fT_4 nicht ausreichend um den SDH-Status zu überprüfen, beispielsweise bei einer Mutation in TRα, der Differentialdiagnose zwischen einer Mutation in TRβ und einem TSH-sekretierenden Hypophysenadenom oder während einer SDH-Substitutionstherapie. Daher sind weitere spezifische Biomarker für schwierige klinische Situationen notwendig, wenn TSH und fT_4 unzureichend sind.

Um diese diagnostische Lücke zu schließen und zukünftige Therapieformen zu verbessern, wurde eine ungerichtete Proteomanalyse in Plasmaproben thyreotoxischer menschlicher Probanden und Mäusen zur Identifizierung möglicher Biomarker durchgeführt. Die resultierenden Datensätze ergaben 16 Proteine, die in gleichgerichteter Weise zwischen den Spezies durch SDH reguliert waren und hauptsächlich aus der Leber, der Milz und den Knochen stammten. Um die zugrundeliegenden Mechanismen und das genaue SDH-Ansprechverhalten zu klären, wurden weiterführende Mausstudien durchgeführt.

Hierbei wurde CD5L, ein von Makrophagen sezerniertes Plasmaprotein, als robustester möglicher Biomarker unter verschiedenen SDH-Stadien und Behandlungszeiträumen identifiziert. Nachfolgende *in vitro* Studien konnten zeigen, dass CD5L hauptsächlich aus proinflammatorischen hepatischen M1 Makrophagen stammt und indirekt durch einen bislang nicht identifizierten Hepatozytenfaktor reguliert wird. Durch die dominante Rolle von TRα in Zellen des angeborenen Immunsystems und des durch TRβ kontrollierten Hepatozytensignals, ist die *Cd5l*-Expression abhängig von beiden Rezeptorisoformen.

Die in dieser Arbeit gewonnen Ergebnisse identifizierten 16 neue Zielproteine mit einem Potential als SDH-Biomarker, wobei CD5L der vielversprechendste und sensitivste Kandidat ist. Obwohl weitere Studien zur Validierung der Spezifität der Biomarker notwendig sind, könnte CD5L zukünftig genutzt werden, um das Zusammenspiel von Hepatozyten mit Makrophagen in Abhängigkeit von SDH-Spiegeln zu untersuchen, und bei der differentiellen Diagnose von SDH-Defekten wie der SDH-Resistenz hilfreich zu sein.

Abstract

The Thyroid hormones (TH) T_4 and T_3 play a pivotal role in development and homeostasis, therefore their secretion is regulated by the hypothalamic hormone TRH and the pituitary hormone TSH. TSH and unbound T_4 (fT_4) are the most important clinical parameters to monitor TH status due to their peripheral secretion into the blood stream, their distinct physiological range and the quality of the available detection immunoassays. However, these parameters only represent the general TH status within a patient and not the tissue-specific TH status. This discrepancy strongly depends on several proteins of the TH metabolism and the two TH receptor isoforms α and β (TRα and TRβ). Thus, under certain clinical conditions, TSH, fT_4 or both are not sufficient to evaluate thyroid economy, for instance in cases of a mutation in TRα, the differential diagnosis between a mutation in TRβ and a TSH-secreting adenoma in the pituitary or upon TH substitution therapy. Therefore, new biomarkers, indicative of peripheral TH status, are urgently needed to provide an additional diagnostic tool where TSH and fT_4 fail.

To fill this diagnostic gap and improve future therapies, TH-dependent plasma proteins were identified in an untargeted proteomics approach in plasma samples of thyrotoxic humans and in thyrotoxic mice. The resultant data sets revealed 16 plasma proteins that were concordantly differentially abundant under T_4 treatment compared to euthyroid controls across the two species and they originated predominantly from liver, spleen and bone. Subsequent mouse studies were used to identify the target gene expressing tissues and the involvement of the two different TH receptors (TR) as well as the kinetics of target gene response to changes in TH concentrations.

CD5L, a macrophage-derived plasma protein, could be identified as the most robust putative biomarker under different serum TH states and treatment periods. Subsequent *in vitro* studies confirmed that CD5L originates from pro-inflammatory hepatic M1 macrophages, which are similar to liver-residing Kupffer cells, and is regulated by an indirect mechanism requiring the secretion of a yet unknown factor from hepatocytes. In agreement with the role of TRα in immune cells and the TRβ dependent hepatocyte-derived signalling, the regulation of *Cd5l* expression depended on both TR isoforms.

Our results identified 16 novel targets of TH action in plasma with CD5L as the most robust marker. Although further studies are required to validate the specificity of these targets, CD5L seems to be a promising candidate to assess TH action in hepatocyte-macrophage crosstalk and to support the differential diagnosis of TH disorders like resistance to TH.

Table of contents

1 Introduction

1.1 Thyroid hormones

Thyroid hormones (THs) belong to the class of non-peptide hormones and are iodine-containing tyrosine derivatives that play a pivotal role in vertebrate embryonal and postnatal development and homeostasis [1]. They occur in the storage form 3,3',5,5'-tetraiodo-L-thyronine (L-thyroxine or T_4) and in the biologically more active form 3,3',5-triiodo-L-thyronine (T_3). These molecules act in virtually all tissues and cell types through specific receptors, called TH receptors (TRs) [1, 2]. These TRs control, among other funtions, neuronal development [3], cardiac functions [4], growth [5] and metabolic activity [6] in mammals.

1.1.1 Thyroid hormone synthesis

Thyroid Hormones are produced by the thyroid gland which is situated at the front of the neck attached to the trachea and consists of two lobes with a small tissue connection termed as isthmus that creates its typical butterfly-like shape [7]. The thyroid in healthy people weights between 15 – 20 g, is around 10 cm long and 2 – 2.5 cm thick. It is composed of follicular cells or thyrocytes which produce and secrete THs into the periphery as well as C cells producing calcitonin [7]. TH secretion is regulated by a negative feedback loop that involves the hypothalamus, the pituitary and the thyroid gland and is hence referred to as the hypothalamus-pituitary-thyroid axis (HPT axis). The paraventricular nucleus of the hypothalamus synthesises the tripeptide hormone thyrotropin releasing hormone (TRH), which is transported via the portal capillary plexus to the anterior pituitary. Here, TRH secretion is recognised by TRH receptors on thyroid-stimulating hormone (TSH) – secreting cells in the anterior pituitary, termed thyrotropes. TSH also known as thyrotropin, a 28 kDa glycoprotein, is then released into the periphery and stimulates follicular cells in the thyroid gland for TH production. Subsequent increases of peripheral TH concentrations are sensed by both TRH- and TSH-secreting cells and cause a reduction in TRH- and TSH-release. Hence, this negative feedback loop is a self-regulating system that allows for a fine adjustment of peripheral TH concentrations and a rapid reaction towards endo- or exogenous disturbing factors and is depicted in **Figure 1** [1].

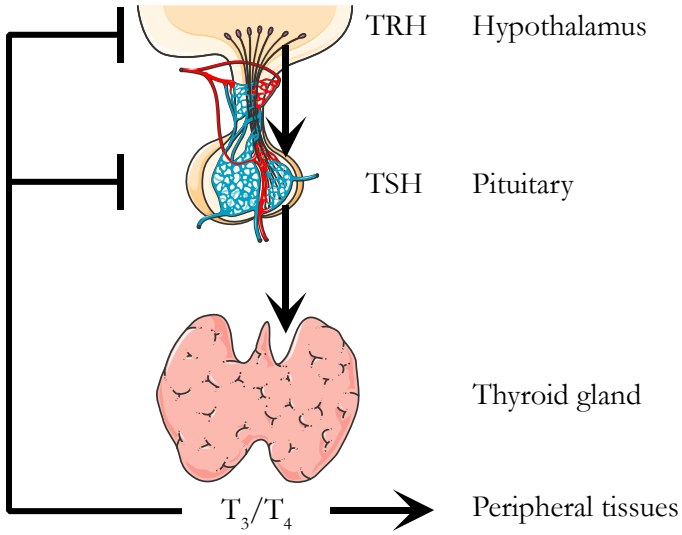

Figure 1 | Schematic illustration of the HPT axis. TSH secretion in the pituitary is stimulated by hypothalamic TRH. Peripheral distributed TSH stimulates TH production and release in the thyroid gland which in turn reduce TRH and TSH secretion. HPT axis – hypothalamus-pituitary-thyroid axis; TH – Thyroid hormone; TRH – thyrotropin releasing hormone; TSH – thyroid-stimulating hormone.

The synthesis of THs in the thyroid gland is strongly stimulated by the binding of TSH with its corresponding TSH receptor (TSHR). It increases among others the gene expression of sodium/iodide symporter (NIS), which facilitates the iodine uptake and results in concentrated iodide ions in thyrocytes by 20 – 40-fold compared to plasma [8]. Iodide import by NIS is driven by a sodium ion gradient that is actively generated by Na^+/K^+-ATPase pumps. Excessive amounts of potassium ions are then exported by voltage-gated K^+-channels KCNQ1 and KCNE2 [9]. NIS activity is inhibited by thiocyanate (SCN^-) or perchlorate ions (ClO_4^-), but due to potentially toxic effects of SCN^-, only ClO_4^- is used in *in vivo* studies to induce states of TH deficit. In addition, excessive amounts of iodine in the plasma also inhibit NIS-mediated import of iodide, which is named after their discoverers, Wolff-Chaikoff effect, and it is utilised in areas with nuclear fallout to prevent people from the uptake of radioactive iodine isotopes, by applying iodine tablets [10]. Incorporated iodide is rapidly transferred by iodide channels like pendrin, ClC5 or anoctamin-1 across the apical plasma membrane into the follicular lumen [11-13]. This process is termed iodide efflux. In the follicular lumen, I^- ions are oxidised into hypo-iodite (IOH) or iodinium ions (I^+) by the transmembrane heme protein thyroid peroxidase (TPO), which requires the presence of hydrogen peroxide (H_2O_2) to oxidise and hence activate the heme group of TPO [14]. The H_2O_2 production is facilitated by the dual oxidase 2 (DUOX2) and its associated activator DUOXA2, which are transmembrane proteins that are located in the apical thyrocyte membrane [15]. TPO catalyses the fixation of activated iodinium to tyrosyl residues of the protein thyroglobulin (TG) in sequential steps, which leads to mono- or diiodotyrosine (MIT or DIT) and is called as organification of iodine [16]. TPO represents an important part in TH synthesis and its inhibition with 1-methyl-2-mercaptoimidazole, also called methimazole (MMI), results in severe states of TH

deficit [17]. The MIT and DIT residues are subsequently oxidised and coupled into iodothyronines with three or four bound iodine atoms, known as T_3 and T_4, which are still bound to TG. Both the production of H_2O_2 and the coupling of iodotyrosyl residues require highly oxidative reaction conditions, which is why the production of THs occurs exclusively in tightly demarcated cavities like the follicular lumen. The dependence of TH synthesis on direct interactions of TG with TPO let all reaction steps happen in close proximity to the apical thyrocyte membrane, which facilitate the endocytosis of iodinated TG molecules. The incorporated endosomes fuse with lysosomes, which induce a proteolysis and hence a release of T_3 and T_4, but also MITs and DITs that are deiodinated by the iodotyrosine dehalogenase 1 (DEHAL1) and subsequently recycled [18]. Liberated T_3 and T_4 molecules are mainly exported by the monocarboxylate transporter 8 (MCT8) and to a minor extend by L-type amino acid transporter 2 (LAT2) [19]. A schematic illustration with the key points of TH synthesis can be found in **Figure 2**.

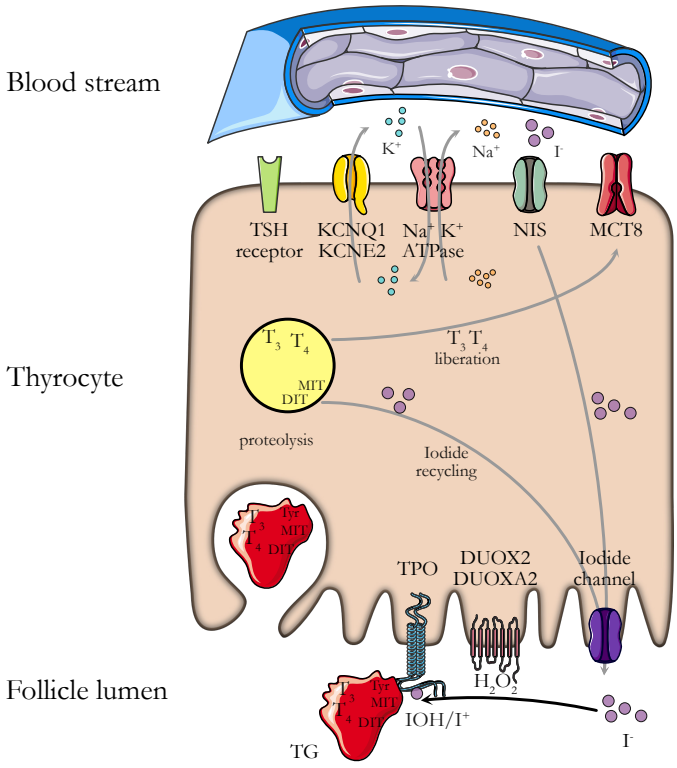

Figure 2 | Schematic illustration of TH synthesis. Iodide is imported by NIS, which is driven by a sodium gradient that is established by Na^+/K^+-ATPase and KNCQ1 / KNCE2. Iodide ions are transported into the follicular lumen and there they are oxidised by TPO, supported by DOUX2- and DUOXA2-derived H_2O_2. Iodinated and T_3/T_4-containing TG is endocytosed and proteolytically cleaved to liberate T_3/T_4, which are exported into the blood stream by MCT8. The whole synthesis machinery is stimulated by intracellular cAMP levels that originate from TSH- activated TSHR signalling. cAMP – cyclic adenosine monophosphate; DOUX2/DOUXA2 – dual oxidase 2/activator 2; I^- - Iodide ion; KNCQ1/KCNE2 – voltage-gated K^+ channels; MCT8 – monocarboxylate transporter 8; NIS – sodium iodide transporter; TG – Thyroglobulin; TH – Thyroid hormone; TPO – Thyroid peroxidase; TSH receptor – Thyroid-stimulating hormone receptor.

1.1.2 Thyroid hormone metabolism & actions

The vast majority of secreted T_4 and T_3 are bound to serum proteins like thyroxine-binding globulin (TBG), transthyretin and albumin. Only 0.03 – 0.05% of T_4 and 0.3% of T_3 are unbound or free distributed in the blood stream and are therefore referred to as free T_4 (fT_4) and free T_3 (fT_3) [20]. Both forms of THs, free and bound, account for the total amounts of T_4 in T_3 in the periphery and are termed as tT_4 and tT_3. The TH storage form tT_4 occurs in 40-fold higher concentrations compared to tT_3, but only the free forms are able to enter cells [1]. The half-life of TH in the circulation varies strongly between organisms. In humans, the half-life of T_4 and T_3 are 7 d and 1 d, respectively, while in rodents they are much shorter with 8 h and 2 h, respectively [21]. It was the prevailing opinion for decades that TH are able to enter cells by passive diffusion, but this dogma was challenged twenty years ago with the identification of transmembrane transporters that are essential for TH to pass this barrier. To date, three classes of TH transporters are identified, which are monocarboxylate transporter 8 and 10 (MCT8/10), organic anion-transport polypeptides family (OATP) and L- and T-type amino acid transporters 1 and 2 (LAT1/2). The transporters differ in tissue abundance and a preference for T_3 or T_4, but as passive transporters they allow for im- as well as export of TH [22-26]. Despite the existence of different classes of TH transporters, MCT8 is the most important transporter discovered to date due to its high specificity and binding affinity for THs [27].

As mentioned above, only a minority of THs exists in the biologically active form T_3, therefore the primarily abundant storage form T_4 requires further activation to fulfil signalling activity. This process is performed by a class of specialised selenoproteins that remove single iodine atoms from the THs. This class is termed as deiodinases and three different proteins with special properties are found in mammals with two distinct tasks. First, the type I and type II deiodinases (DIO1 and DIO2) are able to activate T_4 by outer ring deiodination which leads to the production of T_3. Second, the type I and type III deiodinases (DIO1 and DIO3) are able to inactivate both T_4 and T_3 by inner ring deiodination and the production of 3,3',5'-triiodo-L-thyronine also known as reverse T_3 (rT_3) or by either inner or outer ring deiodination for the production of different T_2 derivatives which have a reduced affinity for TRs and are prone to further degradation. The inactive role of T_2 is still under debate, since studies have shown an activating role for outer ring deiodinated 3,5-T_2 on the resting metabolic rate of rodents, but continuous problems in robust T_2-isoform detection, discrimination and quantification raised questions about the reliability of T_2-related findings [28-30]. Activation of T_4 is mainly processed by DIO2 which has, compared to DIO1, a 100 to 1 000-fold higher affinity for outer ring iodine atoms and is hence primarily responsible for peripheral T_3 concentrations [31]. The production of TH in humans is about 100 μg T_4 and 30 μg

T_3 per day and the thyroid gland contributes with only 5 µg T_3, hence the majority of circulating T_3 is produced by peripheral organs. Of the residual 25 µg T_3, 20 µg are produced by DIO2 and 5 µg by DIO1, indicating the importance of DIO2 within the TH metabolism [32]. In addition to peripheral T_3 concentrations, deiodinases are important for intracellular T_3 concentrations as well. Depending on the tissue-specific needs for TH-mediated signalling, deiodinases show a distinct expression pattern. Despite overlapping abundance in numerous cell types, DIO1 is predominantly expressed in liver, kidney and the thyroid gland, while DIO2 is the primary isoform in the brain, the pituitary and brown adipose tissue [32, 33]. In contrast, DIO3 expression strongly depends on spatiotemporal aspects and is high in embryonal tissues to suppress excessive prenatal growth [34]. In mature organisms, DIO3 expression is also high in the brain and the skin [33]. The exact mechanism of how deiodinases contribute to peripheral TH concentrations remain still enigmatic, since transgenic mice devoid of both outer ring deiodinases or all 3 types of deiodinases are viable and have normal serum tT_3 concentrations, despite increased fT_4 and TSH concentrations [35]. The different actions of deiodinases and resulting products of the sequential deiodination steps are illustrated in **Figure 3**.

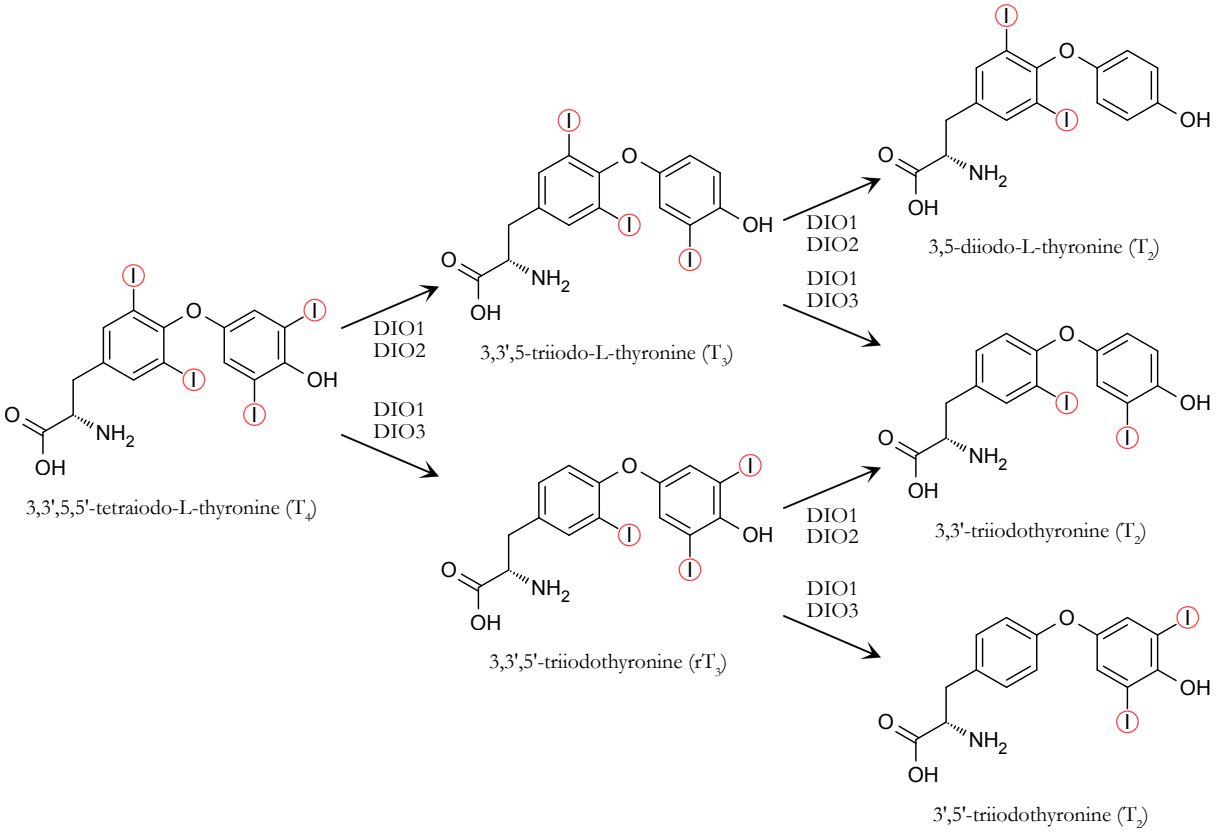

Figure 3 | Sequential deiodination steps in TH degradation.

As mentioned before, THs act mainly through regulating gene expression of responsive genes. The regulation bases on the recognition of THs by specific nuclear receptors, termed as TH receptors (TRs). In mammals, two TRs are known which are encoded by two different genes, *THRA* and

THRB and both belong to the nuclear receptor superfamily. The identification of TRs was successful in 1986, when two groups independently identified an endogenous homolog to the viral oncogene v-erb-A as a TH binding protein termed as c-erb-A [36]. *THRA* was later found to be encoded on chromosome 17 and expresses two splice variants that encode for THRA1 (TRα1) and THRA2 (TRα2), but only TRα1 was found as a functional TR. *THRB* is located on chromosome 3 and encodes for three splice variants of which two only TRβ1 and TRβ2 are functional TRs. The amino acid sequence of the TRα1 and TRβ1 share a high degree of homology with 82%[1] of coverage and therefore their functional properties show a high degree of overlap. TRs consist of three functional domains and the first is the N-terminal A/B domain which is thought to influence the potency of TR actions and show the highest degree of diversity between the TRs, but so far not much changes in TR functionality between A/B domain variants could be determined and therefore this domain is mostly ignored [37, 38]. The middle domain is the DNA binding domain that recognises the hexanucleotide sequence motif (A/G)GGT(C/A/G)A on the DNA and enables for binding of TRs. The consensus sequence for this motif which is most often referred to is AGGTCA. Two of these binding motifs that are separated by an unspecific linker sequence form the TR response element (TRE). As shown in **Figure 4**, three forms of TREs exist that are defined by specific repeating patterns which are the direct repeat with a typical 4 nt linker sequence, the inverted or palindromic repeat which does not always have a linker sequence and the everted or inverted palindromic which have a typical linker sequence of 6 nt [39]. These TREs represent the most common forms, but this is variable and other linker lengths have also been found in promoter regions of TH target genes and have direct influence on binding pattern [40, 41]. The third domain in TRs is the ligand-binding domain which is responsible for the binding of T_3, but it also enables the receptor to form homo- or, most commonly, heterodimers with the retinoid X receptor (RXR) and to interact with other co-regulatory proteins like co-activators, e.g. nuclear receptor coactivator (NCoA) or steroid receptor coactivator (SRC), or co-repressors, e.g. nuclear receptor corepressor 1 (NCoR1) or silencing mediator of retinoic acid receptor (SMRT) [42-45]. The preference of TRs to either bind co-activators or –repressors depends on the presence

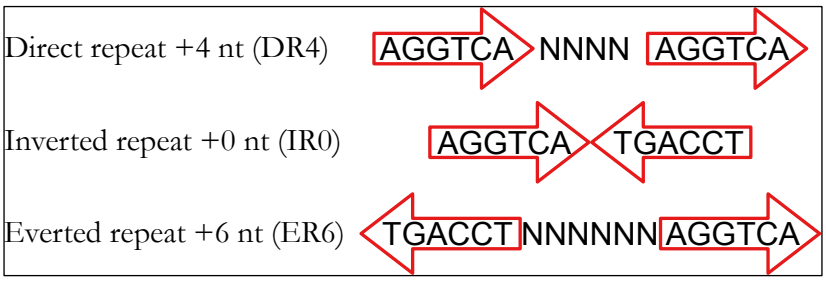

Figure 4 | Motifs of TR responsive elements

[1] Search query with protein blast on https://blast.ncbi.nlm.nih.gov for P10827 and P10828

or absence (aporeceptor state) of bound T_3, which induces strong conformational changes in TRs that results in different binding affinities [46]. In addition, the binding of T_3 to TRs and subsequent changes in coactivator binding with SRC leads to histone acetylation in the promoter region with concomitant increase in target gene transcription [45, 47]. Still the mechanisms and factors that enhance or hamper TR-mediated gene expression are not fully understood [48].

Like TH transporters and deiodinases, TRs are tissue-specific distributed as well. TRα1 is the predominantly expressed TR in heart, bone, intestines and lymphoid tissue. Moreover, metabolically active tissues, like brown adipose tissue or skeletal muscle, express high amounts of TRα1, which makes this receptor essential for the regulation of metabolic activity in an organism [36, 49, 50]. The TRβ isoforms show variations in tissue abundance. TRβ1 is widely distributed across different tissues and predominantly expressed in liver, kidney and the brain, whereas TRβ2 is more restricted and the main TR in the hypothalamus, pituitary and thyroid gland, but also the cochlea and retina [51-53]. The reason for these specific expression patterns, despite overlapping TRE recognition and almost identical target gene regulation [54], remains enigmatic so far, but functional analyses revealed a pronounced role of TRα in the context of embryonal and postnatal development and metabolism, while TRβ is more essential in the control of TH and liver metabolism and homeostasis of mature organisms [55, 56]. The actions of THs and its nuclear receptors as regulator of target gene expression are regarded as their main function. Nevertheless, recent studies also revealed fast and therefore non-genomic actions of thyroid hormones [57, 58]. These actions are mediated by cytoplasmic TRs, which are found to shuttle between nucleoplasm and cytoplasm, but also by transmembrane αvβ3 integrins that are able to bind THs and act via signal transduction towards phosphoinositide 3-kinase (PI3K) and mitogen-activated protein kinase (MAPK) and regulate downstream processes [57, 59-61]. The physiological relevance of these effects is still under debate, as they influence processes of long-lasting effects of the immune system and changes in the extracellular matrix which are not sustainably affected by short term signals [62-64].

1.2 Thyroid hormone disorders

Apart from diabetes mellitus, disorders affecting TH metabolism are most commonly observed in endocrinology. New and better diagnostic tools are urgently needed to capture their variety and complexity highlighted by more recent data on inherited diseases affecting TH receptor alpha where conventional diagnostic tools fail but also in a number of acquired disorders where routine assessment of the HPT axis is insufficient for diagnosis.

1.2.1 Acquired disorders

The most common causes for acquired TH disorders are inadequate iodide supplementation and autoimmune disorders, which are able to induce both an oversupply of THs (hyperthyroidism) or an undersupply of THs (hypothyroidism). The prevalence for hyperthyroidism in iodide-sufficient countries is about 0.7% of the general population and Graves' disease (GD) accounts for 70 – 80% of these cases [65, 66]. Graves' disease is characterised by hyperthyroidism and diffuse goitre, while ophthalmopathy, pretibial myxoedema and acropachy can also occur. The overproduction of autoantibodies against TSH receptor is believed as the initial incident for GD, and women show a higher prevalence with a women-to-men ratio of 8:1, especially in their mid-life period between 30 and 50 years of age [67, 68]. In iodine-deficient countries the most common causes for hyperthyroidism are toxic multinodular goitre and toxic adenomas and account for 50% of all cases, with predominant prevalence in women compared to men at a ratio of 5:1 [69, 70]. Less common causes for hyperthyroidism are thyroiditis, a self-limiting thyrotoxicosis due to excess TH release from the thyroid gland. Painful thyroiditis mostly follows an infectious disease of the respiratory tract, while painless thyroiditis occurs post-partum or due to unspecific destruction of thyrocytes leading to uncontrolled release of TH. The prevalence for thyroiditis is uncertain due to its transient and mostly unsuspicious character, but in Europe it is marked as uncommon [71-73]. Another less common cause for hyperthyroidism is a TSH-secreting pituitary adenoma (TSHoma) which is often misdiagnosed with primary hyperthyroidism despite inadequately increased TSH concentrations. The intervention therapies with thyrostatic drugs, radio-iodine ablation or thyroidectomy were found to worsen post-surgical outcomes after corrected diagnosis and successful transsphenoidal resection [74, 75]. Despite the low prevalence of TSHomas with 2 – 4% of all pituitary adenomas, improved diagnostic tools are required for affected patients to avoid unnecessary worsened outcomes. Extreme rare causes for hyperthyroidism are ectopic forms due to functional thyroid cancer metastases or an ovarian tumour with functional thyroid tissue, called struma ovarii [66, 76]. Hypothyroidism is a common endocrine disorder with a prevalence of about 5% in Europe, depending on iodine supplementation, with an approximately 10 times higher occurrence in women than men [69, 77]. The most common form of hypothyroidism, besides iodine-deficiency induced hypothyroidism, in iodine-replete areas is the chronic form of autoimmune thyroiditis, termed after its discoverer Hakaru Hashimoto as Hashimoto's thyroiditis or Hashimoto's disease (HT) [78]. The cause for developing HT is not known so far, but high titres of anti-TPO and/or anti-TG autoantibodies are a hallmark, despite these autoantibodies are also found in 11% of the general population without disease progression [79]. A graded influence of mutations in autoimmune-related genes, e.g. PTPEN22, SH2B3, VAV3, FOXE1 and PDE8B, may influence

HT development, but also environmental factors like flame retardants or solubilised packing materials [80, 81]. Another important cause for hypothyroidism are measures to treat hyperthyroidism like radioiodine ablation, hemithyroidectomy or neck surgery for cancer therapy [82, 83]. Other drugs and therapies that cause hypothyroidism, which summarised in the term iatrogenic hypothyroidism, are e.g. amiodarone, lithium, immune checkpoint inhibitors and tyrosine kinase inhibitors [84-86].

1.2.2 Congenital disorders

In contrast to acquired TH disorders, congenital TH disorders occur after birth or even at earlier stages of embryonal development. The vast majority of congenital hypothyroidism (CH) are caused by iodine-deficiency or malformations of the thyroid gland (thyroid dysgenesis). The total incidence for CH is between 1 in 1 400 to 1 in 2 800 and thyroid dysgenesis alone accounts for 1 in 4 000 with unknown underlying cause [87].

Alongside thyroid dysgenesis, numerous genetic variations have been identified to cause thyroid dyshormonogenesis and these can occur in all stages of TH metabolism. Mutations of genes related to TH metabolism that are expressed in hypothalamus or pituitary are combined with invasive lesions into the term central hypothyroidism (CeH) and induce hypothyroidism by insufficient stimulation of the otherwise healthy thyroid gland. CeH is characterised as a rare disease with an incidence of 1:16 000 to 1: 100 000 in neonates without a preference in females [88]. Typical causes for CeH besides mutations, which represent the main cause for CeH, are compressive lesions like craniopharyngiomas, gliomas and macroadenomas and drug treatments, but also autoimmune and infective diseases and injuries were described [89, 90]. Various gene mutations were identified to hamper TH production and some are also associated with broaden effects that influence different pituitary functions and are termed as combined pituitary hormone defects [91]. The first and most serious mutations that induces CeH were alteration in *TSHB*, which, if untreated for more than six weeks after birth, is able to cause cretinism, the most serious form of hypothyroidism with severe mental retardation, dwarfism and muscle weakness [92]. *TSHB* encodes for the β-subunit of TSH and mutations are commonly inconspicuous in first infant TH screening. Other mutations that were identified to induce CeH occur in *TRHR* which encodes for TRH receptor. Affected children were inconspicuous for functional TH screening and development prolonged neonatal jaundice and growth retardation [93]. Two more gene mutations with were identified to induce CeH and are X-linked inherited but no prevalence for male infants could be confirmed [94]. The first gene was *IGSF1* that encodes for a transmembrane protein with unknown function in the pituitary and the second gene was *TBL1X*, a subunit for NCoR1 and SMRT and essential for proper transcriptional regulation [95, 96]. Several other genetic variations as in *POU1F1*, *PROP1*, *HESX1*, *PROKR2*, and

SOX2 have been identified to induce CeH but the phenotype is less specific as they are combined with other deficiencies of anterior pituitary functions [94].

Despite mutations that evoke symptoms of CeH, mutations in all genes that are involved in TH biosynthesis and metabolism have the potential to cause congenital hypothyroidism. With the exception of KCNQ1/KCNE2 whose mutations are predominantly implicated in cardiac disorders like the short QT syndrome and increased susceptibility to cardiac arrhythmias [97], mutations in NIS, TPO, DOUX2, TG and the iodotyrosine dehalogenase (DEHAL) are identified in the context of CH. These mutations are inherited in an autosomal recessive manner and therefore occur only in children were both parents are carriers of mutations in the same genes [18, 98, 99]. For TSH receptor, activating and inactivating mutation are described with different pathologies. While inactivating mutations cause CH, also known as resistance to TSH, activating mutations can lead to inadequately active TSH receptors that permanently raise intracellular cAMP levels and therefore increase TH production, termed non-autoimmune hyperthyroidism, and are associated with toxic thyroidal nodules and thyroid tumorigenesis [100, 101].

Mutations in MCT8 lead to a severe undersupply of the whole brain, termed Allan-Herndon-Dudley syndrome (AHDS) with its typical symptoms like spastic quadriplegia, lack of speech, severe intellectual deficit and altered thyroid hormone concentrations in the periphery. The AHDS is inherited in a X-linked recessive manner and characterised as a rare disease [102]. The phenotype is due to the predominant role of MCT8 to transport T_4 and T_3 into the brain which is therefore hypothyroid, while peripheral tissues are able to compensate the loss of MCT8 with other TH transporters. The hypothyroid conditions in the brain lead to increased TSH concentrations and finally to a hyperthyroid periphery with increased tT_3, but also increased renal excretion of T_4 is discussed to contribute to this phenotype [103-105].

In contrast to the residual genes that are involved in TH metabolism, mutations in deiodinases are not described to lead to severe phenotypes. Genome-wide association studies revealed a connection of single nucleotide polymorphisms in *DIO1* with TSH and fT_4 levels, but no connection was found to CH, indicating only moderate influences of mutations on the phenotype [106, 107]. One common mutation in *DIO2* is well described and leads to the missense mutation Thr92Ala, which prolongs the half-life of DIO2, but also induces a localisation at the Golgi apparatus that reduces its activity [108]. Mutations in *DIO3* are not described with any phenotypes, but an upregulation due to tumour progression can induces severe forms of so called consumptive hypothyroidism, which is mainly found in children [109].

In 1967 a mutation in *THRB* was first described and lead to a disorder, later termed resistance to TH due to defective TRβ (RTHβ), which was characterised by a thyrotoxicosis with nonsuppressed TSH levels. This phenotype emerges through a defective TRβ and its role in TH release control.

The prevalence of RTHβ is 1 in 40 000 - 50 000 life births and to date more than 900 cases are known [110]. As mentioned above, actions of the HPT axis depend on functional TRβ signalling and TH recognition. Decreased TRβ-mediated regulation of TRH and TSH secretion result in increased TH secretion by the thyroid gland depending on the degree of severity of the mutation in *THRB* [111]. Hence, tissues predominantly expressing TRβ appear hypo- or euthyroid, while tissues expressing TRα are under chronically and strongly hyperthyroid conditions [112]. Most affected are tissues with a predominant expression of THRA, like heart, bones, skeletal muscles and lymphoid tissues, which trigger typical symptoms like tachycardia, impaired growth or low body mass index [56, 113]. In 80% of the affected families, RTHβ is autosomal dominantly inherited and associated with heterozygous mutations in *THRB* [114]. In 20% of the described patients a *de novo* mutation occurred in *THRB*. Many different mutations were identified in patients positive for RTHβ and include point mutations, in-frame deletions and frame-shift insertions and almost all of them are located in the ligand-binding domain, indicating a dominant-negative role of the aporeceptor state above the intact TRβ receptor and putatively silent mutations in DNA-binding or N-terminal A/B domain [115, 116]. The strength of symptoms corresponds to the respective mutation and a broad range of phenotypes can be detected [117].

A disorder in humans that is associated with mutations in *THRA* has long been suspected and until 2012 only a phenotype based on observation in transgenic mice could be anticipated [118]. In 2012 the first patients matching those suggested phenotypes were identified and the disorder was described as resistance to TH due to a defective TRα (RTHα) [119, 120]. As TRβ in RTHβ, mutations in *THRA* in affected patients with RTHα occur in a dominant-negative manner in the ligand-binding domain. Due to the limited number of identified patient, no prevalence for this disorder can be given and most of the identified patent carry *de novo* mutations, indicating a challenging predictability [121-123]. The most common symptoms of affected patients are similar to symptoms of mild congenital hypothyroidism, like bradycardia, short statute, mental impairments, severe constipation and mild anaemia, but with low-normal fT_4, normal-high fT_3 and normal TSH [124].

1.3 Manifestation of thyroid hormone disorders

TH disorders are characterised by distinct symptoms with varying degrees, depending on the concrete origin, which have to be exactly determined for adequate diagnosis and treatment. Numerous diagnostic tools are available for this purpose and are explained in the following sections.

1.3.1 Clinical symptoms

Clinical parameters are essential for first-line identification of a presumed TH disorder. Typical parameters for hyperthyroidism that clinicians should be aware of are palpitation, fatigue, tremor, anxiety, disturbed sleep, weight loss, heat intolerance, sweating and polydipsia. The use of ultrasound monitoring to examine thyroid size and goitre formation, tenderness, symmetry and nodularity is also indicated. In addition, peripheral symptoms like ophthalmopathy, dermopathy, acropachy and edema should be investigated. In elderly patients, cardiac and pulmonary disorders like increased heart rate, increased blood pressure, increased respiratory rate should more extensively be examined [66, 125, 126].

Typical symptoms for hypothyroidism are fatigue, lethargy, cold intolerance, weight gain, constipation, change in voice and dry skin. Less common are also shortness of breath, impaired memory, muscle weakness, hair loss and deterioration of kidney function [109].

The clinical symptoms for both hyper- and hypothyroidism are relatively unspecific and even in older patients less predictive. For hypothyroid patients, the sensitivity and specificity of clinical assessment methods was superseded by biochemical methods, and only the ankle reflex relaxation time correlates well with the degree of hypothyroidism, but is sparsely used in clinical practise [127]. The symptoms worsen insidiously and are therefore and due to their unspecific nature often overlooked.

1.3.2 Biochemical parameters

In a previous human study, an eight-week thyrotoxicosis did not induce detectable clinical symptoms, but clear alterations of biochemical parameters, which emphasised their superiority over clinical diagnostic tools to identify hyper- or hypothyroidism and to determine its degree of severity [128]. The most important parameter in TH disorder diagnosis is the peripheral TSH concentration due to several reasons. First, nowadays third-generation bioassays for plasma TSH provide robust and sensitive results. Secondly, TSH and fT_4 are connected in a log-linear relationship, thus small changes in fT_4 induce large changes in TSH concentration [129]. In addition, plasma fT_4 is determined routinely to support TSH findings. The measurement of fT_3 is due to financial reasons not routinely performed, albeit mild and early forms of hyperthyroidism are characterised by low TSH and normal fT_4, but increased fT_3 levels [126].

Graves' disease is characterised by increased TSHR auto-antibodies, hence competitive-binding immunoassays are employed to determine occurrence and concentration of these antibodies, with a sensitivity and specificity of 97 and 98%, respectively for third-generation assays [125].

In iodine-replete areas, HT is the most common cause for hypothyroidism, therefore biochemical diagnostics additionally comprise tests to evaluate titres of anti-TPO and anti-TG auto-antibodies using immunoassays. Only positive anti-TPO antibodies allow for predicting a developing hypothyroidism and is therefore recommended in patients with subclinical hypothyroidism, which is a condition of slightly increased TSH with normal fT_4 and fT_3 [79].

1.3.3 Limitations of applied diagnostics

The vast majority of patients with symptoms of TH disorders can be straightforwardly diagnosed, as biochemical markers can be used to assess the degree of severity of the respective disease. Hyperthyroid patients can then be treated with anti-thyroid drugs or in more severe cases with radioiodine ablation or thyroidectomy, while hypothyroid or iatrogenically rendered hypothyroid patients receive, in a lifelong regimen, a single daily oral dose of Levothyroxine ($L\text{-}T_4$) to reach the treatment targets of normalised TSH concentrations in the lower half of the reference range (0.4 – 2.5 mIU/l) and the resolution of physical and mental complaints [68, 109]. It was shown that certain circumstances like critical illness, acute psychosis, TBG excess, TSHomas, RTHβ, disorders in TH metabolism, but also administration of various drugs change TSH concentrations. Of these diseases, the differential diagnosis between TSHomas and RTHβ is the most prominent clinical situation were TSH and TH are no sufficient biomarkers. Moreover, specific antibodies like human anti-animal antibodies and auto-antibodies that can occur in cases of Graves' disease or rheumatoid arthritis can directly bind to detection antibodies of TSH immunoassays and lead to false low TSH values, which are challenging to detect [130, 131].

Despite adjusting TSH into the reference range, excluding technical issues and interfering indications, and restoring physical parameters like serum cholesterol, resting heart rate, anxiety level, sleep pattern and menstrual cycle abnormalities into reference ranges, a subset of patients still complain about impairment in psychological well-being [132, 133]. The origin of these effects is still unknown, but studies identified variations up to 40 – 50% in circadian plasma TSH concentrations, which do in addition also seasonally change and could lead to inadequate replacement therapy [134, 135]. Circadian or seasonal variations could not be detected for fT_4 or fT_3, but these parameters cannot be used for the assessment of the thyroid status due to the $L\text{-}T_4$ administration [135]. Every individual patient has its personal euthyroid range and an endogenous set point for the HPT axis, which is narrower than the general reference range, thus a TSH value within this interindividual range can be suboptimal for a patient and hence induce symptoms of hypo- or hyperthyroidism [136]. This set point depends on the whole range of proteins that are involved in TH metabolism and therefore needs an individual assessment [137]. The problem that TSH alone is insufficient to fine-tune the daily dose of $L\text{-}T_4$ to the optimum was shown in a large

cohort study where 1 811 thyroidectomised patients were compared with 3 875 euthyroid controls. In this study, 7.2% of the patients under L-T_4 monotherapy showed increased fT_4 values, while 15.4% had reduced fT_3 concentrations [138]. More dramatically, 29.6% of the athyreotic patients exhibited a lower fT_3/fT_4 ratio than euthyroid controls, indicating a chronic condition of inadequate TH availability for peripheral tissues. Moreover, L-T_4 monotherapy was not able to induce physiological conditions, because in the patient cohort fT_3 values showed a correlation with log(TSH) values, which was not detectable in the euthyroid control group. Since thyroid disorders and the L-T_4 monotherapy are very common, there is a need for additional and tissue-specific biomarkers to improve treatment success for patients with marginal set points for TH metabolism within the euthyroid reference range [131].

Several TH-responsive serum proteins have been tested for their suitability as tissue markers for TH disorders, including total cholesterol [139], low-density lipoproteins [139], osteocalcin [140, 141], creatine kinase [142], ferritin [142], testosterone-binding globulin [143], tissue plasminogen activator [144], angiotensin converting enzyme [145] and glucose-6-phosphate dehydrogenase [146]. However, none of these markers were recommended for clinical use in recent guidelines due to their low sensitivity and/or specificity or unavailability for routine testing [147]. Many of these markers are predominantly liver-derived like lipid parameters or sex hormone-binding globulin (SHBG), which has been suggested for the differential diagnosis of RTHβ and TSHomas, but it is co-regulated by oestrogens, androgens, insulin and prolactin, and moreover it lacks specificity and sensitivity [148-150].

1.4 Aim of this thesis

During the past years, permanent effort was made to improve the diagnosis of challenging TH disorders and achieve optimal treatment of patients with TH diseases. However, despite all efforts, there is still an enormous need for new diagnostic tools and new therapeutic approaches to alleviate symptoms related to TH disorders. Therefore, the aim of this thesis is to identify new TH-dependent biomarkers using cutting edge OMICs techniques to facilitate diagnosis of TH disorders and guide therapeutical approaches. A suitable marker should be readily detectable in the plasma of humans as well as mice to allow mechanistic studies for involved organs and pathways. Moreover, one aim is to study the underlying regulation mechanisms and kinetics of the identified target genes using mice that will be transiently rendered hyperthyroid or transgenic mouse strains that are models for RTHα or RTHβ and represent chronic thyroid disease states. Further *in vitro* characterisation of the target genes complements the identification of expressing tissues or cell types and target gene suitability as putative TH biomarkers.

2 Materials and Methods

2.1 Materials

2.1.1 Devices and consumable materials

Devices and consumable materials in the following **Table 1** were used during the experiments.

Table 1 | Devices and consumable materials used for experiments

Device	Manufacturer / Supplier
8-strip optical clear flat caps	Sarstedt AG & Co. KG, Nümbrecht, Germany
96 PCR plate half skirt	Sarstedt AG & Co. KG, Nümbrecht, Germany
Atilon ATL-224-I	Acculab by Sartorius AG, Göttingen, Germany
Axiovert 40 CFL	Carl Zeiss Microscopy GmbH, Jena, Germany
BD Falcon 5 ml round-bottom	Becton, Dickinson and Company, Franklin Lakes, NJ, USA
Biofuge fresco	Heraeus Holding GmbH, Hanau, Germany
Biosphere® Filter tips (20 µl, 100 µl)	Sarstedt AG & Co. KG, Nümbrecht, Germany
Cell Scraper 25 cm	Sarstedt AG & Co. KG, Nümbrecht, Germany
ChemiDoc™ Touch Imaging System	Bio-Rad Laboratories GmbH, Munich, Germany
Disposal bag	Sarstedt AG & Co. KG, Nümbrecht, Germany
Dissection tools	Fine Science Tools GmbH, Heidelberg, Germany
Duran® laboratory glass ware	DWK Life Sciences GmbH, Mainz, Germany
E802 power supply	Consort bvba, Turnhout, Belgium
EASYstrainer™ Zellsieb (70 µm)	Greiner Bio-One GmbH, Frickenhausen, Germany
Eismaschine ZBE 70-35	Ziegra Eismaschinen GmbH, Isernhagen, Germany
Epoch + Take3 microplate reader	BioTek Instruments Inc., Winooski, VT, USA
FACS Aria II	BD Biosciences, San Jose, CA, USA
Fisherbrand™ Bead Mill 24 Homogenizer	Thermo Fisher Scientific, Waltham, MA, USA
Green Line IVC Sealsafe PLUS cage system	Tecniplast, Buguggiate, Italy
Hera Cell 150 Incubator	Thermo Fisher Scientific, Waltham, MA, USA
HORIZON® 11·14	Thermo Fisher Scientific, Waltham, MA, USA

Immobilion-P Membrane, PVDF, 0.45 µm	Merck KGaA, Darmstadt, Germany
Incu-Line ILS6	VWR™ part of Avantor, Radnor, PA, USA
Mini-PROTEAN® Tetra Handcast Systems	Bio-Rad Laboratories GmbH, Munich, Germany
Micro tube (1.5 and 2 ml)	Sarstedt AG & Co. KG, Nümbrecht, Germany
Micro tube 1.3 ml LH (25 I.U. Heparin)	Sarstedt AG & Co. KG, Nümbrecht, Germany
Mini Trans-Blot® Cell	Bio-Rad Laboratories GmbH, Munich, Germany
MJ Research PTC-200 Thermal Cycler	Bio-Rad Laboratories GmbH, Munich, Germany
Multifuge 3S-R	Heraeus Holding GmbH, Hanau, Germany
Multiply® - Pro cup 0.2 ml	Sarstedt AG & Co. KG, Nümbrecht, Germany
NanoDrop™ 2000	Thermo Fisher Scientific, Darmstadt, Germany
Neubauer counting chamber	Glaswarenfabrik Karl Hecht GmbH & Co. KG, Sondheim v. d. Rhön, Germany
NitraTex®	Ansell Ltd., Iselin, NJ, USA
OLS200 shaking water bath	Grant Instruments Ltd., Shepreth, UK
Omnifix® Luer syringe 10 ml	B. Braun Melsungen AG, Melsungen, Germany
Omni-Tips™ Disposable	Omni International, Kennesaw, GA, USA
Pasteur pipettes ISO 7712	Glaswarenfabrik Karl Hecht GmbH & Co. KG, Sondheim v. d. Rhön, Germany
Peristaltic Pump P-3	Pharmacia, Uppsala, Sweden
Pipette (max. 2.5, 10, 20, 100, 200, 1000 µl)	Eppendorf AG, Hamburg, Germany
Pipette tip (10 µl, 200 µl, 1 000 µl)	Sarstedt AG & Co. KG, Nümbrecht, Germany
Pipetus® pipetting tool	Hirschmann Laborgeräte GmbH & Co. KG, Eberstadt, Germany
Realplex^2 Mastercycler epgradient S	Eppendorf AG, Hamburg, Germany
Safe 2020 Class II Biological Safety Cabinet	Thermo Fisher Scientific, Waltham, MA, USA
Screw cap tubes (1.5, 15 and 50 ml)	Sarstedt AG & Co. KG, Nümbrecht, Germany
Serological pipettes (2 ml, 5 ml, 10 ml, 25 ml)	Sarstedt AG & Co. KG, Nümbrecht, Germany
SpectroStar nano	BMG Labtech GmbH, Ortenberg, Germany
Sterican® canula G27 x ¾"	B. Braun Melsungen AG, Melsungen, Germany
TC dish 100	Sarstedt AG & Co. KG, Nümbrecht, Germany
TC flask T75	Sarstedt AG & Co. KG, Nümbrecht, Germany

TC plate (6- and 24-wells; Cell+ surface)	Sarstedt AG & Co. KG, Nümbrecht, Germany
TH-02 hard tissue lyser	Omni International, Kennesaw, GA, USA
Thermomixer compact	Eppendorf AG, Hamburg, Germany
Vasofix® Safety catheter G22	B. Braun Melsungen AG, Melsungen, Germany
Vortex-Genie 2	Scientific Industries Inc., Bohemia, NY, USA
VX-65	Systec GmbH, Linden, Germany

2.1.2 Chemicals

The following chemicals in **Table 2** were used during the experiments.

Table 2 | Chemicals used for experiments

Chemicals	**Supplier**
9-cis-Retinoic acid	BIOMOL GmbH, Hamburg, Germany
α-MEM (w nucleosides, 2 g/l $NaHCO_3$, w/o L-Glu	Biochrom GmbH, Berlin, Germany
Agarose NEEO Ultra-Qualität	Carl Roth GmbH & Co. KG, Karlsruhe, Germany
Amberlite® IRA-400 chloride form	Sigma-Aldrich Chemie GmbH, Munich, Germany
Ammonium peroxodisulfate (APS)	Carl Roth GmbH & Co. KG, Karlsruhe, Germany
L-Ascorbic acid 2-phosphate sesquimagnesium salt, BioUltra	Sigma-Aldrich Chemie GmbH, Munich, Germany
Bicinchoninic acid	Sigma-Aldrich Chemie GmbH, Munich, Germany
Bovine Serum Albumin (BSA; Fraction V)	BIOMOL GmbH, Hamburg, Germany
Bromphenol Blue	Sigma-Aldrich Chemie GmbH, Munich, Germany
Cell Staining Buffer	BioLegend Inc., San Diego, CA, USA
Collagenase, type I (Clostridium histolyticum)	Worthington Biochemical Corporation, Lakewood, NJ, USA
Copper sulfate	Merck KGaA, Darmstadt, Germany
DMEM (w 4.5 g/l D-Glucose, w/o L-Glu and sodium pyruvate)	Gibco by Life Technologies, Ltd., Paisley, UK

DMEM/F-12 (1:1; 1x) w L-Glu	Gibco by Life Technologies, Ltd., Paisley, UK
Disodium hydrogenphosphate (Na_2HPO_4)	Merck KGaA, Darmstadt, Germany
Dimethylsulfoxide (DMSO) for molecular biology	Merck KGaA, Darmstadt, Germany
Dulbecco's PBS	Gibco by Life Technologies, Ltd., Paisley, UK
EBSS w/o Ca^{2+}, Mg^{2+} and Phenol Red	Life Technologies, Ltd., Paisley, UK
EDTA (500 mM)	AppliChem GmbH, Darmstadt, Germany
EGTA	Sigma-Aldrich Chemie GmbH, Munich, Germany
Ethanol 70 % + 1 % MEK	Carl Roth GmbH & Co. KG, Karlsruhe, Germany
Ethanol 99.8 %	Carl Roth GmbH & Co. KG, Karlsruhe, Germany
L-Glutamine	PAA Laboratories GmbH, Pasching, Austria
Glycerol	Carl Roth GmbH & Co. KG, Karlsruhe, Germany
β-Glycerophosphate disodium salt, BioUltra	Sigma-Aldrich Chemie GmbH, Munich, Germany
Glycin for electrophoresis, > 99 %	Sigma-Aldrich Chemie GmbH, Munich, Germany
HBSS w/o Ca^{2+}, Mg^{2+} and Phenol Red	Biochrom GmbH, Berlin, Germany
HEPES (1 M)	Gibco by Life Technologies, Ltd., Paisley, UK
Interferon γ, Premium Grade	Miltenyi Biotec GmbH, Bergisch Gladbach, Germany
Isopropanole	Carl Roth GmbH & Co. KG, Karlsruhe, Germany
LB Broth with agar (Lennox)	Sigma-Aldrich Chemie GmbH, Munich, Germany
Lipofectamine 2000	Life Technologies, Ltd., Paisley, UK
Lipopolysaccharides (source *E. coli* O111:B4)	Sigma-Aldrich Chemie GmbH, Munich, Germany
M-CSF murine (recombinant; source *E. coli*)	PeproTech Germany, Hamburg, Germany
β-Mercaptoethanol	Sigma-Aldrich Chemie GmbH, Munich, Germany

Methanol	Carl Roth GmbH & Co. KG, Karlsruhe, Germany
Methimazole, analytical standard	Sigma-Aldrich Chemie GmbH, Munich, Germany
Milk powder, blotting grade	Carl Roth GmbH & Co. KG, Karlsruhe, Germany
Opti-MEM	Life Technologies, Ltd., Paisley, UK
Pen Strep (10 000 units/ml)	Gibco by Life Technologies, Ltd., Paisley, UK
Phenylmethylsulfonyl fluoride (PMSF; 100 mM)	Sigma-Aldrich Chemie GmbH, Munich, Germany
Potassium chloride (KCl)	Merck KGaA, Darmstadt, Germany
Potassium dihydrogenpohosphate (KH_2PO_4)	Carl Roth GmbH & Co. KG, Karlsruhe, Germany
RANKL (recombinant, source *E.coli*)	R&D Systems, Inc., Minneapolis, MN, USA
Red Cell Lysis Buffer (10x)	BioLegend Inc., San Diego, CA, USA
RPMI 1640 (w 4.5 g/l D-Glucose, 2.383 g/l HEPES, L-Glu, 1.5 g/l sodium bicharbonate 110 mg/l sodium pyruvate)	Gibco by Life Technologies, Ltd., Paisley, UK
S.O.C. Outgrowth medium	New England Biolabs GmbH, Frankfurt am Main, Germany
Sodium chloride (NaCl)	Sigma-Aldrich Chemie GmbH, Munich, Germany
Sodium dodecylsulfate (SDS)	Sigma-Aldrich Chemie GmbH, Munich, Germany
Sodium deoxycholate	AppliChem GmbH, Darmstadt, Germany
Sodium hydroxide	Merck KGaA, Darmstadt, Germany
Sodium orthovanadate (Na_3VO_4)	Merck KGaA, Darmstadt, Germany
Sodium perchlorate monohydrate ($NaClO_4$), p.A.	Merck KGaA, Darmstadt, Germany
Sodium selenite, BioReagent	Sigma-Aldrich Chemie GmbH, Munich, Germany
T0901317	Bio-Techne Ltd., Abingdon, UK
TEMED	Carl Roth GmbH & Co. KG, Karlsruhe, Germany

L-Thyroxine (T_4)	Sigma-Aldrich Chemie GmbH, Munich, Germany
Trichloromethane (Chloroform)	Merck KGaA, Darmstadt, Germany
3,3'5-Triidothyronine (T_3)	Sigma-Aldrich Chemie GmbH, Munich, Germany
Tris ultra pure, p.A.	BIOMOL GmbH, Hamburg, Germany
Triton X-100	Sigma-Aldrich Chemie GmbH, Munich, Germany
Trypsin-EDTA 0.05%	Gibco by Life Technologies, Ltd., Paisley, UK
Tween 20	Sigma-Aldrich Chemie GmbH, Munich, Germany

2.1.3 Buffers and solutions

The following buffers and solutions in **Table 3** were used during the experiments and prepared as indicated.

Table 3 | Buffers and Solutions used for experiments

Buffer / Solution	Composition
Phosphate Buffered Saline (PBS) 10x for 1l	NaCl: 80 g KCl: 2 g KH_2PO_4: 2 g Na_2HPO_4 x 2 H_2O: 14.4 g
Electrophoresis Buffer 10x for 1 l	Tris: 12.15 g Glycin: 144.1 g SDS: 10 g
Lämmli Buffer 4x for 20 ml	Glycerol: 10 ml SDS: 2 g Tris/HCl (pH 6.8): 6.25 ml Bromphenol Blue: spade point H_2O dest.: ad 20 ml 400 ml aliquots store at -20 °C add 100 µl β-Mercaptoethanol per aliquot when using

Blotting Buffer **10x for 1 l**	Tris: 30.3 g Glycin: 144.1 g when diluting to 1x add 20 % Methanol
TBS pH 7.4 **10x for 1 l**	Tris: 12.15 g NaCl: 87.6 g for TBS-T add Tween 20 1:1000
Radioimmunoprecipitation assay Buffer (RIPA Buffer) **1x for 100 ml**	Tris: 0.79 g NaCl: 0.9 g H_2O dest.: ad 75 ml stir solution until all solids are solved adjust pH to 7.4 10 % NP-40: 10 ml 10 % Na-deoxycholate: 2.5 ml stir until solution is clear 500 mM EDTA: 0.2 ml 200 mM activated Na_3VO_4: 50 µl for 1 mM 500 mM NaF: 20 µl for 1mM H_2O dest.: ad 100 ml store until use at 4 °C
Cell lysis Buffer **1x for 10 ml**	Add 1 tablet of protease inhibitor complex to 10 ml RIPA Buffer shake until tablet has dissolved store at -20 °C add 100 mM PMSF: 1:100 when using
Collagen medium	DMEM/F12: 46 ml FBS: 2.5 ml 1M HEPES: 0.5 ml Collagen G: 0.5 ml P/S: 0.5 ml
Perfusion Buffer **(for 1 mouse)**	EBSS: 20 ml 50 mM EGTA: 200 µl
Digestion Buffer **(for 1 mouse)**	HBSS: 50 ml Collagenase type I: 15 mg

2.1.4 Oligonucleotides

All oligonucleotides were purchased from Integrated DNA Technologies Inc., Leuven, Belgium in standard desalting quality and were optimised for an annealing temperature of 60 °C. The oligonucleotides were designed by using SequenceAnalysis Version 2.0.

Table 4 | Oligonucleotides used for experiments

Gene name	Abbreviation	Sequence (5' → 3') forward / reverse
ATP binding cassette subfamily G member 5	*Abcg5*	CATGATGCTAGATGAGCCAACC TGTCGAAGTGTTGGAAGAGCT
Actin β	*Actb*	ACTGAGCTGCGTTTTACACCC TGCTCCAACCAACTGCTGTC
Alpha 2-HS glycoprotein (*Fetua*)	*Ahsg*	TGGGGAAGAAGTTTCAGTGG GTCGTGGTAAGTTCGGTGGT
Angiotensinogen (*Angt*)	*Agt*	TAACCCCCAGAGTGTGGTGT AGGCTCTGCTGCTCATCATT
Apolipoprotein A1	*Apoa1*	AAACAGAAGGTGCAGCCCTA GCGCAGAGAGTCTACGTGTG
Apolipoprotein B	*Apob*	TTGGCAAACTGCATAGCATCC TCAAATTGGGACTCTCCTTTAGC
Apolipoprotein C3	*Apoc3*	TACAGGGCTACATGGAACAAGC CAGGGATCTGAAGTGATTGTCC
Apolipoprotein C4	*Apoc4*	TGTTCTTGGTCAGCTTTGTAGC AGGCTGTGGGTCTTGTTTAGG
Apolipoprotein D	*Apod*	TTCACCACAGCCAAAGGACA GCTCGCTGGGATCTTCTCAA
Apolipoprotein E	*Apoe*	CATGGAGGATCTACGCAACCG TGCCTTGTACACAGCTAGGC
Arginase-1	*Arg1*	CCCAGATGTACCAGGATTCTCC AGGTCTCTTCCATCACCTTGC
Abnormal spindle microtubule assembly	*Aspm*	TTCGCGATGAGAAGGAAGTT GTGCATCTTTTGCACCCTTT
bone gamma-carboxyglutamate protein (*Ocn*)	*Bglap*	GCGCTCTGTCTCTCTGACCT ACCTTATTGCCCTCCTGCTT
Cathelicidin antimicrobial peptide	*Camp*	GTCTTGGGAACCATGCAGTT CAGGTCCAGGAGACGGTAGA

CD5 molecule like	*Cd5l*	GATCGTGTTTTTCAGAGTCTCCA
		TGCAGTCAACCCCTTGAATAAG
CD28 antigen	*Cd28*	TCACACCACACTCTGCCTTG
		GCTGACCTCGTTGCTATCTACC
CD3 antigen, delta polypeptide	*Cd3d*	CATCCTGTGGCTTGCCTCTATT
		GATGCATGACGCTGGTATTGC
Ceruloplasmin	*Cp*	CTTAGCCTTGGCAAGAGATAAGC
		GGCCTAAAAACCCTAGCCAGG
Colony stimulating factor 1	*Csf1r*	CAATGGCAGTGTGGAATGGG
receptor (*CD115*)		AAGCTCGGTACAACGGTAGG
Cathepsin K (*CatK*)	*Ctsk*	AAGTGGTTCAGAAGATGACGGGAC
		TCTTCAGAGTCAATGCCTCCGTTC
Deiodinase, iodothyronine, type	*Dio1*	GCTGAAGCGGCTTGTGATATT
I		GTTGTCAGGGGCGAATCGG
Fibulin 1	*Fbln1*	TGAATGCCCCGAGAACTATC
		CTCAGGACGGGTGAACTCTC
Hypoxanthine guanine	*Hprt*	GCAGTACAGCCCCAAAATGG
phosphoribosyl transferase		AACAAAGTCTGGCCTGTATCCAA
Glyceraldehyde-3-phosphate	*Gapdh*	AGGTCGGTGTGAACGGATTTG
dehydrogenase		TGTAGACCATGTAGTTGAGGTCA
Interleukin-1β	*Il1b*	TATCACTCATTGTGGCTGTGGA
		CATCTCGGAGCCTGTAGTGC
Interleukin 1 receptor accessory	*Il1rap*	GTACTGGACCAGGCAAGACC
protein		GCTGTCCTTCTGAACAACTTCC
Interleukin-10	*Il10*	ATGCAGGACTTTAAGGGTTACTTG
		TAGACACCTTGGTCTTGGAGCTTA
Lumican	*Lum*	GATCAAGCATCTGCGCTTGG
		CCACCAGCAACGAGAAGGAT
Membrane-spanning 4-domains,	*Ms4a1*	TTGGGGGCTGTCCAAATCATG
subfamily A, member 1 (*CD20*)		ACTCAAACAGATGGGTGCGAA
Nitric oxide synthase, inducible	*Nos2*	ACATCGACCCGTCCACAGTAT
		CAGAGGGGTAGGCTTGTCTC
Osteocalcin	*Ocn*	GCGCTCTGTCTCTCTGACCT
		ACCTTATTGCCCTCCTGCTT

Osteopontin	*Opn*	TGAAAGTGACTGATTCTGGCA
		GGACGATTGGAGTGAAAGTGT
Oxysterol receptor LXR-α	*Nr1h3*	CAATCGAGGTCATGCTTCTGGA
		GAGTTGCAGCTCATTCATGGC
Paired box 5	*Pax5*	GGAGGATCCAAACCAAAGGTTG
		GTCCGAATGATCCTGTTGATGG
Peptidoglycan recognition protein 2 (*Pgrp2*)	*Pglyrp2*	CTCTGGATCGTGCTTGGATT
		GAATTGTGGGTGCTGGAGTT
Platelet glycoprotein 4 (CD36)	*Cd36*	ATGGGCTGTGATCGGAACTG
		GTCTTCCCAATAAGCATGTCTCC
Secretory leukocyte peptidase inhibitor (*Alp*)	*Slpi*	CTACTTGTGTGGCGTGAAGG
		CTGGTGGCATCTCGTTATCC
Sclerostin	*Sost*	CGTGCCTCATCTGCCTACTT
		TGACCTCTGTGGCATCATTC
Sterol regulatory element binding transcription factor 2 (*Srebp2*)	*Srebf2*	GGAAGCAGGCAGACCTAGACC
		AGGCTGTAGCGGATCACATTCC
Thyroid hormone responsive (*Spot14*)	*Thrsp*	CCTGCTGACAGTCATGGATCG
		TGGTCCACTTCTACACAGATGC
Transthyretin	*Ttr*	TTGCCTCGCTGGACTGGTA
		TTACAGCCACGTCTACAGCAG
Tumour necrosis factor α	*Tnfa*	TCTCATCAGTTCTATGGCCC
		GGGAGTAGACAAGGTACAAC
Vascular cell adhesion molecule 1	*Vcam1*	CCCGTCATTGAGGATATTGG
		GGTCATTGTCACAGCACCAC
	Primer for human genes	
Angiotensinogen (Angt)	*AGT*	GACACCGAAGACAAGTTGAGG
		ATTGCCTGTAGCCTGTCAGC
Apolipoprotein A1	*APOA1*	GCGGCAGAGACTATGTGTCC
		CTCCAGATCCTTGCTCATCTCC
Apolipoprotein B	*APOB*	CCAGGATCAACTGCAAGGTT
		ACCTGCTTCCCTTCTGGAAT
Apolipoprotein C3	*APOC3*	CAGCTTCATGCAGGGTTACA
		GGTCCAAATCCCAGAACTCAG

Apolipoprotein C4	*APOC4*	GGTGAACAGGACCAGAGACG
		TCCCTCAGGTGGTCGTCATA
Apolipoprotein D	*APOD*	GGTGCAGGAGAATTTTGACGTG
		GGTGGCTTCACCTTCGATTTG
Alpha 2-HS glycoprotein (*FETUA*)	*AHSG*	AGAGGCAGCCAAGTGTAACC
		GCTTCATTGGCACCTTCTGG
Abnormal spindle microtubule assembly	*ASPM*	TTGGCTGTTGTCCTACAATCC
		TCTATACAGGTGAGGAACAGTGG
CD5 molecule like	*CD5L*	GTCATGGCTCTGCTATTCTCC
		CAGCCACGTCCTTAATGTCC
Cathelicidin antimicrobial peptide	*CAMP*	CCCAGGTCCTCAGCTACAAGG
		TCTGGTGACTGCTGTGTCGTC
Deiodinase, iodothyronine, type I	*DIO1*	AGCCACGACAACTGGATACC
		CCAGTGGCCTATTACCTTGC
Fibulin 1	*FBLN1*	CCTACACGTGCCAGAAGAACG
		GACACACATCCTGCTGATGCC
Hypoxanthine guanine phosphoribosyl transferase	*HPRT*	TTGCTCGAGATGTGATGAAGG
		GATGTAATCCAGCAGGTCAGC
Interleukin 1 receptor accessory protein	*IL1RAP*	TGATGGATTCTCGCAATGAGG
		CATAGCTGCGCTTGAGATCC
Lumican	*LUM*	CAGACTGCCTTCTGGTCTCC
		AGGACAGATCCAGCTCAACC
Peptidoglycan recognition protein 2 (*Pgrp2*)	*PGLYRP2*	TCTGGATCCTACTCGGATTGC
		AGTGGTAGAGGCGATTGTGG
Thyroid hormone responsive (*SPOT14*)	*THRSP*	TCCGGGATGCTTCTCTACCT
		CGAGGGGAGCAGTGAATAGC
Thyroid hormone receptor β	*THRB*	TGACAAAGCCACCGGGTATC
		AAAGCGACATTCCTGGCACT
Transthyretin	*TTR*	AGCAGCCATCACAGAAGTCC
		CAGAGGACACTTGGATTCACCG
Vascular cell adhesion molecule 1	*VCAM1*	GAAGATGGTCGTGATCCTTGG
		TGCTGCAAGTCAATGAGACG

2.1.5 Antibodies

The following antibodies were used for Western Blot or cell sorting experiments.

Table 5 | Antibodies used for experiments

Antibody	Species	Dilution	Clone	Manufacturer
Primary antibodies for Western Blot				
anti-AIM	rat	1:1000	23B12 (#36)	TransGenic Inc., Kobe, Japan
anti-Ceruloplasmin	goat	1:1000	Ab19171	Abcam plc, Cambridge, UK
Primary antibodies for flow cytometry				
APC anti-CD115	rat	1:200	AFS98	BioLegend Inc., San Diego, CA, USA
BV421 anti-CD3ε	American Hamster	1:800	145-2C11	BioLegend Inc., San Diego, CA, USA
CD16/32 Fcγ blocker	rat	1:100	93	BioLegend Inc., San Diego, CA, USA
FITC anti-CD45	rat	1:400	I3/2.3	BioLegend Inc., San Diego, CA, USA
PE anti-CD19	rat	1:400	1D3	BD Biosciences, Heidelberg, Germany
Secondary antibodies for Western Blot				
HRP anti-goat IgG	rabbit	1:5000	P0449	Dako Denmark A/S, Glostrup, Denmark
HRP anti-rat IgG	goat	1:2000	#7077	Cell Signaling Technology Inc., Frankfurt am Main, Germany

2.1.6 Plasmids

The following Plasmids were used during the experiments.

Table 6 | Plasmids used for experiments

Plasmid	Manufacturer
pcDNA3.1	provided by Lars Möller – Universitätsklinik Essen
pcDNA3.1-TRβ	provided by Lars Möller – Universitätsklinik Essen

2.1.7 Kits

The following kits were used during the experiments.

Table 7 | Kits used for experiments

Kit	Manufacturer
Clarity and Clarity Max Western ECL Substrate	Bio-Rad Laboratories GmbH, Munich, Germany
cOmplete ULTRA tablets Mini, Easy Pack	Roche Diagnostics International AG, Rotkreuz, Switzerland
Direct-zol RNA Miniprep Kit	Zymo Research Europe GmbH, Freiburg, Germany
Fast Start Universal SYBR Green Master (ROX)	Roche Diagnostics International AG, Rotkreuz, Switzerland
NucleoSpin® RNA Clean-up Kit	Macherey-Nagel GmbH & Co. KG, Düren, Germany
Plasmid Mini Kit	Qiagen GmbH, Hilden, Germany
Plasmid Maxi Kit	Qiagen GmbH, Hilden, Germany
QIAzol Lysis Reagent	Qiagen GmbH, Hilden, Germany
RevertAid First Strand cDNA Synthesis Kit	Thermo Fisher Scientific, Waltham, MA, USA
Total T3 ELISA 96 wells	NovaTec Immunodiagnostica GmbH, Dietzenbach, Germany
Total T4 ELISA 96 wells	DRG Instruments GmbH, Marburg, Germany
TGX Stain-Free™ FastCast™ Acrylamide Kit 10%	Bio-Rad Laboratories GmbH, Munich, Germany
Zombie NIR™ Fixable Viability Kit	BioLegend Inc., San Diego, CA, USA

2.1.8 Software

The following software for MacOS Mojave Version 10.14.1 64-bit was used for the experiments.

Table 8 | Software used for experiments

Software	Manufacturer
Affinity Designer Version 1.7.2	Serif Ltd., Nottingham, UK
Image Lab™ Version 6.0.0 build 26	Bio-Rad Laboratories GmbH, Munich, Germany
MySQL Workbench Version 6.3.10	Oracle Corporation, Redwood Shores, CA, USA

Office 2016 for Mac Version 15.41	Microsoft Corporation, Redmont, WA, USA
Prism 6.0h	GraphPad Software, Inc., San Diego, CA, USA
R Version 3.5.1	The R Foundation for Statistical Computing, Vienna, Austria
Realplex Version 2.2.10 (for Windows XP)	Eppendorf AG, Hamburg, Germany
RStudio Version 1.1.383	RStudio Inc., Boston, MA, USA
SequenceAnalysis 2.0	Informagen Inc., Greenland, NH, USA

2.2 Methods

2.2.1 Animal husbandry and induced thyrotoxicosis

Animals were housed in groups under constant 12h/12h light/dark cycle at ambient temperature (22 ± 1 °C) and had ad libitum access to food and water. TRβ-/- [151] and TRα1+/m [152] as described previously, were bred in the GTH Lübeck animal core facility and compared with TRβ+/- or TRα1+/+ littermates. Wild type C57BL/6NCrl (BL6) animals were purchased from Charles River Laboratories GmbH (Erkrath, Germany) and rendered hypothyroid with methimazol (0.1% m/v) and sodium perchlorate (0.2% m/v) for three weeks in the drinking water. Mild or severe thyrotoxicosis was induced by either adding T_4 at 1 mg/l or T_3 at 0.5 mg/l to the drinking water for 2 weeks, respectively. For the investigation of short term effects of TH on mice, animals were treated either with T_4 at 1 mg/l for 4 days or with T_3 at 0.5 mg/l for 24 h. To minimise avoiding drink behaviour, bovine serum album (BSA, 0.1% m/v) was added into the drinking water of T_4 or T_3 treated groups and untreated control groups and 4 tablets of sucralose sweetener per bottle were added into MMI/ClO_4^- - treated groups. All animal procedures were approved by the MELUND Schleswig-Holstein (Ministerium für Energiewende, Landwirtschaft, Umwelt, Natur und Digitalisierung).

2.2.2 Proteomics and transcriptomics

The proteome and transcriptome analyses were performed by the staff of the Department for Functional Genomics at the Ernst-Moritz-Arndt University of Greifswald.

2.2.2.1 Determination of plasma proteome

The results and methodological procedures were already published and will here only be briefly described [128]. Six highly abundant plasma proteins were removed by using an Agilent technologies MARS6 column, before precipitating the non-bound proteins. The protein concentration was determined using a Bradford assay kit, and subsequently the protein solutions were prepared for mass spectrometric analysis For the mass spectrometer analysis, a Thermo Electron LTQ-Orbitrap Velos was used and MS/MS fragmentation was brought about by collision induced dissociation. For data pre-processing, the GeneData Refiner MS version 7.6.6 software was employed with a 3-step protocol, followed by a data search against the human Swissprot/Uniprot database (rel. 2012/08). The data of all 80 samples were deposited to the ProteomeXchange Consortium with the identifier PXD004815.

2.2.2.2 Determination of Liver Transcriptome

The methodological procedure of transcriptome determination has been published before and will be only briefly described here [153]. Total RNA was isolated by homogenising frozen liver tissue in TRIzol reagent. After quality control in an Agilent 2100 Bioanalyzer, the transcriptome was measured in accordance with manufacturer's instructions after using the WT Expression Kit and GeneChip WT Terminal Labeling Kit, on a GeneChip Mouse Gene 1.0 ST array (all Affimetrix).

2.2.2.3 Target gene identification

For the identification of concordantly altered targets between human and mouse plasma proteome and their further specification by combination with the mouse liver transcriptome, the unfiltered data sets were provided by the Department of Functional Genomics. For a better handling of the transcriptome data set, containing 35 500 entries, a MySQL database was set up, with MySQL Workbench version 6.3.10 on a local server, where all raw data sets were deposited without any pre-selections. The following data sets were created and included the mentioned tables with their associated columns:

1. **humane_proteome** (name, Description, FT4_p_FDR, FT4_est(beta), %tualer Anstieg je einer Einheit ft4, %tualer Anstieg je 10 Einheiten ft4)
2. **serum t4 vs co no fc** (Swissprot accession entry, protein name, annotation, BH Q-Value, Ratio, P-Value, FC)
3. **serum t4 vs rec no fc** (Swissprot accession entry, protein name, annotation, BH Q-Value, Ratio, P-Value, FC)
4. **liver_transcriptome_t4** (Primary Sequence Name, name, Post Hoc P-value0-Control_T4, P-value [Control vs. T4] (Ratio Experiment), Ratio [Control vs. T4] Fold Change (Ratio Experiment))
5. **liver_transcriptome_rec** (Primary Sequence Name, name, Post Hoc P-value0-Control_T4, P-value [Control vs. T4] (Ratio Experiment), Ratio [Control vs. T4] Fold Change (Ratio Experiment))

The data set of the human proteome only contains fold change values after 8 weeks of treatment compared to baseline level at the beginning of the trial, therefore no further selection step was available. For the mouse plasma proteome and liver transcriptome, the fold change values between all groups were available, which allows detecting target genes that alter upon T_4 treatment, but also return back to baseline within the recovery period. This additional information required an overlay between the tables "serum_proteome_t4" with "serum_proteme_rec" and "liver_transcriptome_t4" with "liver_transcriptome_rec", which was achieved with the MySQL code found in the Appendix.

The command referred to above, generated the new table "FC 1.05 proteome overlay" which includes all common entries from "serum t4 vs co no fc" and "serum t4 vs rec no fc". In addition, this command already comprises a filter step which excludes genes or proteins with a fold change < |1.05|, which is the vast majority of unregulated targets. The next level in data preparation was the exclusion of statistically non-significant targets with a p-value > 0.05 from the data sets, which necessitate the creation of the tables "p-cutoff humane proteome", "p-cutoff proteome overlay" and "p-cutoff transcriptome overlay" using the commands found in the Appendix.

The resultant data sets completed the pre-processing procedure and were now compared to identify shared targets. The different methodological techniques with their specific annotation styles hampered the comparability and necessitate more sophisticated substring comparison of the first four annotation symbols to combine the tables, which is shown in the commands in the Appendix. The applied algorithm used a "join" command to combine the respective data sets, which implies the problem of duplet creation. To remove these duplets, an auxiliary table copy was used to identify artificial copies which share the same Swissprot accession entry, but have different unique IDs and exclude them from the final list. The applied command can be found in the Appendix.

A final check was then performed to exclude incompletely annotated genes or proteins, using the commands shown in the Appendix.

2.2.3 Cell sorting

For cell sorting experiments the FACS Aria II device in the Cell Analysis Core Facility (CanaCore) of Institute for systemic inflammation research (ISEF) was used. The cell sorting procedure bases on the principle for flow cytometry, which uses fluorophore-coupled antibodies that recognise cell type specific surface molecules. Several antibodies with different coupled fluorophores enable the discrimination of different cell types. With a cell sorting approach, this discrimination does not simply count the abundance of different cell types, but allows to sort specific cell types to perform subsequent analysis with these cells. The antibodies used here are listed in **Table 5** and allowed to distinguish between Monocytes ($CD45^+$; $CD115^+$), B cells ($CD45^+$; $CD19^+$) and T cells ($CD45^+$; $CD3\varepsilon^+$) [154-156]. For this purpose, Heparin-stabilised blood was diluted in 14 ml Cell Staining Buffer (CSB) and centrifuged with 350 g for 5 min at 4 °C. The supernatant was carefully decanted and discarded. The pellet was resuspended in 3 ml Red Cell Lysis buffer (RCL buffer) and incubated until total clearance for about 5 min on ice. The lysis was stopped by addition of 10 ml CSB and the solution was centrifuged with 350 g for 5 min at 4 °C and supernatant was discarded and the washing step with 10 ml CSB was repeated. The pellet was resuspended in 10 ml CSB and cell number was determined using a Neubauer counting chamber. The suspension was centrifuged

with 350 g for 5 min at 4 °C and the supernatant was discarded. For the distinction of live and dead cells, the pellet was resuspended in 100 µl of a 1 : 100 dilution of Zombie NIR™ dye and incubated for 15 min at room temperature in the dark, followed by a centrifugation with 350 g for 5 min at 4 °C. After discarding the supernatant, the resultant pellet was resuspended in a required volume CSB to obtain a final concentration of $1 \cdot 10^6$ cells/ml. Unspecific binding sites were blocked using an anti-CD16/32 Fcγ-inhibitor antibody with concentration of 5 µg/ml for 10 min on ice. This step was followed by the incubation with fluorophore-labelled antibodies at specific concentrations between 1 : 200 – 1 : 800 for 20 min in the dark on ice. Henceforward, the cells were stored in the dark on ice to avoid photo bleaching of the fluorophores. The pellet was washed twice with 2 ml CSB, centrifuged with 350 g for 5 min at 4 °C and finally resuspended in 500 µl PBS for cell sorting.

2.2.4 Cell culture

To dissect the different actions of TH *in vitro*, several cells lines were used. The cell specific conditions and cultivation procedures are described in the following section.

2.2.4.1 Depletion of TH from serum

For determination of target gene expression under TH-free conditions, fetal bovine serum (FBS) was incubated at 4 °C for 24 h with sterile Amberlite IRA-400 chloride form resin, aliquoted in 50 ml falcons and stored at -20 °C. The effect of this procedure was described before [111, 157] and the validation of the TH removal from the serum was determined by fT_4 and fT_3 immunoassays conducted by the department for clinical chemistry and revealed a reduction of 79% for fT_3 and 89% for fT_4.

2.2.4.2 LX-2 cell line

The LX-2 cell line is derived from human hepatic stellate cells (Ito cells) and was artificially generated by spontaneous immortalisation under low serum concentration conditions in 2005 [158]. The cells were grown in Dulbecco's Modified Eagle Medium (DMEM) supplemented with 2% heat-inactivated Foetal Bovine Serum (FBS) and 1% Penicillin / Streptomycin (P/S) at 37 °C in a humidified 5% CO_2 containing atmosphere. Cells were split every 2 – 3 days when they reached 95% confluency in 1:5 dilution. For this purpose, they were firstly washed with Dulbecco's Phosphate-Buffered Saline (DPBS), followed by an incubation at 37 °C with a mixture of trypsin and EDTA for 5 min. This detaching process was stopped by adding a 2-fold trypsin volume of serum-containing medium.

The LX-2 cell line was kindly provided by Prof. Dr. rer. nat. Hendrik Ungefroren.

2.2.4.3 HepG2 cell line

Since its first description in 1979, the HepG2 cell line played an important role for immunology, cancer and pharmacology research, which is due to their similar properties compared to the scarcely available primary hepatocytes [159]. HepG2 cells were cultured in Roswell Park Memorial Medium (RPMI) 1640, containing 10% FBS and 1% P/S, at 37 °C in a humidified 5% CO_2 containing atmosphere. Cells were split every 2 – 3 days when they reached 95% confluency in 1:15 dilution as described for LX-2 cells.

The HepG2 cell line was kindly provided by Dr. rer. nat. Nina Perwitz.

2.2.4.4 Primary osteoclasts

In 1988, the present gold standard method for the murine primary osteoclast (OCs) culture was established [160]. With slight adaptations, this protocol was used to differentiate OCs from hematopoietic stem and progenitor cells (HSPCs) and was performed as follows. Mice were sacrificed with CO_2 followed by cervical dislocation. The skin was removed and the leg was dislocated to allow clear view for the cut in the gap between the articular head and articular cavity, which releases the whole bone. Surrounding soft tissue was removed and tibia and femur were separated and stored until further usage in ice-cold phosphate buffered saline (PBS). From here, all further steps were performed under sterile conditions. Tibiae and femora were sterilised with 70% ethanol, bone ends were broken off with a scissor and bone marrow was flushed out with 15 ml serum-free α – Minimum Essential Medium (α-MEM). Cells were centrifuged at 483 g for 5 min and the pellet was resuspended in 1 ml of α-MEM and cell number was determined in a 1:100 dilution with an improved Neubauer counting chamber. Cells were then seeded at a density of $1 \cdot 10^6$ cells/cm^2 in α-MEM with nucleosides containing 10% FBS, 1% P/S supplemented with 1 mM L-Glutamine and 20 ng/ml Macrophage colony-stimulating factor (M-CSF). After 5 days, the medium was changed and 50 ng/ml Receptor Activator of NF-κB Ligand (RANKL) were added to stimulate the fusion and differentiation of osteoclastic progenitors into mature osteoclasts. After 24 h the medium was changed and contained henceforward 1% FBS. 12 h later the cells were poised for the stimulation with desired stimuli.

2.2.4.5 Primary osteoblasts

From 1976 it was known, that the parathyroid hormone together with high amounts of p-orthophosphate are essential for osteoblast (OB) development from HSPCs [161]. Hence a protocol, similar to the isolation protocol for OCs was established as follows. After isolation of HSPCs, as described for OCs, cells were seeded at a density of $1 \cdot 10^6$ cell/cm^2 in α-MEM, containing 20% FBS and 1% P/S. After 5 days, medium was changed and from this time point on

DMEM, containing 10% FBS, 1% P/S, 10 mM β-Glycerophosphate and 100 µM ascorbate phosphate, was used as differentiation medium (DM) for 14 days. For stimulation purposes, starvation medium with 1% FBS and 1% P/S was added to the cells 12 h before stimulation beginning.

2.2.4.6 Primary bone marrow-derived macrophages

Macrophages are known to be first line defence cells in mammals. The here used macrophage population differentiated from hematopoietic and progenitor stem cells (HPSCs). Therefore, murine stem cells were isolated from femurs and tibiae as previously described for primary osteoclasts. Cells were seeded at a density of $1 \cdot 10^5$ cells/cm^2 in RPMI 1640, containing 10% FBS, 1% P/S and 20 ng/ml M-CSF. After three days, the same amount of medium with the same formulation was carefully added to the cells. After two days, the medium was removed and cells were washed with Hanks Buffered Saline Solution (HBSS) without Ca^{2+} and Mg^{2+} and RPMI medium, containing 10% FBS, 1% P/S, 100 ng/ml Lipopolysaccharide (LPS) and 20 ng/ml Interferon γ (IFN γ) to induce the polarisation from resting state MΦ macrophages into activated M1 macrophages [162]. The polarisation medium was removed after 24 h and after washing with HBSS, starving medium, containing RPMI 1640 supplemented with 1% FBS and 1% P/S, was added to the cells. After 12 h of starvation, cells were stimulated for 24 h in RPMI 1640 medium containing 1% FBS, 1% P/S and the respective stimulation compound.

2.2.4.7 Primary hepatocytes

For accurate validation and interpretation of *in vivo* findings, primary hepatocytes are a more suitable model compared to hepatic cell lines, since these cells still show a gene expression pattern similar to the gene expression of tissue hepatocytes and were isolated and cultivated as follows. Perfusion buffer, collagenase solution and RPMI 1640 medium, containing 10% FBS and 1% P/S were pre-warmed to 37 °C. After sacrificing the mouse with CO_2 but without cervical dislocation, the abdomen was opened to release the liver and the port vein. A 22G butterfly cannula was carefully injected into the caudal vena cava and draining of perfusion buffer was allowed by cutting through the portal vein. The perfusion and digestion buffer were injected by a peristaltic pump with a constant speed of 5 ml per minute. The liver should immediately loose its blood derived red colour. Perfusion was stopped when leaking fluid became colourless and was directly replaced by collagenase solution. The success of the collagenase digestion of the liver was controlled by evolving white spots on the liver lobes. After complete digestion, the liver was taken in one piece and the gall bladder was removed. The liver was placed in 13 ml RPMI 1640 medium and transported under the sterile work bench. Here, the hepatocytes were squeezed out the lobes by carefully pushing a cell scraper on the tissue. For higher cell numbers this process was repeated 3

times to end up with a total medium volume of 50 ml (3 x 13 ml + 11 ml). The cell suspension was centrifuged for 10 min at 43 g and 4 °C. The supernatant was removed and cells were resuspended with 25 ml RPMI 1640 medium (+ 10% FBS, + 1% P/S) and centrifuged for 5 min at 43 g and 4 °C. After repeating this step, the cells were resuspended in 20 ml RPMI 1640 medium and diluted 1:10 in a 1:10 Trypan Blue solution to determine the total cell number. Importantly, only the cells with a clear or slightly blue nucleus were considered and counted as living and vital cells. The cells were seeded at a density of $2 \cdot 10^5$ cells/ml in collagen-coated 6-well plates in RPMI 1640 medium, containing 10% FBS and 1% P/S. After 3 h, medium was changed and the cells were incubated for 24 h, before starving them for 16 h in RPMI 1640, containing 5% FBS and 1% P/S. After starvation, the cells were incubated in starving medium and the respective compound for 24 – 48 h.

2.2.5 Plasmid amplification & transfection

Circular extra-chromosomal bacterial DNA strands or Plasmids enable for an efficient and defined genetic modification of mammalian cells by induced incorporation of these nucleic acids. The plasmids used in the experiments here were shipped lyophilised on Whatman paper and were reconstituted at a concentration of about 0.1 µg/µl in TE buffer.

2.2.5.1 Amplification of plasmids

For the amplification of plasmids, 50 µl of commercially available competent NEB5α cells were thawed on ice and incubated with 10 µl plasmid solution for 20 min on ice, followed by a heat shock at 42 °C for 45 s and an immediate return on ice. The bacteria were recovered in 900 µl S.O.C. media without antibiotics at 37 °C for 1 h and 300 rpm. The bacteria solution was then diluted 1 : 100 in LB medium and 400 µl of the dilution was plated out on LB agar with Ampicillin (100 µg/ml) at 37 °C overnight. After incubation, single bacteria colonies were picked with a pipette tip at transferred into 15 ml tubes containing 3 ml of LB medium with Ampicillin (100 µg/ml) and incubated at 37 °C and 300 rpm for 6 – 8 h. DNA was isolated from 1 ml of the bacteria suspensions using a Plasmid MiniPrep Kit. The purified DNA was analysed for plasmid-specific sequences in a polymerase chain reaction (PCR) and the 10 µl reaction mix contained 1 µl 10 x reaction buffer, 1 µl primer mix (forward and reverse) (5 mM), 1 µl dNTPs (100 mM), 0.1 µl DreamTaq DNA Polymerase, 4.9 µl distilled water and 1 µl of sample DNA. The PCR protocol for plasmid DNA was as follows.

Table 9 | Protocol for Plasmid insert PCR

Step number	Step	Temperature	Time	
1	Denaturation	95 °C	30 s	} 40 x
2	Annealing	50 °C	30 s	
3	Elongation	72 °C	30 s	
4	Final elongation	72 °C	2 min	
5	Hold	4 °C	∞	

Amplified fragments were then analysed by agarose gel electrophoresis. For this purpose, 2 µl of 6 x loading dye were added to the PCR reaction mixtures and pipetted into a 1% agarose gel, containing SYBR Safe (1 : 10 000) to visualise DNA under UV light emission, in TBE buffer. The gel run was performed with a constant voltage of 100 V until the marker front had reached the end of the gel. The DNA bands were detected in a Bio-Rad ChemiDoc™ by UV light excitation. Bacteria clones with a verified plasmid insert were prepared for a Maxiprep procedure. Therefore, 100 µl bacteria suspension were pipetted into 100 ml LB medium with Ampicillin (100 µg/ml) and incubated for 16 – 18 h at 37 °C and 200 rpm. Plasmid DNA of the final bacteria suspensions were isolated with Qiagen EndoFree Plasmid Maxi Kits by following manufacturer's instructions, which bases on the principle of the alkaline plasmid extraction [163]. The isolated DNA was stored at -20 °C in TE buffer (pH 7.4)

2.2.5.2 Transfection of mammalian cell lines

Cells were seeded at a density of 500 000 cells/well in a 6-well format and were allowed to grow for 24 h. On the next day, the transfection mixture was prepared. For this purpose, 2.5 µg Plasmid-DNA and 7.5 µl Lipofectamine 2 000 reagent were diluted separately in 150 µl Opti-MEM each, to allow for optimal dilution of the DNA and the lipid-based transfection reagent. Both dilutions were combined and incubated for 5 – 10 min at room temperature to create DNA – Lipofectamine – complexes. Meanwhile, the cells were washed with PBS and new medium without antibiotics was added to the cells. The absence of antibiotics during cell transfection improves the survival rate of the cells, which are vulnerable during this process due to cellular membrane deficiencies caused by the transfection reagent. A volume of 250 µl of the transfection mixture was added into the cells, which were incubated for 24 h before starting the respective stimulation of the cells.

2.2.6 Gene expression analysis

Classical cellular processes mediated by nuclear receptors manifest by changes in the amount of mRNA content of regulated target genes. These differences in mRNA copy numbers between certain cohorts are an important measure to quantify the effects of a specific treatment and were analysed as follows.

2.2.6.1 RNA isolation and cDNA synthesis (tissue, cells)

Soft Tissue: For RNA isolation from soft tissues like liver or spleen, 20 – 30 mg of deep frozen organs were cut off into a 1.5 ml reaction tube filled with 1 ml of QIAzol lysis reagent and five lysis beads. The organ piece was then homogenised in a tissue lyse device with an impulse frequency on level 5 for 60 s. The resultant suspension was centrifuged for 15 min with 12 000 g at 4 °C and the supernatant was transferred into a new tube. The separation of nucleic acids and proteins was initiated by adding 200 µl trichloromethane (Chloroform) and gentle inverting of the tubes. After 2 – 3 min of incubation the solution was centrifuged for 15 min with 12 000 g at 4 °C and the resultant upper RNA-containing aqueous phase was transferred into a new tube. RNA precipitation was achieved by adding 500 µl of propane-2-ol (Isopropanol) and an incubation time for 10 min, followed by centrifugation for 10 min with 12 000 g at 4 °C. After discarding the supernatant, the RNA pellet was washed with 1 ml ethanol (75% v/v) and centrifuged for 7 min with 8 000 g at 4 °C. After removing the supernatant, the pellet was draught for 10 - 30 min, depending on the residual amount of Ethanol, before resolving it in 100 µL RNase-free water. Isolated RNA solution was purified with the Macherey-Nagel NucleoSpin® RNA Clean-up kit, to remove residual genomic DNA and further contaminations. For this purose, 300 µl RA1 buffer were mixed with 300 µl ethanol (100% v/v) for each sample and added to the RNA solution. The whole volume was transferred into the provided spin columns and centrifuged for 1 min with 8 000 g at room temperature. Resultant RNA was stored at - 80 °C.

Bone Tissue: For the RNA isolation of hard tissues like bone, the soft tissue-free femur and tibiae were deep frozen in liquid nitrogen and immediately added into 1 ml QIAzol. The bones were then shredded with a hard tissue lyser and undissolved fragments were removed by centrifugation for 10 min at 12 000 g at 4 °C and transferred the clear supernatant into a new reaction tube. Further isolation steps correspond to the isolation protocol for soft tissues.

Cell Culture: The relatively small amounts of applied cells, compared to tissue samples, and the high quantity of single samples required the use of the Zymo Research DirectZol RNA isolation kit. This kit allows the use of RNA, still dissolved in QIAzol, without the time-consuming chloroform and isopropanol precipitation. For this purpose, cells in a 6-well format were lysed by addition of 500 µl QIAzol. To this solution an equal QIAzol volume of ethanol (100% v/v) was

added and the mixture was transferred into the DirectZol spin columns and centrifuged for 1 min with 12000 g at room temperature. After washing the columns with 400 µl RNA washing buffer, 80 µl of the DNA digestion solution was added into the middle of the column without touching the surface and incubated at room temperature for 15 min. The DNA digestion solution consists of DNase I solution, which was diluted 1:16 with DNA digestion buffer. After DNA digestion was completed, the columns were washed twice with 400 µl RNA pre-wash buffer, followed by a final washing step with 700 µl RNA washing buffer. All washing steps were followed by a centrifugation for 1 min with 12000 g at room temperature. To remove buffer residues, the columns were transferred into a new collection tube and centrifuged for 3 min with 12000 G. After the final centrifugation, the columns were transferred into new 1.5 ml tubes and 40 µl nuclease-free water were added into the middle of the columns. Eluted RNA was stored at -80 °C.

2.2.6.2 Determination of RNA concentration

The resultant amounts of RNA were quantified by using either a ThermoFisher Scientific NanoDrop™ 2000 spectrophotometer or a BioTek® Epoch spectrophotometer with a Take3 microplate adapter. For both devices, a total volume of 2 µl sample or water as blank was used. RNA concentration for each sample was calculated with the following formula: c = OD * D * F (OD – optical density; D – path length; F – extinction coefficient; c - concentration).

2.2.6.3 cDNA synthesis by reverse transcription

For the reverse transcription of RNA into cDNA, the ThermoFisher Scientific RevertAid first strand cDNA synthesis kit was used. For this purpose, 500 – 1000 ng RNA, depending on the available amounts of obtained RNA, were pipetted into 200 µl PCR tubes and filled up with nuclease-free water up to 11 µl and 1 µl of Oligo-dT primer were added. The mixtures were warmed up to 65 °C for 5 min to open secondary RNA structures and allow for optimised primer binding at the mRNA poly-A-tails. In the meantime, the reverse transcription master mix was prepared, consisting of 4 µl 5 x reaction buffer, 2 µl dNTPs (100 mM) and 1 µl of reverse transcriptase and RiboLock, respectively. After adding the master mix to the RNA, the solution was incubated at 42 °C for 1 h to achieve complete transcription from mRNA into cDNA, followed by an incubation at 72 °C for 10 min to inactivate all involved enzymes. Finally, cDNA were diluted 1:20 in nuclease-free water and stored at -20 °C.

2.2.6.4 Quantitative real-time polymerase chain reaction

To determine the amounts of gene specific amounts of original RNA, also referred to as gene expression, a quantitative real-time polymerase chain reaction (qPCR) was used. To measure gene expression, 4 µl of cDNA were pipetted in duplicates into 96-well plates. For each target gene, a

specific master mix was necessary and consisted of 10 µl 2 x FastStart Universal SYBR green master (ROX) reaction mix, 4 µl nuclease-free water and 2 µl primer mix with 0.5 µM of forward and reverse primer. After finishing and pipetting all reaction mixtures into their specific wells, the plate was sealed with 8-tube qPCR stripes and spin down at 2500 g for 3 min. The 96-well plate was placed into a RealPlex^2 Mastercycler and the protocol for a 2-step qPCR was started, which was as follows:

Table 10 | Protocol for the 2-step qPCR

Step number	Step	Temperature	Time	
1	Initial denaturation	95 °C	10 min	
2	Denaturation	95 °C	15 s	} 40x
3	Annealing & Elongation	60 °C	60 s	
4	Melting curve	95 °C	15 s	
5		60 °C	15 s	
6		60 °C → 95 °C	20 min	
7		95 °C	15 s	

After completing the measurement with step 7 of the qPCR protocol, the plate was discarded and results were exported into a MS Excel spreadsheet.

2.2.6.5 Determination of gene expression

Gene expression of target genes was determined in relation to excessively and constantly expressed genes, termed as housekeepers. Housekeeping gene suitability was validated by a one-way ANOVA with a Holm-Sidak's multiple comparisons test to identify regulations between regarded groups and the geometric mean of at least two independent housekeeping genes was used, otherwise stated. Target gene expression was then calculated by the difference of the target gene Ct values and the mean Ct value of the housekeeping genes, called ΔCt. The Ct value represents the point in the fluorescence curve at which the transition from the linear to the exponential growth occurs and crosses a measurement-specific threshold. Since gene expression and Ct measurements are in a log-linear relationship, the ΔCt needs to get exponentiated by the efficiency of the qPCR measurement. This efficiency (E) was calculated with the slope of a standard curve for each gene separately, using the following equation: $E = 10^{(-1/slope)}$. Gene expression was further calculated as E to the power of –ΔCt: Gene expression = $E^{-\Delta Ct}$. For a proper comparison between different genes under certain conditions, the group means were divided by the mean value of a control group to normalise the gene expression and illustrate the fold changes of the gene expressions between involved groups.

2.2.7 Enzyme-linked immunosorbent assay

A fast and easy way to quantify analytes and an alternative for mass spectrometric or other sophisticated detection methods of diluted compounds from all types of body fluids or tissues lysates is the enzyme-linked immunosorbent assay (ELISA). There are several different specific ELISA techniques, suitable for many different applications, but they all share the principle of adhering either an analyte-specific mono- or polyclonal antibody or the analyte itself to the surface of a reaction chamber or a microtiter plate. By using one of numerous detection methods, a colour reaction, depending on the analyte concentration in the investigated fluid, is induced and by using a standard curve the analyte concentration can be calculated [164].

2.2.7.1 Total T_4 (tT_4)

For the detection of total T_4, including free and protein-bound T_4, the commercially available total T_4 ELISA kit from DRG was used, which bases on the principle of a competitive ELISA. This type of assays is commonly used for small antigens, like small molecules or peptides, which do not have the size to provide multiple antibody binding sites. Therefore, the surface of a 96-well microtiter plate was coated by the supplier with a monoclonal mouse anti-T_4 antibody. After pipetting 25 µl serum or standard solution as singlets into their respective wells, 100 µl of the conjugate solution were added. This conjugate solution contains horseradish peroxidase-linked (HRP-linked) T_4 to compete with serum T_4 molecules for antibody binding sites and 8-anilino-1-napthalene sulfonic acid (ANS), which is responsible for the release of protein-bound T_4 in the serum and enables the assay to determine total and not just free T_4. Since the standards and samples are pipetted first into the wells, unbound T_4 in serum has a time advantage over HRP-linked T_4 in the conjugate solution, but free T_4 accounts only for 0.03% of the total T_4 pool. Therefore, this point can be neglected. The mixture was incubated for 1 h at room temperature. This incubation step was followed by a thorough wash procedure with 5 wash steps of 300 µl distilled water per well. All remaining liquid residues had to be removed by brisk shaking on absorbent paper. In the next step, 100 µl of HRP substrate 3,3',5,5'-Tetramethylbenzidine (TMB) containing substrate solution was added and incubated for 20 min in the dark before the colour reaction was stopped with 100 µl 0.5 M Sulfuric acid (H_2SO_4). The change of the pH, induced by sulfuric acid, causes a protonation of TMB leading to a colour change from blue to yellow, which can be detected by a spectrophotometer at a wavelength of 450 nm within 15 min. The concentrations of 6 standard solutions, provided by the manufacturer, were 0, 2, 5, 10, 15 and 25 µg/dl. By taking the concentrations and their respective extinction values for standards solutions and perform a non-linear regression analysis with a substrate inhibition algorithm, the concentrations of the serum samples could be interpolated.

2.2.7.2 Total T_3 (tT_3)

The principle of the NovaTec total T_3 ELISA kit is similar to the DRG total T_4 ELISA kit described above. The primary anti-T_3 antibody is immobilised on a microtiter plate surface and T_3 has to compete with HRP-linked T_3 for free antibody-binding sites. Free T_3 accounts only for 0.3% of the total T_3 pool, therefore the time advantage over the HRP-linked T_3 can be neglected, due to a comparable principle described for the T_4 ELISA. After an incubation of 1 h at room temperature, the microtiter plate was washed 5 times with 300 µl washing buffer. The colour reaction was induced with 100 µl TMB for 15 min in the dark, stopped with 100 µl 0.5 M Sulfuric acid and detected with a spectrophotometer at 450 nm within 5 min.

2.2.8 Western blot

The term Western Blot describes a quantitative method to measure the amounts of specific proteins in a variety of biological samples. Several consecutive steps were performed, which will be explained in more detail in the sections described below.

2.2.8.1 Protein quantification

The protocol for the protein quantification used here, bases on the bicinchoninic acid assay (BCA assay) [165]. For an optimal protein determination and a secure storage, proteins were kept in lysis buffer, which consists of modified RIPA buffer + 1 mM phenylmethylsulfonyl fluoride (PMSF). To obtain sufficient amounts of protein, 10 mg tissue or one fully covered 75 cm^2 cell culture flask were needed. For tissue samples, 5 ceramic beads together with 100 µl lysis buffer and tissue sample itself were given into screw cap tubes and lysed for 30 s at medium level in a tissue lyser. Cells from cell culture flasks were removed with a cell scraper, lysed in 100 µl lysis buffer and collected in a new 1.5 ml reaction tube. Lysed tissue or collected cells were centrifuged for 15 min with 13 000 rpm at 4 °C and protein containing supernatant is then transferred into a new 1.5 ml reaction tube. For the BCA assay, 5 µl of the protein solution and the standard solutions are pipetted into a 96-well plate in duplets. The BCA solution needs to be prepared directly before measurement by mixing bicinchoninic acid with copper sulphate ($CuSO_4$) at a ratio of 51 : 1 and 100 µl of the final BCA solution is added to the protein and standard solutions and incubated for 30 min at 37 °C. After incubation has finished, the plate is cooled for 15 min at 4 °C before measuring the extinction at 562 nm in a spectrophotometer. The concentration of the protein solution is calculated by interpolating a non-linear fitting hyperbola of the standard solutions in a range between 25 – 0.78 mg/ml.

2.2.8.2 Sodium dodecyl sulphate polyacrylamide gel electrophoresis

The principle used here for the sodium dodecyl sulphate polyacrylamide gel electrophoresis (SDS-PAGE) bases on standard protocol introduced by Ulrich Lämmli [166]. TGX Stain-free cast gels were prepared in advance by combining 4.5 ml of Resolver A and B with 45 µl Ammonium persulphate (10 % m/v) and 7.5 µl Tetramethylethylenediamine (TEMED) for the final separation gel. Directly after the separation gel was poured into a casting mould with 1.5 mm in diameter and 10 cm in length, the stacking gel was prepared by combining 1.5 ml Stacker A and B with 15 µl APS and 4.5 µl TEMED and poured directly upon the unpolymerised separation gel and the ridge for the sample pockets was placed at the top of the casting mould. The fully polymerised gel can be stored wrapped in wet tissue at 4 °C for one week.

The total amount of protein used for western blot depended on the target protein and its abundance in the target cells in a range between 25 – 50 µg per lane. Protein solutions were diluted with lysis buffer to allow for a volume of 15 µl per lane in a 15-lane gel. For the final protein preparation, 4x sample buffer was added and the protein solutions were heated at 98 °C for 10 min. The prepared gels were fixed in the gel apparatus, before filling the apparatus with running buffer. First and/or last lane were loaded with PageRuler marker followed by fully prepared protein samples. The power supply was set to 120 V and the run was stopped when the sample buffer front line reached the bottom end of the gel.

2.2.8.3 Blotting

When SDS-PAGE approximates its end, polyvinylidene difluoride (PVDF) membrane were equilibrated in methanol for 1 min and afterwards washed with distilled water before finally kept in blotting buffer. The SDS-PAGE gel was extracted from the apparatus and unloaded areas together with the stacking gel were removed. For the later total protein normalisation, it is necessary to activate the stain-free trihalo compound by irradiating the gel with UV light for 60 s to form covalent trihalo - tryptophan bonds on proteins, which develop an UV light-inducible fluorescence for detection on the membrane [167]. During this activation step the blotting apparatus was prepared by equilibrate the filter tissues in blotting buffer and position the membrane onto the cathode-oriented filter tissue. The SDS-PAGE gel is placed straight on the PVDF membrane and the anode-oriented filter tissue is placed free of air bubbles onto the gel before the whole blotting apparatus is closed and locked and filled with blotting buffer. To avoid over-heating, an ice block was used and constant stirring allows a sufficient temperature exchange within the apparatus. The blotting process was started by applying 100 V for 1 h. Afterwards the apparatus was dismantled and a picture of the whole protein on the membrane was taken by exposing the membrane to UV light in the gel documentary device. The membrane was then ready for antibody staining.

2.2.8.4 Antibody staining

Unspecific binding sites on membrane-bound proteins were blocked by incubating for 1 h in dry-milk solution (5% m/v in TBS-T). The antigen-specific primary antibody was diluted, as mentioned in the materials section, in 5 ml dry-milk solution and put, together with the blocked membrane, into a 50-ml falcon tube and incubated on a shaker over night at 4 °C. At the next day, the membrane was washed with TBS-T five times for 10 min each before it was incubated in 25 ml secondary antibody solution at room temperature for 1 h. The secondary antibodies were reactive against epitopes occurring in primary antibody producing host antibodies and were coupled with HRP. The membrane was subsequently washed 5 times for 10 min with TBS-T and then ready to take a chemiluminescence picture. For this purpose, the Clarity Max kit from Bio-Rad was used, which bases on the principle of enhanced chemiluminescence (ECL), where the antibody-bound HRP catalyses the conversion of a light-emitting substrate. This reaction is enhanced by the presence of several phenols and depends directly on the amounts of bound antibodies, which in turn directly depends on the amounts of recognised target protein on the membrane. The emitted light signal, to draw conclusion about target protein abundance, was measured by a gel documentary device. After taking the ECL picture of the membrane, the intensity of the signal band was normalised by diving it by the total protein intensity for the respective lane. The result is a value with an arbitrary unit, which can be compared with control or treated groups. If necessary, bound antibodies were removed by an incubation with stripping buffer for 15 min at room temperature, followed by an incubation in 5% dry milk in TBS-T for 1 h at room temperature. The membrane was then prepared for another primary antibody staining as described above. Otherwise, the membrane can be stored in TBS-T at 4 °C.

3 Results

3.1 Identification of circulating thyroid hormone target genes

Identification and validation of TH dependent biomarkers in humans is challenging, due to high inter-individual differences of physiological TH metabolism and the sparse tissue sample availability on the one side and a clear definition of the duration and extend of thyroid dysfunction on the other. Therefore, the present search for potential new targets started by analysing plasma proteome data sets of humans and wild type mice under the conditions of an experimentally induced thyrotoxicosis to identify concordantly altered proteins. To minimise the influence of inter-individual variances on the proteome data sets, the human trials were planned as longitudinal studies with three sampling time points for each volunteer.

3.1.1 Induced thyrotoxicosis in human and mice

The initial step in target identification was the analysis of data sets of two previously conducted studies. In the first study, 16 healthy volunteers received an oral single daily dose of 250 µg L-T_4 for eight weeks followed by an eight-week recovery period without T_4 intake. Blood samples were drawn at the first day of administration and at the last days of the administration and recovery period [128]. In the second study, mice were rendered hyperthyroid by adding T_4 at 1 mg/l in the drinking water for two weeks compared to control mice with no treatment. A third group within this study, similar to the human study, underwent the T_4 treatment followed by a recovery period for two weeks. Blood samples and liver tissues from all groups were taken after sacrifice of the animals at their respective experimental endpoints [168].

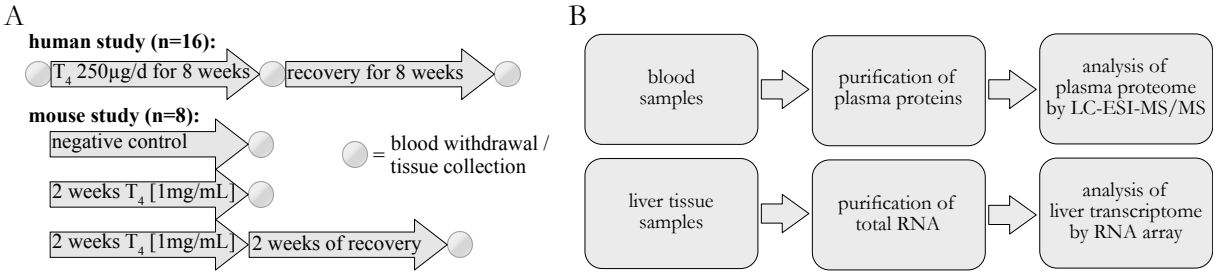

Figure 5 | Design of human and mouse thyrotoxicosis studies. (A) Schematic overview of the human and mouse study for Omics comparison of baseline, hyperthyroid and recovery state. (B) Blood and liver tissue samples were processed as indicated and described in more detail in the methods section to determine plasma proteome and liver transcriptome for target identification.

The obtained plasma proteome data sets were combined in a MySQL database and the source code for this procedure can be found in the Appendix section on page 112. After excluding proteins that did not met the exclusion criteria of a p-value < 0.05 and a fold change $> |1.5|$ the human plasma proteome data set revealed 148 proteins with altered abundance before and after the

treatment, which normalised after the recovery period, while in mice 167 proteins were found with p-value < 0.05 and fold change > |1.05| as exclusion criteria, as illustrated in **Figure 6A**. As shown in **Table 11**, 32 common proteins between these data sets could be identified, of which 16 were concordantly regulated. These 16 proteins were Angiotensinogen (ANGT), Apolipoproteins A1, B, C3, C4 and D (APOA1, APOB, APOC3, APOC4 and APOD), Abnormal spindle-like microcephaly-associated protein (ASPM), CD5 antigen-like peptide (CD5L), Cathelicidin antimicrobial peptide (CAMP), Fibulin-1 (FBLN1), Fetuin A (FETUA), Interleukin-1 receptor accessory protein (IL1AP), Lumican (LUM), Peptidoglycan recognition protein 2 (PGRP2), Transthyretin (TTR) and Vascular cell adhesion protein 1 (VCAM1). The high metabolic activity of the liver, together with its long-known high dependence on TH serum concentrations predestined this tissue as a major source for TH dependent circulating proteins [60, 169, 170]. Hence, the liver transcriptome of thyrotoxic mice compared to untreated or recovered mice transcriptome data, was used to identify liver specific targets and highlight these proteins as high priority targets. The comparison of the 16 identified plasma targets with the list of regulated liver transcripts, which was created by using a p-value < 0.05 and a fold change > |1.05| as inclusion criteria, identified three genes (*Cd5l*, *Il1ap* and *Ttr*) with a common regulation profile as shown in **Figure 6B**. The heatmap, depicted in **Figure 6C**, visualises the effect sizes as fold change of target gene expression and highlights the targets that were also found to be regulated in liver transcriptome with the black rectangle.

Table 11 | Shared proteins between human and mouse plasma proteome

protein name	RefSeq accession number		fold change (control vs. T_4 group)				concordance of abundance alteration
	human	mouse	human	p-value	mouse	p-value	
AMPB	NM_001633; NP_001624	NM_007443; NP_031469	1,79	7,313E-03	-1,62	6,833E-03	no
ANGT	NM_000029; NP_000020	NM_007428; NP_031454	-1,58	3,788E-02	-1,37	9,583E-04	yes
APOA1	NM_000039; NP_000030	NM_009692; NP_033822	-1,46	4,146E-02	-1,48	1,400E-06	yes
APOB	NM_000384; NP_000375	NM_009693; NP_033823	-1,99	2,017E-03	-2,80	2,512E-10	yes
APOC3	NM_000040; NP_000031	NM_023114; NP_075603	-2,19	1,728E-02	-1,88	1,046E-04	yes
APOC4	NM_001646; NP_001637	NM_007385; NP_031411	-2,08	5,670E-03	-4,61	5,515E-04	yes
APOD	NM_001647; NP_001638	NM_007470; NP_031496	-2,77	7,444E-04	-3,10	8,990E-06	yes
ASPM	NM_018136; NP_060606	NM_009791; NP_033921	2,30	2,017E-03	2,00	6,452E-04	yes
CD5L	NM_005894; NP_005885	NM_009690; NP_033820	1,73	1,806E-02	1,77	5,126E-03	yes
CFAH	NM_000186; NP_000177	NM_009888; NP_034018	1,61	2,656E-02	-1,24	3,121E-03	no
CFAI	NM_000204; NP_000195	NM_007686; NP_031712	1,45	3,615E-02	-1,72	1,781E-06	no
CHLE	NM_000055; NP_000046	NM_009738; NP_033868	1,84	1,419E-02	-8,11	1,826E-05	no
CO3	NM_000064; NP_000055	NM_009778; NP_033908	1,49	3,313E-02	-2,36	2,931E-08	no
CO8A	NM_000562; NP_000553	NM_146148; NP_666260	1,23	7,679E-04	-1,39	6,003E-06	no
CO8B	NM_000066; NP_000057	NM_133882; NP_598643	2,03	2,017E-03	-1,40	3,270E-06	no
CO8G	NM_000606; NP_000597	NM_027062; NP_081338	2,44	1,350E-03	-1,33	6,683E-05	no
CAMP	NM_004345; NP_004336	NM_009921; NP_034051	-2,67	9,352E-03	-15,04	2,515E-08	yes
FA9	NM_000133; NP_000124	NM_007979; NP_032005	1,98	5,419E-03	-1,80	2,958E-02	no
FBLN1	NM_006486; NP_006477	NM_010180; NP_034310	1,74	1,061E-02	1,31	9,959E-05	yes
FETUA	NM_001622; NP_001613	NM_013465; NP_038493	1,77	1,187E-02	1,25	3,523E-02	yes
IC1	NM_000062; NP_000053	NM_009776; NP_033906	1,64	2,030E-02	-2,42	1,393E-06	no
IL1AP	NM_002182; NP_002173	NM_008364; NP_032390	-2,75	4,671E-03	-1,54	3,370E-05	yes
ITIH1	NM_002215; NP_002206	NM_008406; NP_032432	1,65	1,808E-02	-1,70	1,956E-04	no
LUM	NM_002345; NP_002336	NM_008524; NP_032550	2,20	2,017E-03	1,45	2,754E-03	yes
MASP2	NM_006610; NP_006601	NM_001003893; NP_001003893	3,07	1,350E-03	-1,27	8,329E-04	no
NCAM1	NM_181351; NP_851996	NM_001081445; NP_001074914	-2,07	3,056E-02	1,67	1,264E-02	no
PEDF	NM_002615; NP_002606	NM_011340; NP_035470	1,98	6,288E-03	-1,19	3,274E-02	no
PGRP2	NM_052890; NP_443122	NM_021319; NP_067294	1,84	5,419E-03	1,51	7,946E-05	yes
SODE	NM_003102; NP_003093	NM_011435; NP_035565	-1,53	2,966E-02	1,34	4,242E-02	no
TTR	NM_000371; NP_000362	NM_013697; NP_038725	-1,61	2,805E-02	-2,17	1,958E-03	yes
VCAM1	NM_001078; NP_001069	NM_011693; NP_035823	2,75	1,631E-02	1,52	4,397E-04	yes
ZA2G	NM_001185; NP_001176	NM_013478; NP_038506	1,75	1,419E-02	-1,51	9,856E-04	no

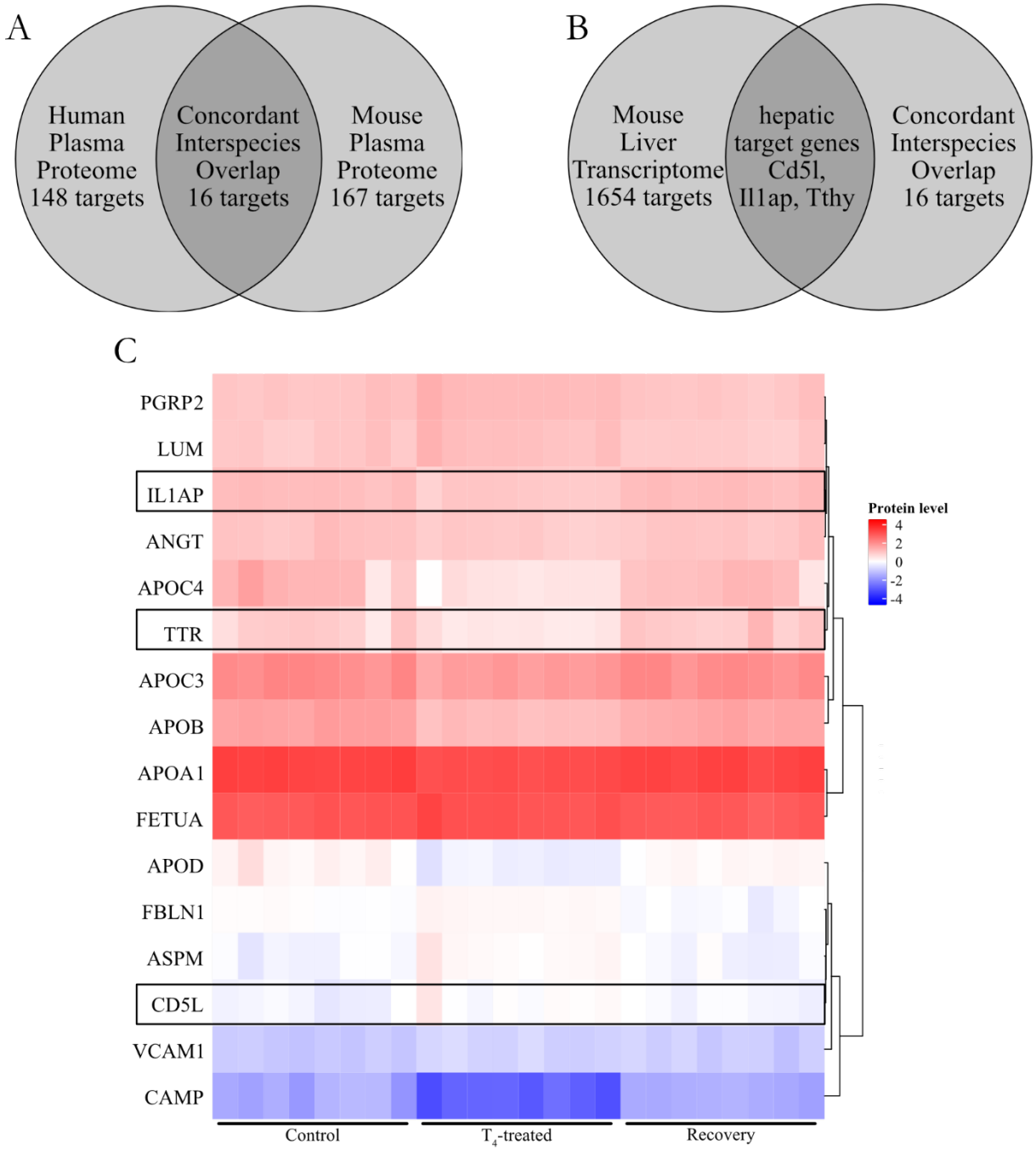

Figure 6 | Overlap of regulated targets in human and mouse plasma and liver tissue by TH. (A) Overlap of concordantly altered plasma proteins between human and mouse upon acute thyrotoxicosis revealed 16 targets. (B) Overlap of the 16 identified plasma targets with the hepatic transcriptome revealed 3 shared proteins. (C) Heat map of the expression levels of the 16 plasma protein targets. The proteins highlighted with black rectangles were also found regulated in the liver transcriptome.

For further validation of the identified target genes, the gene expression atlas[2] of the European Bioinformatics Institute (EBI) was used and the four highest target gene expressing organs are listed in **Table 12**.

Table 12 | Organs with highest target gene expression

target gene	*Angt*	*Apoa1*	*Apob*	*Apoc3*	*Apoc4*	*Apod*	*Aspm*	*Cd5l*
expressing organ	liver	liver	liver	liver	liver	brain	bone	liver
	kidney	colon	colon	colon	adrenal	heart	spleen	spleen
	lung	kidney	kidney	kidney	kidney	lung	thymus	bone
	adrenal	brain	intestine	brain	brain	intestine	lymph node	thymus

target gene	*Camp*	*Fbln1*	*Fetua*	*Il1ap*	*Lum*	*Pgrp2*	*Tthy*	*Vcam1*
expressing organ	liver	lung	adrenal	liver	bone	liver	liver	bone
	bone	heart	stomach	lung	adrenal	colon	brain	testis
	spleen	colon	liver	bone	ovary	lung	colon	ovary
	thymus	bone	intestine	brain	skin	thymus	kidney	spleen

The search in the gene expression atlas revealed the liver, as expected, as the organ with the highest expression potential for 10 out of the 16 target genes, which includes the three targets from the liver transcriptome data set as well. Besides liver, spleen showed a high potential in target gene expression and was therefore also taken into account for further target gene validations. Surprisingly, bone as a tissue with a predominant TRα abundance, was found to be the primary origin for *Aspm, Lum* and *Vcam1* expression and shared to the same extent as the liver, highest expression levels for *Camp* expression. These three tissues were now regarded as the first priority tissues for target gene expression and were investigated to far more detail during the following studies.

3.1.2 Thyroid hormone target genes in biological context

To improve the understanding of the connection between THs and the discovered regulated genes, a gene ontology (GO) analysis was conducted using the PANTHER GO-slim tool[3] to determine the likelihood of protein functions on the biological, cellular and molecular level. The functions were sorted by p-values, indicating their statistical significance in the context of the whole subset of regulated proteins. The results of this analysis are shown in **Figure 7**.

[2] https://www.ebi.ac.uk/gxa/home
[3] http://pantherdb.org (Version 14.1)

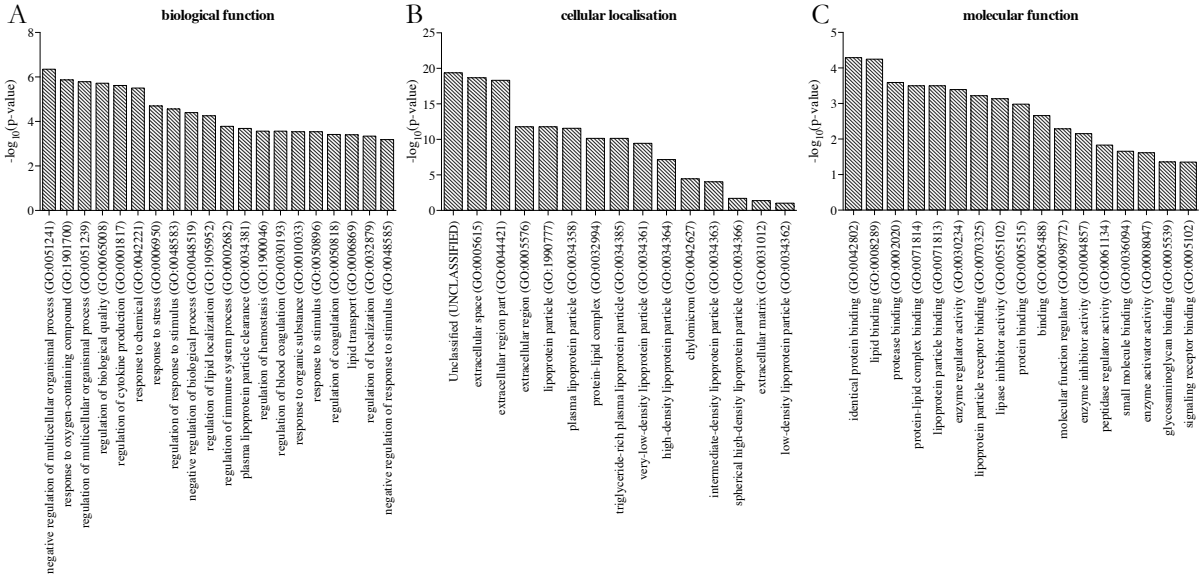

Figure 7 | Gene Ontology analysis of mouse plasma proteins upon transient thyrotoxicosis. (A) Statistically significant regulated biological functions by TH regulated mouse plasma proteins. (B) Statistically significant regulated cellular functions by TH regulated mouse plasma proteins. (C) Statistically significant regulated molecular functions by TH altered mouse plasma proteins.

Although the GO analysis was not invented to be a quantitative measure to determine the exact effect size of a factor on the distinct biological, cellular or molecular function, it can give first indications of what might be influenced by this factor or how this contributes to certain phenotypes. Here, the GO analysis revealed that the proteins found are most likely tissue-originated proteins, since 12 of 20 biological functions are related to multicellular organisation, responses to cellular stress or handling of lipids and only 5 functions were related to blood cells or blood cell functions. For the cellular function, this is even more clear, since 14 of 15 functions are in the context of extracellular lipids or apolipoproteins, while the molecular functions were more diverse and unspecific, but even here 6 of the 10 most significant function were related to lipids or lipoproteins. Taken all of these functions together, they indicate a pronounced role of secreting tissue cells which are also involved in some way either in lipid metabolism and/or stress response.

3.2 Validation of thyroid hormone targets in hypo- and hyperthyroid mice

Using additional transient intervention studies in mice, we aimed to further validate putative TH-dependent target genes and their specificities for TH concentrations.

3.2.1 Acute thyrotoxicosis and hypothyroidism for two weeks

For the validation of target gene TH-dependence, an additional mouse study was conducted. In this study, BL6 mice (n=6) were rendered hyperthyroid by administering T_4 (1 mg/l) or T_3

(0.5 mg/l) in the drinking water for two weeks. The treatment with T_4 was in accordance with the previously conducted study for a better comparability of the results [168], which induced an increase of circulating tT_4 of about 2.5-fold. The treatment with T_3 was used to identify potential ligand-specific differences in target gene expression and results in an approximate 10-fold increase of serum tT_3. Of note, the increase of tT_3 by exogenous application, results in a downregulation of TRH and TSH release and subsequently a decrease in peripheral T_4 concentration, whereas exogenous T_4 application results in an increase of tT_4 and tT_3, since the administered T_4 will be deiodinated into T_3 by intracellular DIO1 and DIO2 [31]. Another group of BL6 mice (n=6) was rendered hypothyroid by administering a mixture of the thyrostatic drugs methimazole (MMI; 0.1% m/v) and sodium perchlorate (0.2% m/v) in the drinking water for three weeks. In contrast to the thyrotoxic groups, these mice were treated for an additional week to ensure for the complete wash out of residual TH. Wild type BL6 mice (n=8) of the same age were kept for same period and served as a negative control for the treated groups. A schematic overview of the study is shown in **Figure 8A**. The effect of the respective treatment on peripheral TH concentration was verified by measuring tT_3 and tT_4 in the serum with commercially available ELISA kits and the results are illustrated in **Figure 8B+C**. The MMI/ClO_4^--treated animals had significantly reduced concentrations of tT_3 as well as tT_4 and can therefore be regarded as hypothyroid during the study, although higher effect sizes were expected as compared to previous studies [21]. The water intake of the mice, as a measure for the efficiency of the treatment shown in **Figure 8D**, stayed constant over the study in control and T_4-treated mice, while there was a slight but constant increase in the T_3-treated mice group without reaching statistical significant difference compared to the control group. The MMI/ClO_4-treated mice showed a reduced water intake during the first week of the treatment, which evolved into a periodically fluctuating pattern during the second week of the treatment. This repellent drinking behaviour every other day could be remedied by daily changes of the drinking water, which also increased the water intake on the level of control mice for the last week of the treatment.

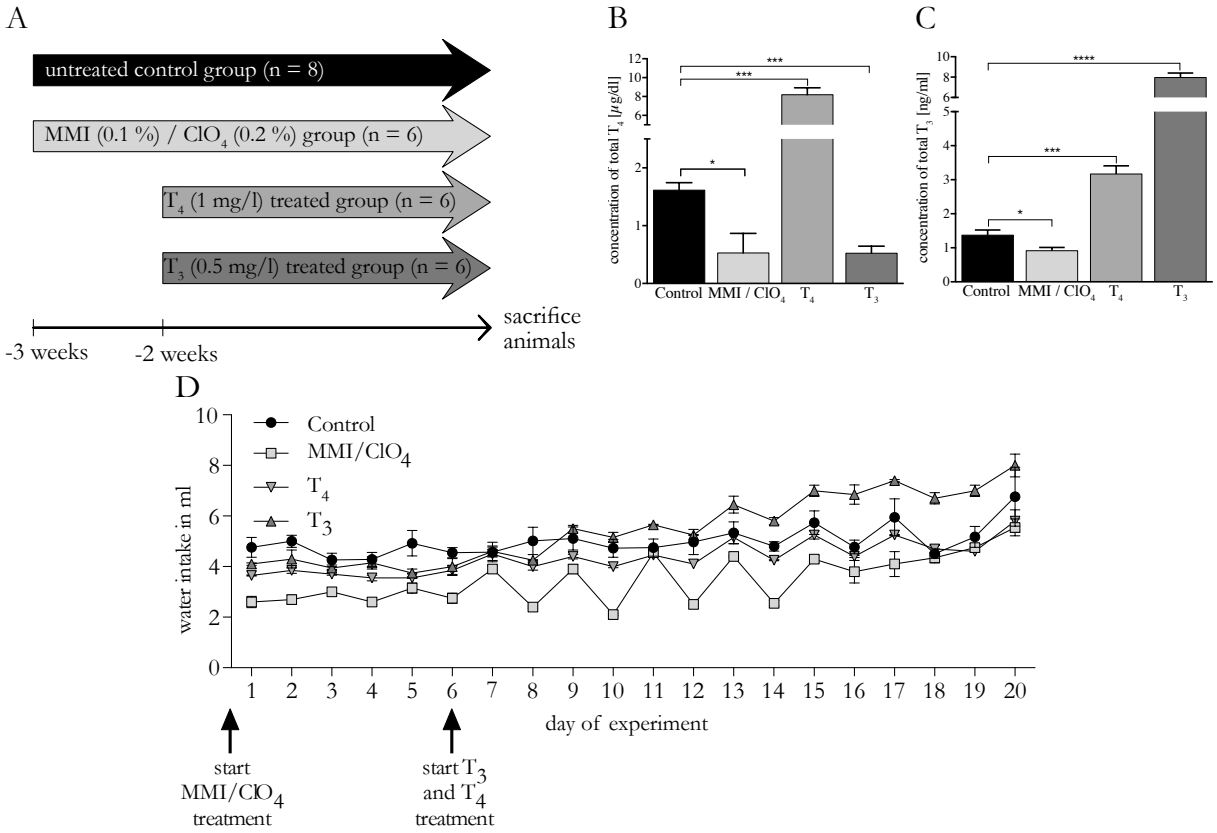

Figure 8 | Intervention study for 2 weeks with hypo- and hyperthyroid groups. (A) Schematic depiction of the intervention study for 2 weeks with one hypothyroid group treated with methimazole (MMI; 0.1%) and $NaClO_4$ (0.2%) in the drinking water for three weeks, and two hyperthyroid groups treated with either L-Thyroxine (T_4; 1 mg/ml) or 3,3',5-triiodothyronine (T_3; 0.5 mg/ml) in the drinking water for two weeks. (B) Measurement of total T_4 in the serum of the mice by ELISA. (C) Measurement of total T_3 in the serum of the mice by ELISA. (D) Water intake per mouse during treatment per day. Statistically significant differences between groups were determined with a One-way ANOVA and Holm-Sidak Post-hoc test for D, or an unpaired two-tailed Student's t-test with Welch's correction and was considered significant at $p<0.05$ (*), $p<0.01$ (**), $p<0.001$ (***) and $p<0.0001$ (****) for B+C. Values are illustrated as mean ± SEM.

After sacrificing the animals, RNA from deep frozen liver, spleen and bone tissues was isolated and reverse transcribed into cDNA for subsequent qPCR analyses to determine target gene expression. As depicted in **Figure 9A**, gene expression of already described TH-dependent genes Thyroid hormone response protein (*Thrsp* or *Spot14*) and deiodinase 1 (*Dio1*) was determined and revealed a strong induction in the hyperthyroid groups with a grading between T_4- and T_3-treated animals, in accordance with the determined TH concentrations. The induction of a hypothyroid state by MMI/ClO_4^--treatment resulted in a significant reduction of *Dio1* expression, while *Spot14* only tended to be decreased. Under hyperthyroid conditions changes in hepatic gene expression were found in *Apoc3*, *Apoc4*, *Cd5l*, *Lum* and *Vcam1*, with a grading between T_4 and T_3 in *Apoc3*, *Cd5l* and *Lum*. The induction of hypothyroid conditions altered the hepatic gene expression significantly of *Apoa1*, *Apoc3*, *Fetua*, *Lum* and *Pgrp2*. As mentioned above, the metabolic and secretory activity of the liver emphasise this tissue for biomarker research, since 14 of the 16

identified target genes were expressed there. The activity of spleen and bone to express secreted factors was lower, which is displayed by the expression of only six target genes, respectively. In spleen, only the hypothyroid state induced significantly alterations in gene expression of *Cd5l* and *Vcam1*, although T_3-treated spleen also tended to show increased *Cd5l* expression, as shown in **Figure 9B**. In bone, solely *Cd5l* showed a response in gene expression upon T_3 treatment, as depicted in **Figure 9C**.

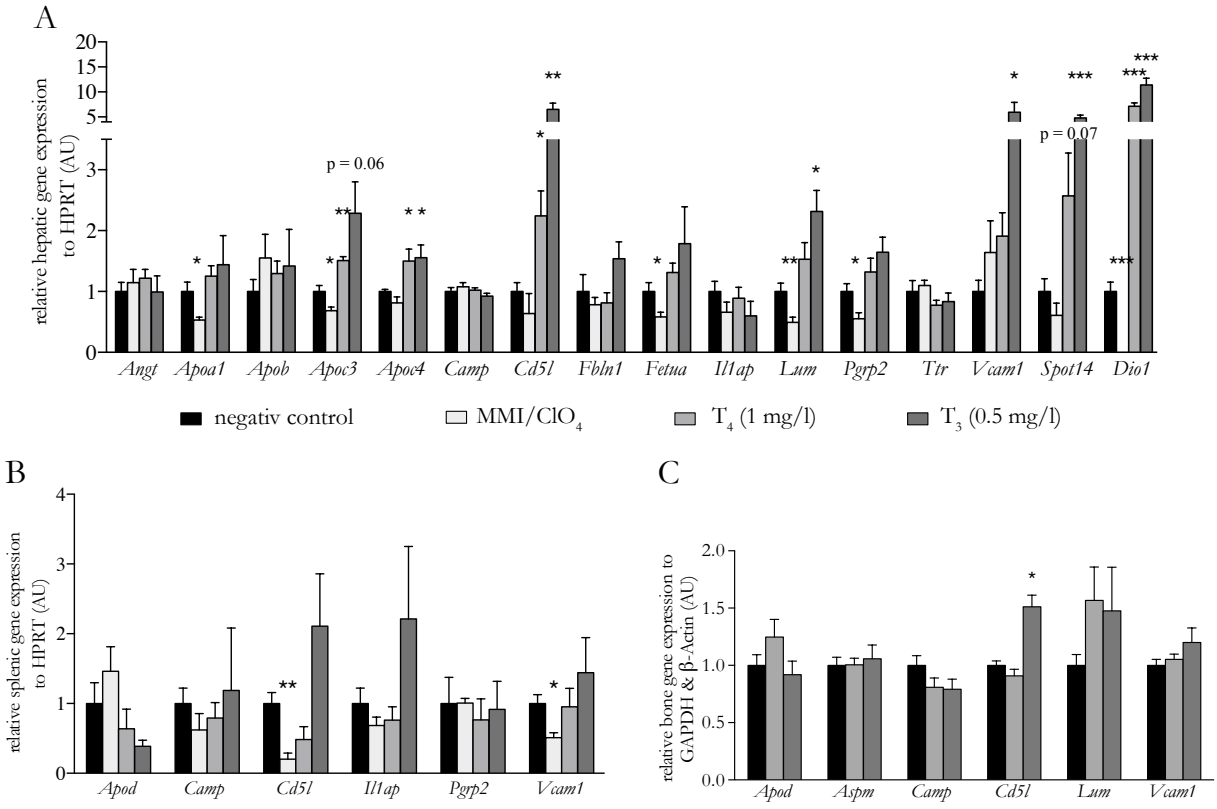

Figure 9 | Target gene expression after acute thyrotoxicosis or hypothyroidism. (A) Determination of target gene expression by qPCR in the liver. (B) Determination of target gene expression by qPCR in the spleen. (C) Determination of target gene expression by qPCR in the bone. Statistically significant differences between groups were determined with an unpaired two-tailed Student's t-test and Welch's correction and was considered significant at $p<0.05$ (*), $p<0.01$ (*) and $p<0.001$ (***). Relative expression values are illustrated as mean ± SEM. n=6-8.

The vast majority of the identified target genes was expressed in the liver and showed a significant TH-dependence. To dissect these effects furthermore, a Pearson correlation was performed for gene expression of each gene for the individual animal with its respective tT_3 or tT_4 concentrations. Of the 14 expressed genes, 5 showed a significant correlation with serum tT_3 and tT_4, which were *Apoc3*, *Apoc4*, *Cd5l*, *Fetua* and *Lum*, and one gene (*Vcam1*) showed a correlation exclusively with tT3, as depicted in **Figure 10A-L**. For the correlation of the target gene expression with its tT_4 concentrations, the T_3-treated group had to be excluded, due to the fact that the treatment with T_3 leads to a reduction of serum tT_4 levels, which does not reflect the hyperthyroid state in these animals anymore and therefore falsifies the correlation.

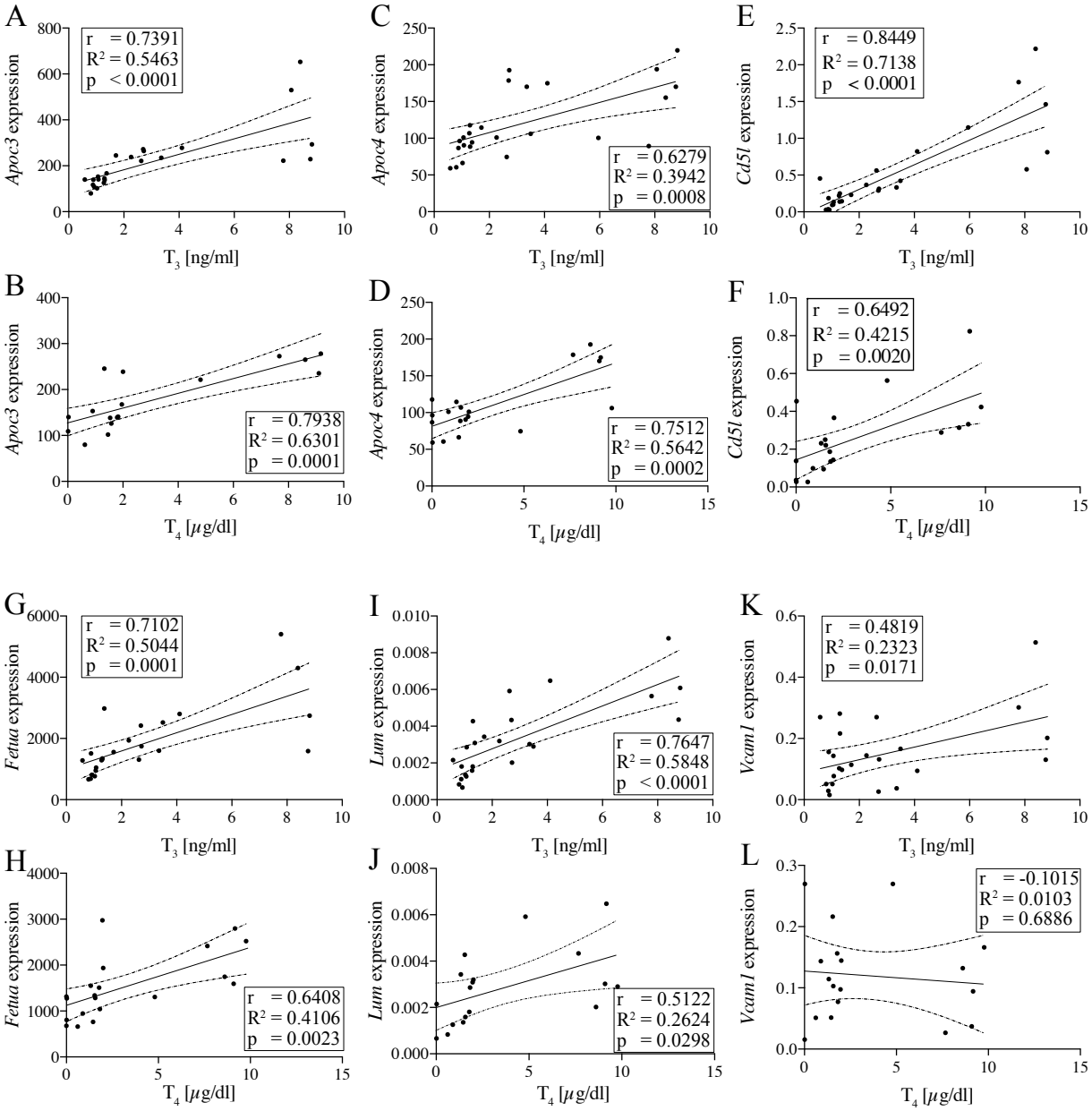

Figure 10 | Correlations of significantly altered target genes with TH concentrations. (A, C, E, G, I, K) Pearson correlation of target gene expression against the respective tT_3 concentration. (B, D, F, H, J, L) Pearson correlation of target gene expression against the respective tT_4 concentration. r – Pearson correlation coefficient; R^2 – coefficient of determination; p – p-value; dashed lines indicate 95% confidence interval.

To test whether the observed changes on mRNA expression would also be reflected on the protein level, we used Western Blot for CD5L, as this was the only gene which showed alterations in gene expression across all investigated tissues. For the validation ceruloplasmin (CP) was used which had been described as a liver-secreted protein with a high dependence on peripheral TH concentrations [171]. The detection of protein in mouse serum was determined by Western Blot analysis as shown in **Figure 11A.** Surprisingly, despite a small but not significant decrease in MMI/ClO_4^--treated mice, CD5L was reduced in T_4-treated mice and only slightly increased in

T_3-treated mice. In accordance to the previously conducted study, CP showed no changes under hypothyroid conditions, but was increased after TH administration.

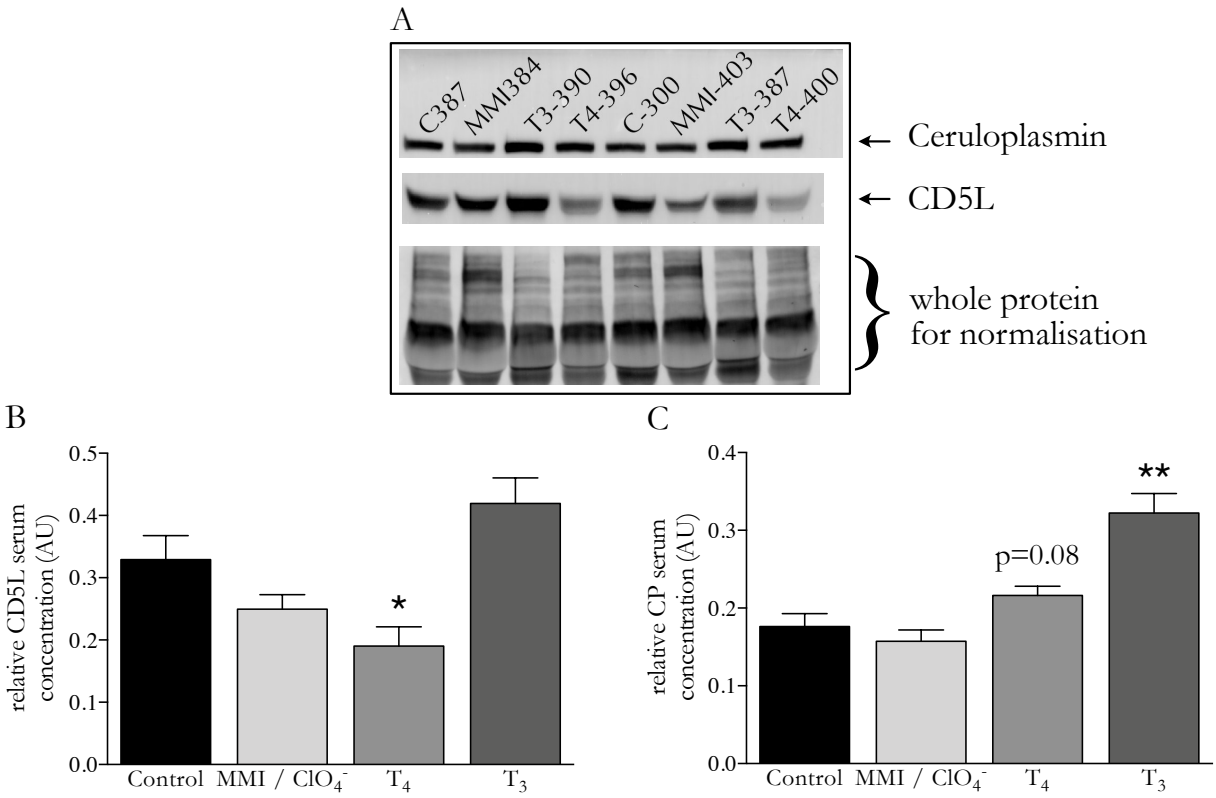

Figure 11 | Serum protein concentrations of CD5L and CP after 2-week treatment. (A) Representative Western Blot of 2µl undiluted mouse serum per sample incubated with goat anti-CP or rat anti-CD5L antibody and normalised to stain-free whole protein. (B) Western Blot analysis of rat anti-CD5L against whole protein for the respective group. (C) Western Blot analysis of goat anti-CP against whole protein for the respective group. Statistically significant differences between groups were determined by an unpaired two-tailed Student's t-test with Welch's correction and were regarded and illustrated as statistically significant when $p < 0.05$ (*) and $p < 0.01$ (**). Values are represented as mean ± SEM. n=6-8.

The effects of CD5L and CP secretion were further investigated by Western Blot analysis of liver tissue as their suspected origin. As shown in **Figure 12A**, liver homogenates were stained, after blotting, with goat anti-CP and rat anti-CD5L antibodies and normalised against stain-free whole protein. In accordance to the serum content, **Figure 12B** shows CD5L abundance as decreased in all groups compared to control group and for the T_4-treated group this effect was statistically significant. Conversely, **Figure 12C** shows the expected protein content of CP with a graduated increase under hyperthyroid conditions, despite unchanged protein concentration in MMI/ClO_4^--treated. The Western Blot analyses of CP protein abundance in serum and liver confirm the hypo- and hyperthyroid conditions within these tissues, as this protein has been described as TH-dependent before [171], at least under hyperthyroid conditions. In contrast to the results from plasma proteomics and liver mRNA determinations, which imply a direct correlation between TH and CD5L concentration, CD5L was decreased in liver and serum under T_4 treatment by Western Blot analysis, while the residual treatments induced no significant changes.

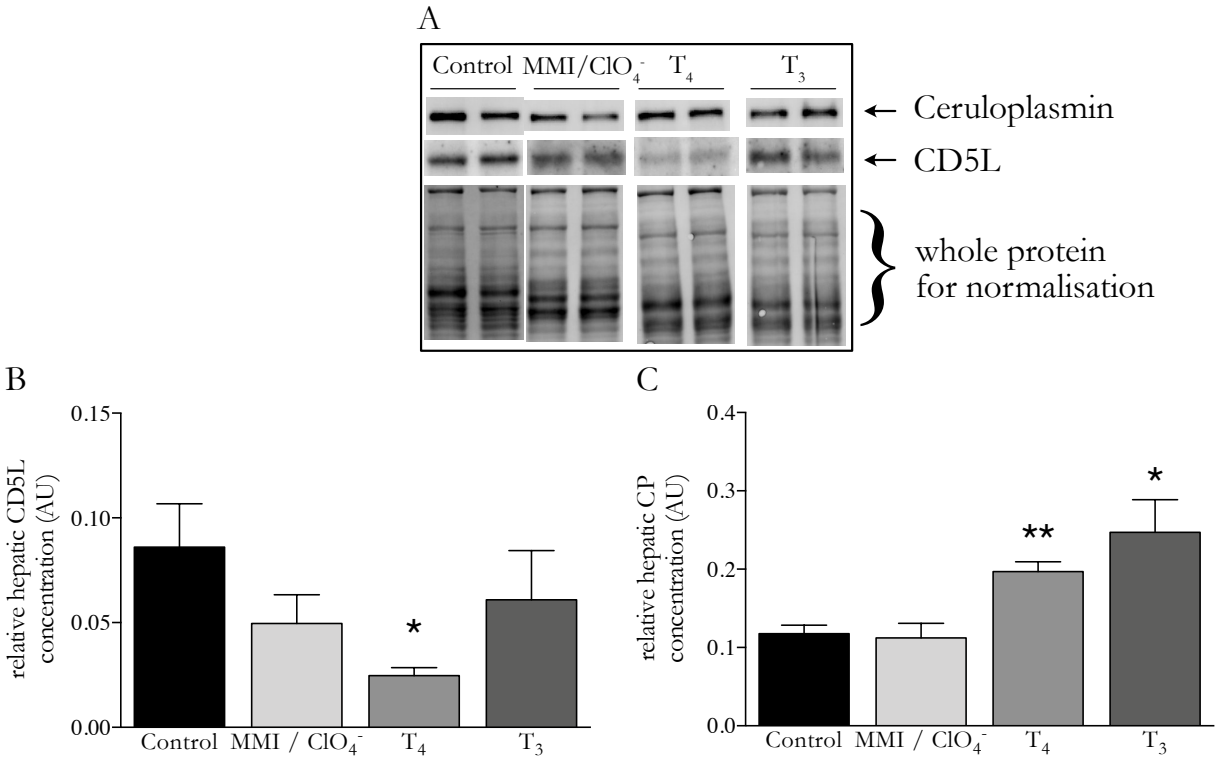

Figure 12 | Liver protein concentrations of CD5L and CP after 2-week treatment. (A) Representative Western Blot of 10 mg mouse liver tissue per sample incubated with goat anti-CP or rat anti-CD5L antibody and normalised to stain-free whole protein. (B) Western Blot analysis of rat anti-CD5L against whole protein for the respective group. (C) Western Blot analysis of goat anti-CP against whole protein for the respective group. Statistically significant differences between groups were determined by an unpaired two-tailed Student's t-test with Welch's correction and were regarded and illustrated as statistically significant when $p < 0.05$ (*) and $p < 0.01$ (**). Values are represented as mean ± SEM. n=6-8.

3.2.2 Acute short-term thyrotoxicosis

The kinetics of TH-responsive genes has been determined by other groups in advance and they reported very fast responses of *Dio1* within six hours which last for weeks [172, 173]. Therefore, the kinetics of the identified target genes should be determined to detect putative contrary effects in the adaption phase of the thyrotoxic state and to outline rational timeframes for usage of future biomarkers. For this purpose, another animal study was conducted with a control group, one group treated with T_3 for one day and one group treated with T_4 for four days, as schematically represented in **Figure 13A**. **Figure 13B+C** illustrate the serum concentrations of tT_3 and tT_4 of the respective groups. For the T_4 treatment, the resultant values were in the expected range with an approximately 2.5-fold increase of tT_4. The T_3 treatment worked exceedingly successful, since tT_3 values were approximately 20-fold increased, instead of the planned 10-fold increase. The reason for this effect can be found in **Figure 13D**, where the water intake of all animals is visualised. While the water intake of the control and T_4-treated animals stayed unchanged during the experiment, the T_3-treated animals drank 50% more upon administration. As this was not

observed over the course of the first two weeks lasting study and no chemicals or concentrations were changed, the reason for this behaviour could not be explained, but the animals were definitely hyperthyroid and thus subsequently analysed.

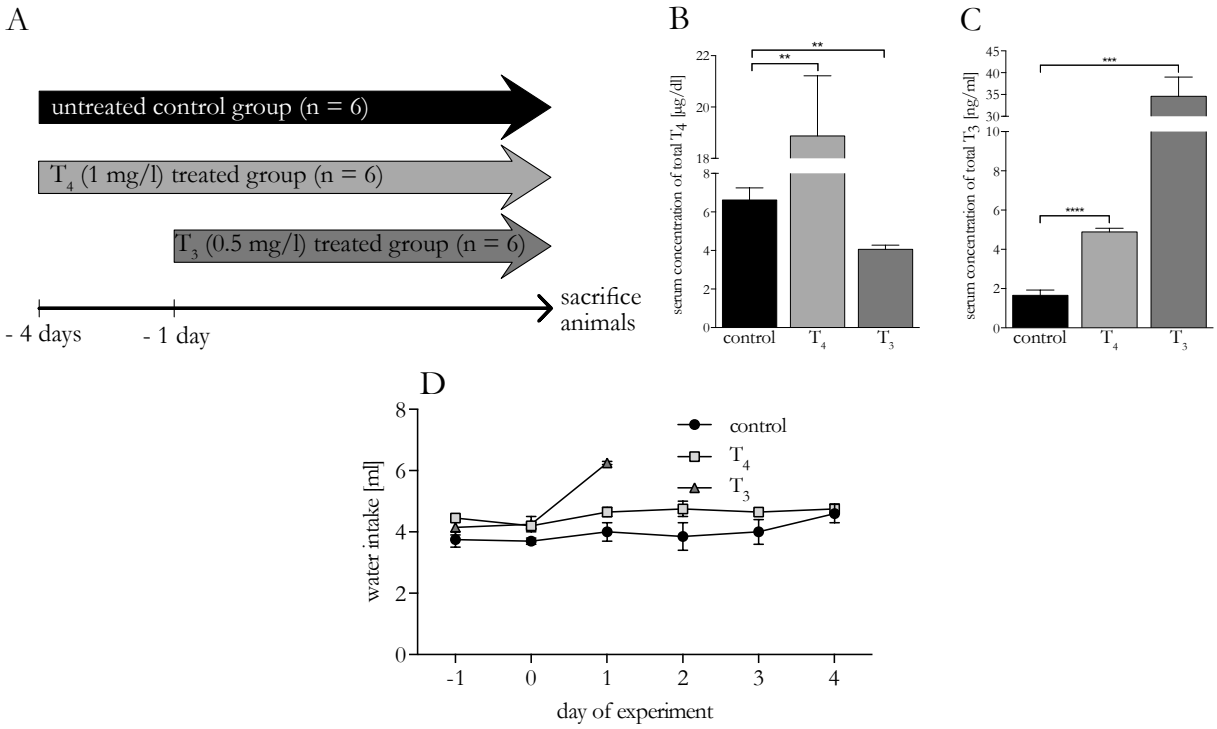

Figure 13 | Short-term intervention study with T_4 for 4 days or T_3 for 1 day. (A) Scheme of the short-term intervention study with wild type C57BL/6NCrl mice. The T_4 group was treated with 1 mg/l T_4 in the drinking water for four days, while the T_3-treated animals received the administration for 1 day. (B) Measurement of total T_4 in the serum of the mice by ELISA. (C) Measurement of total T_3 in the serum of the mice by ELISA. (D) Water intake per mouse during the study per day. Statistical significance was determined with an unpaired two-tailed Student's t-test and Welch's correction and was considered significant at $p<0.05$ (*), $p<0.01$ (*), $p<0.001$ (***) and $p<0.0001$ (****). Values are illustrated as mean ± SEM. n=6

Of top priority was again the measurement of target gene expression in the liver and here especially the expression of *Dio1* and *Spot14* to assess the efficiency of the treatment. As shown in **Figure 14A**, both gene expression levels of *Dio1* and *Spot14* were highly increased in the thyrotoxic groups compared to control group, but the graduation between the two hyperthyroid groups was no longer detectable. This is also the case for *Cd5l* and *Fbln1*, which are increased after T_4 treatment and tend to be increased after T_3 treatment. A Pearson correlation analysis of *Cd5l* gene expression against serum tT_3 and tT_4, as shown in **Figure 14B+C**, revealed a significant correlation which could already be determined after the two-week treatment and affirm the robustness of this effect. *Angt* was reduced after T_4 administration, while *Ttr* tend to be increased after T_3 administration and both effects were not detectable after two-week treatment in the previous study. The gene expression in bone displayed in **Figure 14D**, did not reveal many alterations, as already seen after the two-week treatment, but *Cd5l* and *Lum* were downregulated upon T_3 treatment, indicating a biphasic response.

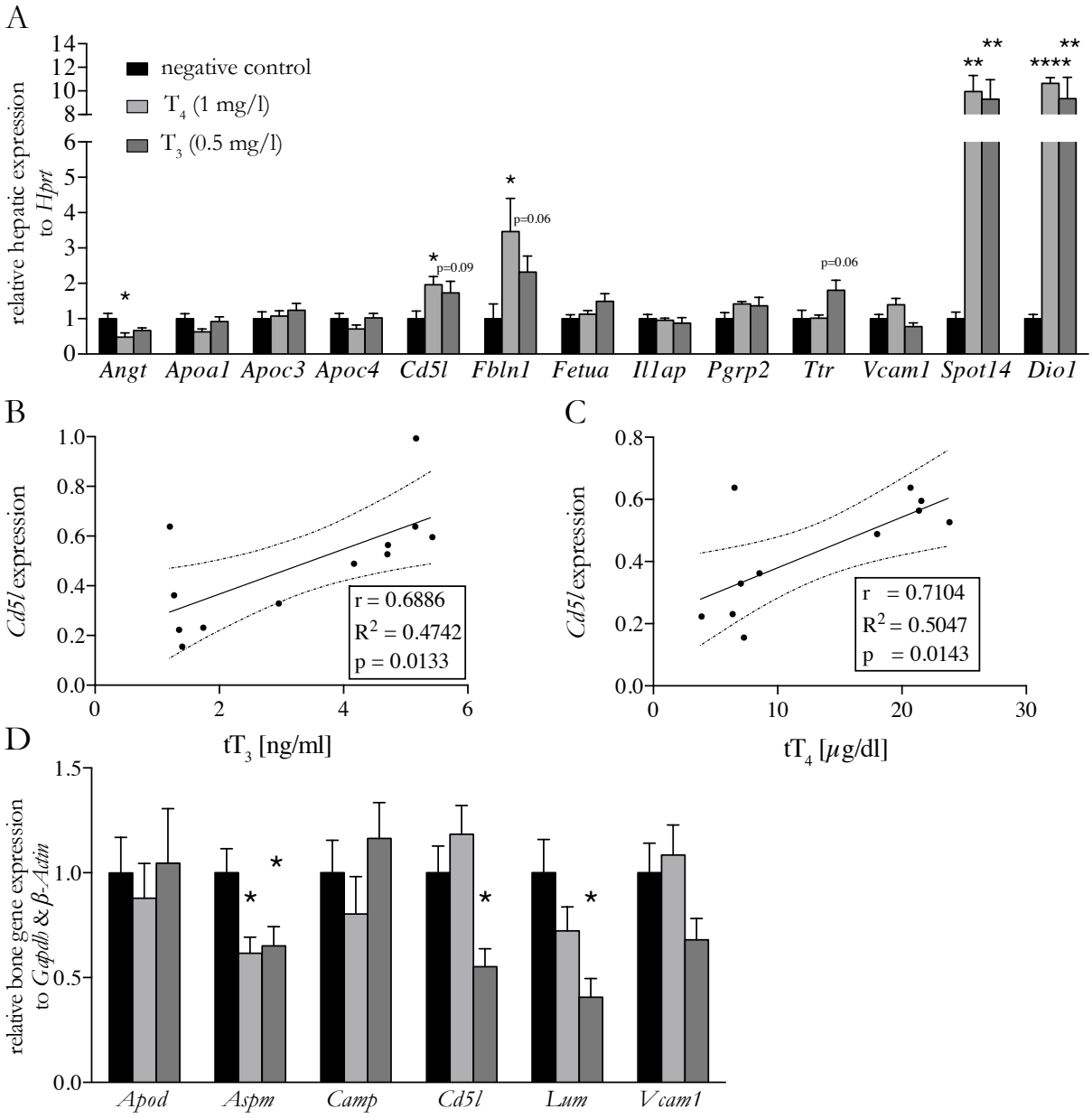

Figure 14 | Target gene expression in the liver after short term treatment. (A) Determination of target gene expression by qPCR in the liver. (B) Pearson correlation of *Cd5l* expression against the respective tT_3 concentration. (C) Pearson correlation of *Cd5l* expression against the respective tT_4 concentration; r – Pearson correlation coefficient; R^2 – coefficient of determination; p – p-value; dashed lines indicate 95% confidence interval. (D) Determination of target gene expression by qPCR in the bone. Statistical significance was determined with an unpaired two-tailed Student's t-test and Welch's correction and was considered significant at $p<0.05$ (*), $p<0.01$ (**), $p<0.0001$ (***) and $p<0.0001$ (****). Relative expression values are illustrated as mean ± SEM. n=6.

3.3 Validation of thyroid hormone targets in TR mutant mice

For the validation of target gene TH-dependence under chronic pathophysiological conditions and to characterise the role of the individual TR isoforms, the expression patterns in tissues of TRα1+/m and TRβ-/- mice with appropriate littermate controls were determined. Liver gene expression of TR mutant mice in **Figure 15A** revealed changes in *Dio1* expression for both TR mutants, but not in *Spot14* expression, highlighting the strong differences of gene expression upon

acute or chronic pathologies. The mutation in TRα1+/m lead to increased *Apoa1*, *Dio1*, *Fetua* and *Pgrp2* expression while *Cd5l* tend to be decreased. The knock-out of TRβ suppressed *Dio1* expression, despite their elevated circulating TH levels [151], but did not change target gene expression with exception for *Camp*, which was highly increased. Gene expression in the spleen of TR mutants is shown in **Figure 15B** and revealed the sole influence of TRα on target gene expression in this tissue, as knock-out of TRβ did not change expression of any target gene. A statistically significant increase was found for *Apoa1*, *Apoc3*, *Camp* and *Fbln1*, whereas *Pgrp2* was decreased in TRα1+/m spleen. A slight increase in TRβ-/- tissue for *Cd5l* could be detected, but did not meet significance criteria. As already seen in spleen, the knock-out of TRβ did not alter target gene expression in bone, which is shown in **Figure 15C**. An increase in gene expression in bone tissue with the TRα1+/m mutation could be measured for *Apod*, *Aspm* and *Camp*, while *Lum* was decreased.

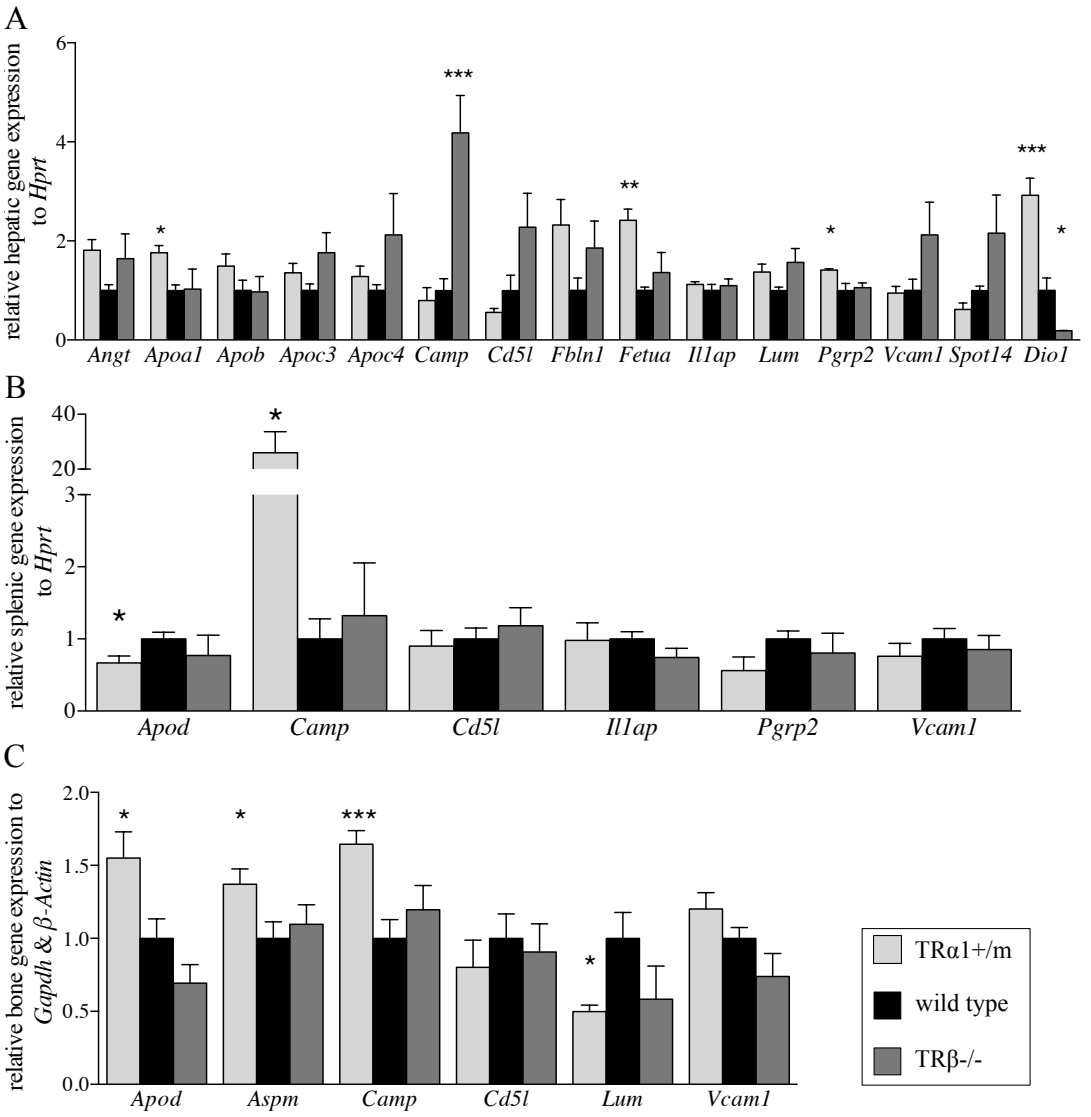

Figure 15 | Target gene expression in TR mutant mice. (A) Determination of target gene expression by qPCR in the liver. (B) Determination of target gene expression by qPCR in the spleen. (C) Determination of target gene expression

by qPCR in the bone. Statistically significant differences were determined with an unpaired two-tailed Student's t-test and Welch's correction and were considered significant at $p<0.05$ (*), $p<0.01$ (**) and $p<0.0001$ (***). Relative expression values are illustrated as mean ± SEM. n = 3-12.

The results of the gene expression analysis were subsequently tested on protein level by Western Blot analysis of serum and liver samples. Yet, as shown in **Figure 16A-C**, statistically significant differences between wild type mice and TR mutant mice in serum could not be determined for CD5L or CP, although CP in TRβ-/- mice tend to be increased, which would be discordantly with *Dio1* expression and indicate a different TR preference. Protein levels of CD5L and CP in liver differed from serum as shown in **Figure 17A-C**, where CP in TRβ-/- was significantly increased compared to wild type controls.

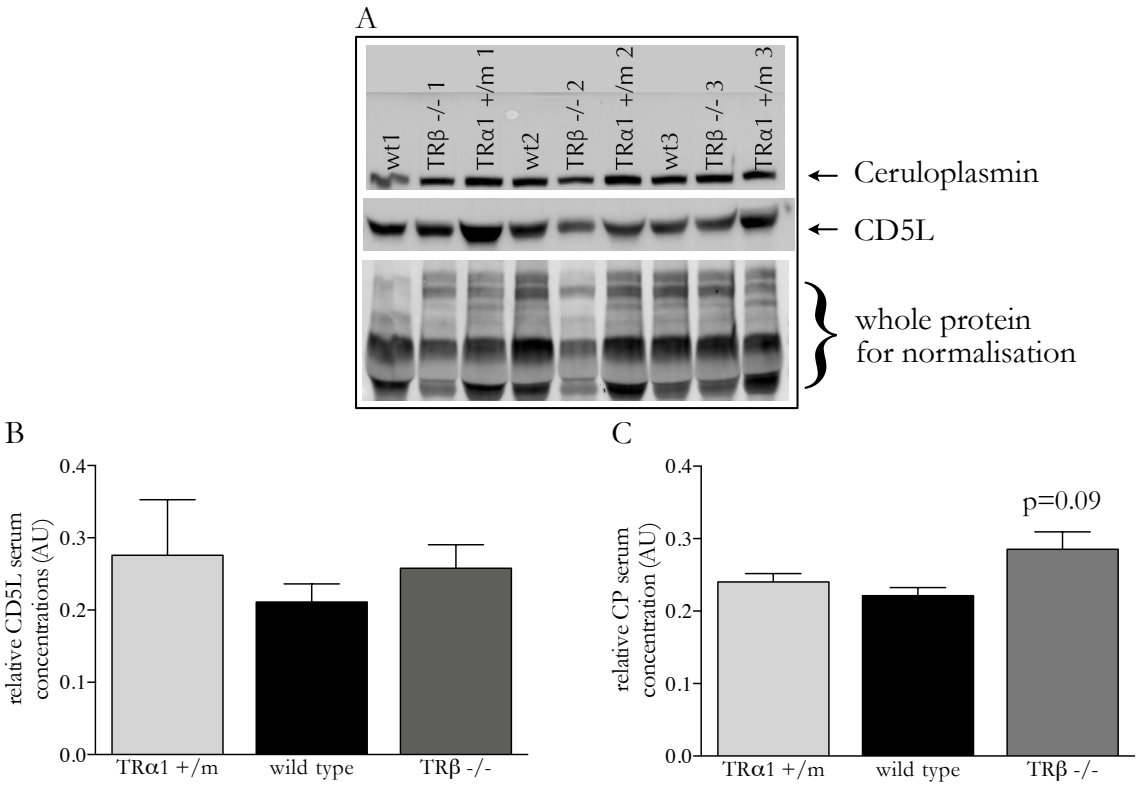

Figure 16 | Serum protein concentrations of CD5L and CP in TR mutant mice. (A) Representative Western Blot of 2µl undiluted mouse serum per sample incubated with goat anti-CP or rat anti-CD5L antibody and normalised to stain-free whole protein. (B) Western Blot analysis of rat anti-CD5L against whole protein for the respective group. (C) Western Blot analysis of goat anti-CP against whole protein for the respective group. Statistically significant differences between groups were determined by an unpaired two-tailed Student's t-test with Welch's correction and were regarded and illustrated as statistically significant when $p < 0.05$ (*). Values are represented as mean ± SEM of n=3.

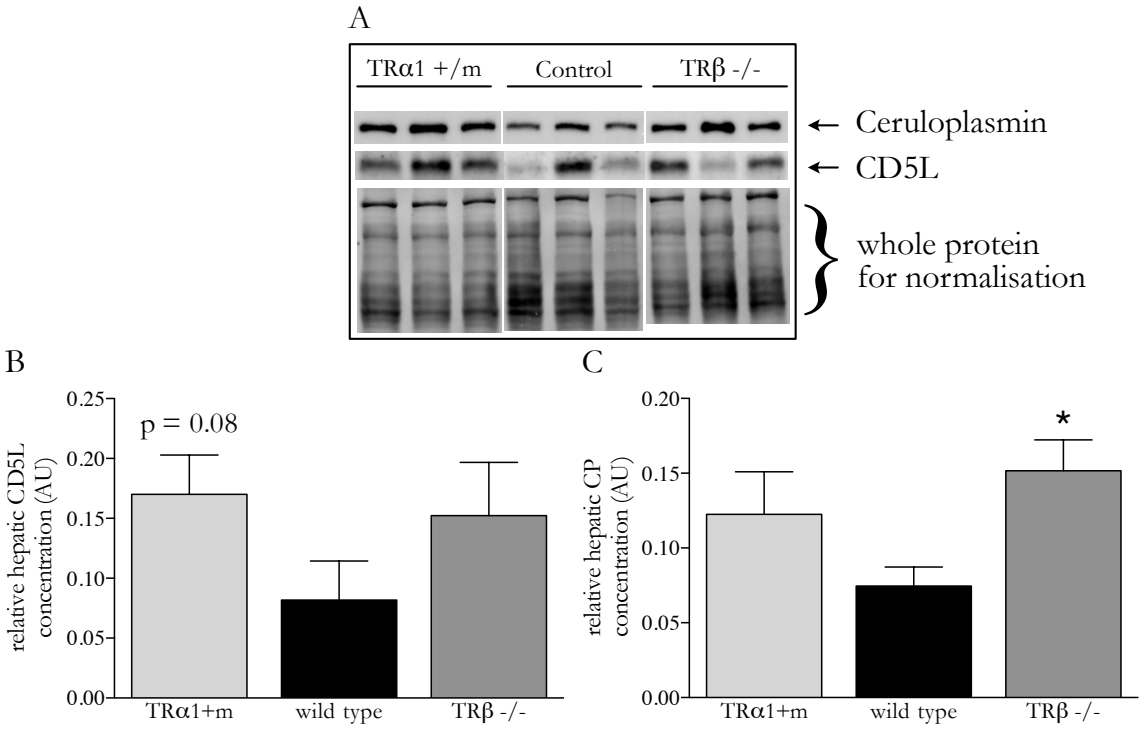

Figure 17 | Liver protein concentrations of CD5L and CP in TR mutant mice. (A) Representative Western Blot of 10 mg mouse liver tissue per sample incubated with goat anti-CP or rat anti-CD5L antibody and normalised to stain-free whole protein. (B) Western Blot analysis of rat anti-CD5L against whole protein for the respective group. (C) Western Blot analysis of goat anti-CP against whole protein for the respective group. Statistically significant differences between groups were determined by an unpaired two-tailed Student's t-test with Welch's correction and were regarded and illustrated as statistically significant when $p < 0.05$ (*). Values are represented as mean ± SEM of n=3.

3.4 Validation of thyroid hormone targets in cell lines and primary cell culture

The *in vivo* results indicate promising correlations of liver-originated genes. To dissect the underlying mechanisms, cells lines and primary cells under different conditions were used.

3.4.1 Target gene expression in HepG2 cell line

The human hepatocellular carcinoma cell line HepG2 was used to validate TH-dependent target gene expression in a well-established cellular system. As shown in **Figure 18A**, 12 of the 16 target genes were expressed in HepG2 cells, but none of these genes were altered under hypo- or hyperthyroid conditions. The known TH-dependent genes *SPOT14* and *DIO1* did also show significant but minor changes under hyperthyroid conditions, while hypothyroid conditions did only change *DIO1* expression. To investigate whether these minor effects occur due to hampered TR expression as a result of the dedifferentiation process during cancerogenesis [174-176], HepG2 cells were transiently transfected with an TRβ expressing pcDNA3.1 plasmid vector under control of a constitutively active Cytomegalovirus (CMV) promoter. The TRβ expression of

pcDNA3.1TRβ-transfected HepG2 cells was compared to pcDNA3.1-transfected HepG2 cells to evaluate transfection success and increased about 25-fold as shown in **Figure 18B**. As previously determined in untransfected cells, minor but significant changes were exclusively detectable for *DIO1* expression in response to TH concentrations, while no TH target expression was altered.

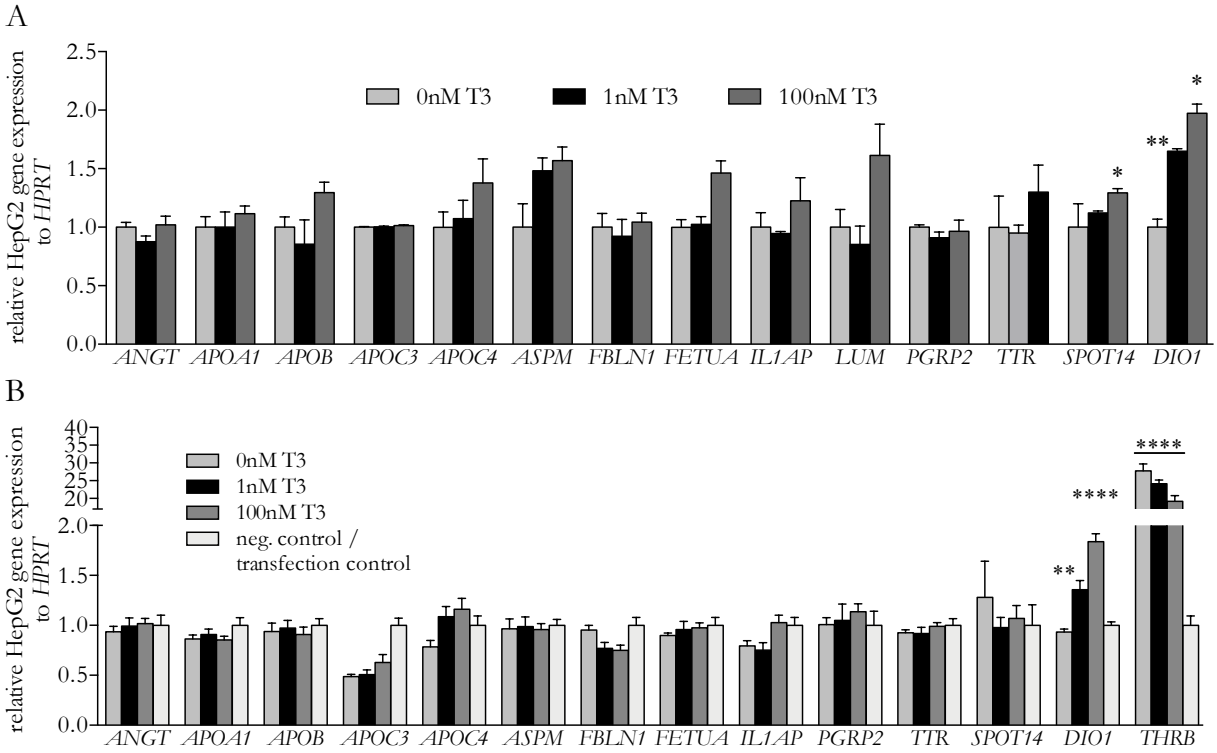

Figure 18 | Target gene expression in HepG2 cell line. (A) Determination of target gene expression by qPCR in HepG2 cell line after 24h incubation in TH depleted medium or TH supplemented medium. (B) Determination of target gene expression by qPCR in HepG2 cell line, transiently transfected with a *THRB* overexpression plasmid or empty vector, after 24h incubation in TH-depleted medium or TH-supplemented medium. Statistically significant differences between groups were determined by an unpaired two-tailed Student's t-test with Welch's correction and were regarded and illustrated as statistically significant when $p < 0.05$ (*). Relative expression values are represented as mean ± SEM of n=3.

3.4.2 Target gene expression in isolated blood cells

The TH dependence of *Cd5l* across different tissues in human and mouse together with its absence in HepG2 cells, as a model system for human hepatocytes, the possibility of circulating CD5L source was then investigated. As CD5L has already been reported as being expressed by Th17 cells [177, 178] but also macrophages [179, 180], the main leucocyte populations were sorted using a fluorescence-activated cell scanning (FACS) sorting panel from freshly isolated blood. The purity of the sorted B cell, T cell and monocyte populations was verified by determining class-specific marker genes and revealed almost 100% pure populations, as shown in **Figure 19**. Nevertheless, *Cd5l* expression could be determined in neither cell type population, clearly demonstrating that circulating cells do not contribute to the CD5L serum levels.

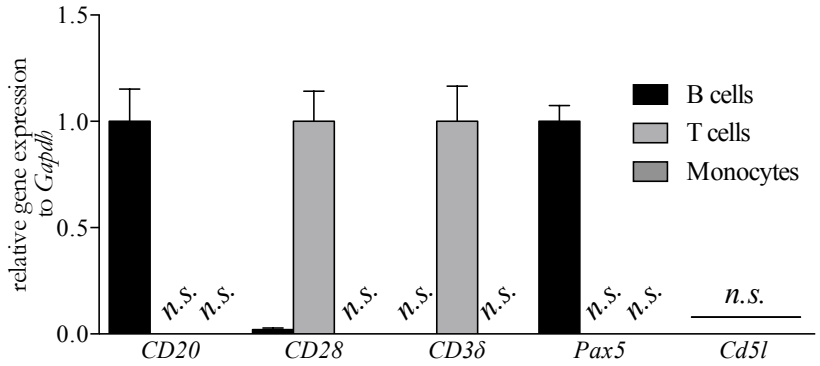

Figure 19 | Gene expression in purified leukocyte populations. Relative expression values are represented as mean ± SEM of n=9. n.s. – no signal detectable

3.4.3 Target gene expression in bone cells

Bone tissue predominantly expresses TRα and was therefore of main interest for the identification of TH-dependent biomarkers. Since the isolation of differentiated bone cells by collagenase digestion of bone tissue is an inefficient and time and material consuming technique, the main active bone cell populations, osteoblasts and osteoclasts, were differentiated from HSPCs located in the bone marrow. Fully differentiated and partly ossified osteoblasts are shown in **Figure 20A** after 12 days under stimulating culture conditions with its characteristic high cellular density and dark phosphate-enriched bone matrix areas. Fully differentiated osteoclasts after 5 days under stimulating culture conditions are shown in **Figure 20B** with the characteristic large multi-nuclear cells. The purity of the cell cultures was determined by measuring gene expression of cell type specific markers. For OBs, a set of different genes was used for the characterisation, which contained secretory leukocyte peptidase inhibitor (*Alp*), osteocalcin (*Ocn*) and osteopontin (*Opn*). For osteoclast and osteocyte characterisation catepsin K (*CatK*) and sclerostin (*Sost*) were used, respectively, and the results are shown in **Figure 20 C+D**. In the osteoblast culture, no expression of *CatK* or *Sost* was measured and the ratio between *CatK* and *Ocn* in OC culture was about 7000:1, indicating a very high purity of both primary cell cultures.

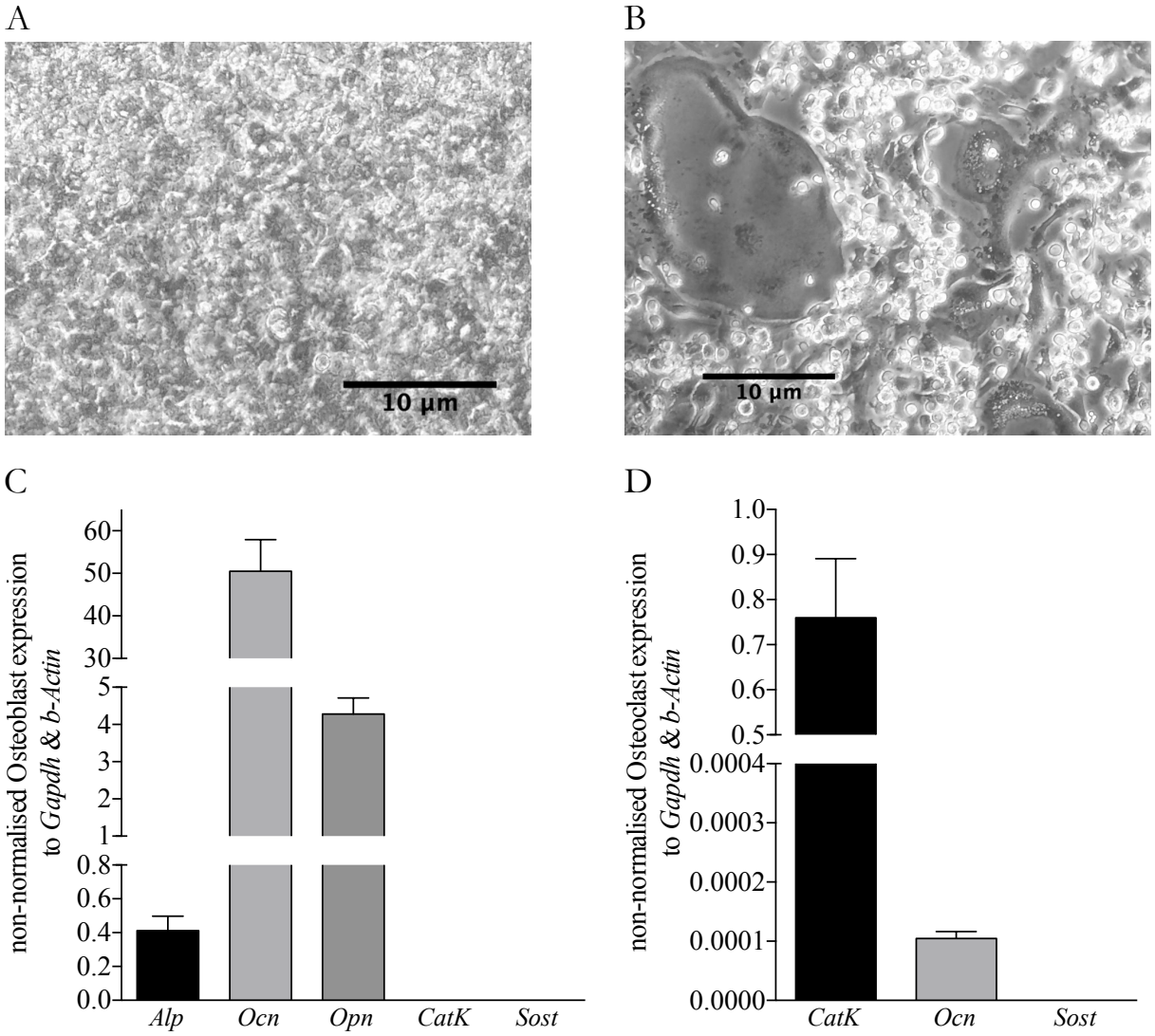

Figure 20 | Differentiation and characterisation of mouse Osteoblasts and Osteoclasts from hematopoietic stem and progenitor cells. (A) Representative picture with 40x magnification of *in vitro* differentiated osteoblasts on day 12 after seeding; darker areas indicate zones with progressed calcification and ossification. (B) Representative picture with 40x magnification of *in vitro* differentiated osteoclasts on day 5 after induction of differentiation. Light grey zones indicate large multinuclear osteoclasts with dark grey zones in the periphery containing multiple nuclei and other cellular compartments. (C) Expression of characteristic osteoblast, osteoclast and osteocyte marker genes in osteoblast cell culture. (D) Expression of characteristic osteoclast, osteoblast and osteocyte marker genes in osteoclast cell culture. Statistically significant differences between groups were determined by an unpaired two-tailed Student's t-test with Welch's correction and were regarded and illustrated as statistically significant when $p < 0.05$ (*). Relative expression values are represented as mean ± SEM of n=5.

The effects of the individual TR isoforms on target gene expression were already shown in whole bone mRNA (**Figure 15C**), therefore primary osteoblasts and osteoclasts from TR mutant mice were cultured. Despite the absence of an effect of TRβ on target gene expression in whole bone, in primary osteoblasts the knock-out of TRβ results in reduced *Cd5l* and *Lum* expression and a mutation in TRα has no significant effect, as shown in **Figure 21A**. Primary Osteoclasts from TRβ knock-out mice showed an increased expression of *Cd5l*, while *Lum* expression was increased in osteoclast carrying the TRα mutation, as illustrated in **Figure 21B**. Although both *Cd5l* and *Lum*

showed a TR-dependent expression in osteoblasts and osteoclasts, their expression was not altered under different TH concentrations, as depicted in **Figure 21C**.

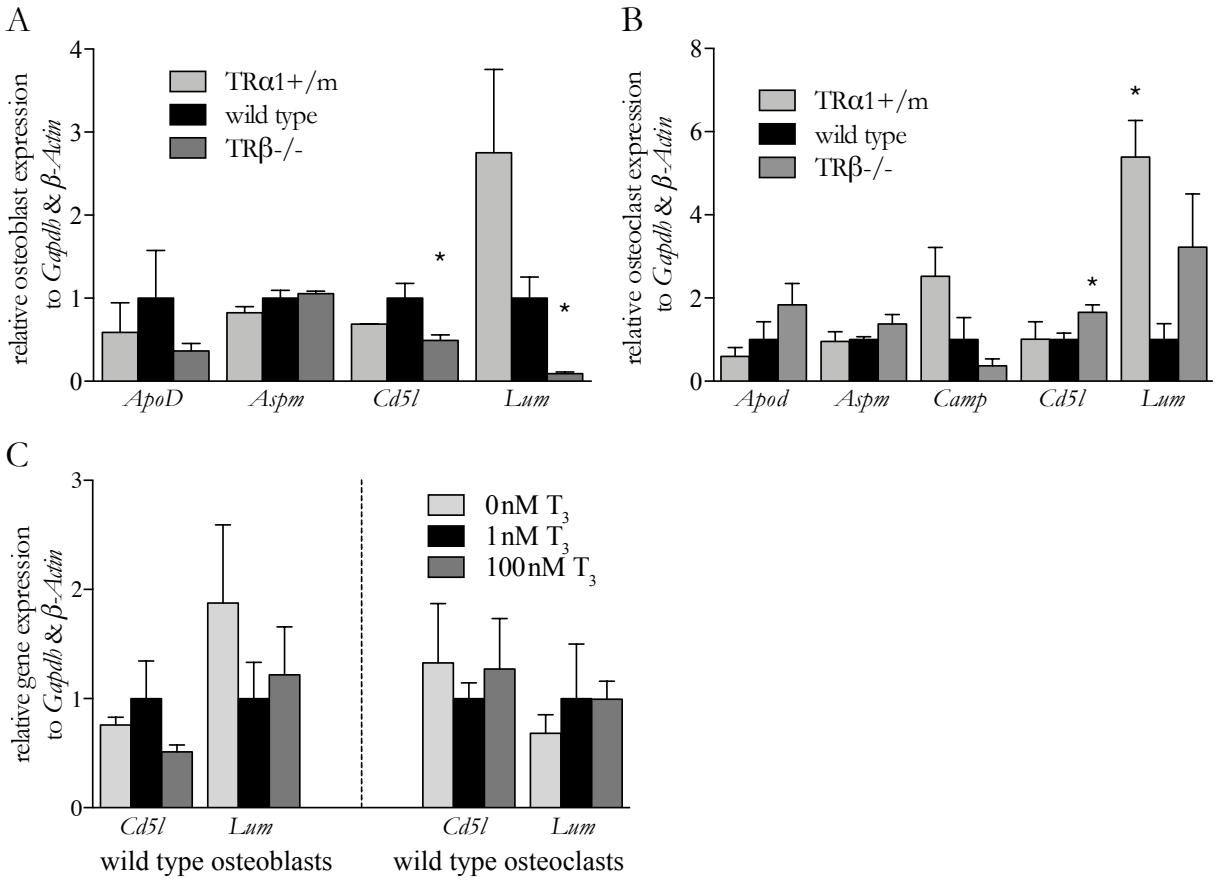

Figure 21 | Target gene expression in differentiated mouse Osteoblasts and Osteoclasts from hematopoietic stem and progenitor cells. (A) Target gene expression in primary mouse osteoblasts after 20 days of differentiation. (B) Target gene expression in primary mouse osteoclasts after 5 days of differentiation. (C) *Cd5l* and *Lum* expression in primary osteoblasts and osteoclasts of wild type mice under hypo-, eu- or hyperthyroid conditions after 24 h incubation. Statistically significant differences between groups were determined by an unpaired two-tailed Student's t-test with Welch's correction and were regarded and illustrated as statistically significant when $p < 0.05$ (*). Relative expression values are represented as mean ± SEM of n=5.

3.4.4 Target gene expression in primary hepatocytes

The *in vitro* cultivation of primary hepatocytes is an established method to investigate hepatic effects and avoid artefacts, induced by dedifferentiation processes. The isolated hepatocytes, as shown in **Figure 22A**, need 24 h to settle onto the cell culture dish surface and can at that point easily be detected, as they carry a characteristic second nucleus, which can be seen in **Figure 22B**. Since the hepatocytes were separated by collagenase digestion of the liver lobes, the primary hepatocyte cell culture contains all cell types that occur in liver tissue, as there are also mono-nuclear cells detectable in **Figure 22B**. The primary hepatocytes culture was mainly used to produce conditioned medium to stimulate BMDM cell culture by transferring the medium. Therefore, the hepatocytes were incubated with different TH concentrations for 48 h to allow for sufficient release of secreted and putatively *Cd5l* releasing factors into the medium. To assess the treatment, gene

expression of TH, liver X receptor (LXR) and retinoid X receptor (RXR) dependent marker genes *Apoe*, *Abcg5*, *Cp*, *Dio1*, *Spot14* and *Srebp2* was measured. The only significant alteration was detectable for *Abcg5*, after stimulation with LXR agonist T0901317 (T1317) and RXR agonist 9-cis retinoic acid (9cRA). *Dio1* expression was induced upon T_3 treatment, albeit not statistically significant. As already detectable in HepG2 cells (**Figure 18B**), *Spot14* was unaffected by different TH concentrations. With the exception of *Camp* and *Lum*, all TH target genes detectable in liver mRNA could be retrieved in primary hepatocytes, but none of them showed significant alterations. *Cd5l* expression tends to be altered upon different TH concentrations, but did not attain statistical significance.

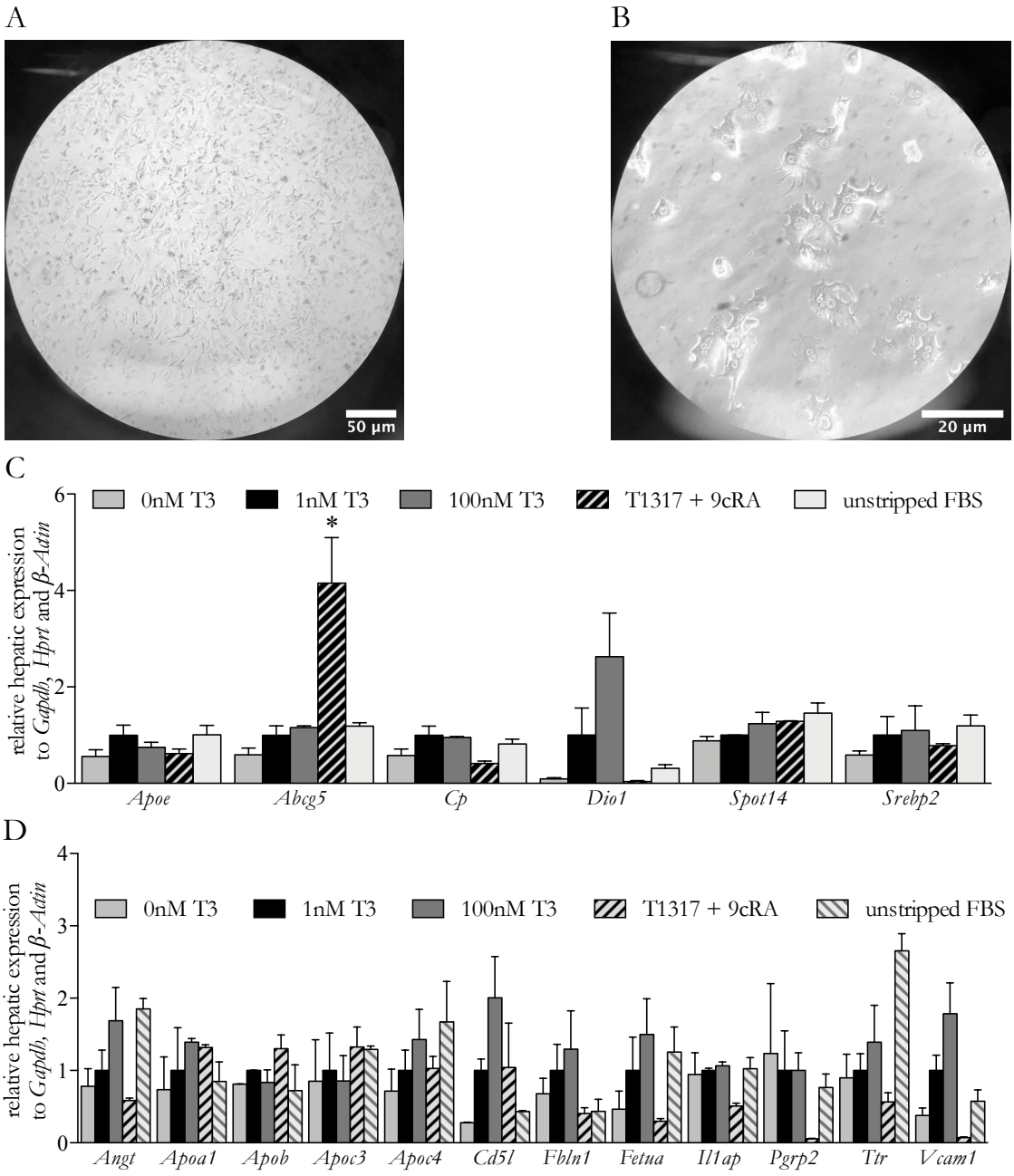

Figure 22 | Gene expression of primary hepatocytes. (A) Representative picture with 10x magnification of *in vitro* cultivated hepatocytes on day 2 after seeding. (B) Representative picture with 40x magnification of *in vitro* cultivated

hepatocytes on day 2 after seeding. Hepatocytes are detectable by a second nucleus. (C) Gene expression of TH, LXR or RXR marker genes after 48 h incubation. (D) Target gene expression in primary hepatocytes after 48 h incubation. Statistically significant differences between groups were determined by an unpaired two-tailed Student's t-test with Welch's correction and were regarded and illustrated as statistically significant when $p < 0.05$ (*). Relative expression values are represented as mean ± SEM of n=2.

3.4.5 *Cd5l* expression in bone marrow-derived macrophages

Tissue residing macrophages are described as major source of CD5L and especially liver-residing Kupffer cells could be the source for the TH-dependent CD5L expression in the liver and proteome data [179, 180]. Therefore, bone marrow-derived macrophages (BMDMs) were differentiated from HSPCs using macrophage colony stimulating factor (M-CSF) and polarised into M1 macrophages by stimulation with LPS and IFN-γ for 24 h. After polarisation BMDMs metamorphose from a flat and laminar shape into a round-shaped form as shown in **Figure 23A**. As hypothesised, *Cd5l* expression could be detected in BMDMs and was additionally downregulated in cells carrying the mutation in TRα1+/m, while TRβ knock-out or different TH concentrations had no effect, as shown in **Figure 23B+C**. As described in a previous study, *Cd5l* expression is regulated by LXR binding on specific LXR response elements (LRE) [181]. Activation of LXR binding on the LRE in *CD5L* promoter region by the LXR-specific agonist T1317 increased Cd5l expression in wild type and TRα1+/m mutant mice, while this increase was hampered in TRβ knock-out mice, which is depicted **Figure 23D**. The differences of *Cd5l* expression between the TR mutant mice could not be excluded from differences in M1 polarity, since TRα1+/m mice show significantly higher *Il10* expression, indicating a higher anti-inflammatory potential, but none of the pro-inflammatory markers tested were altered between these genotypes, as shown in **Figure 23E**.

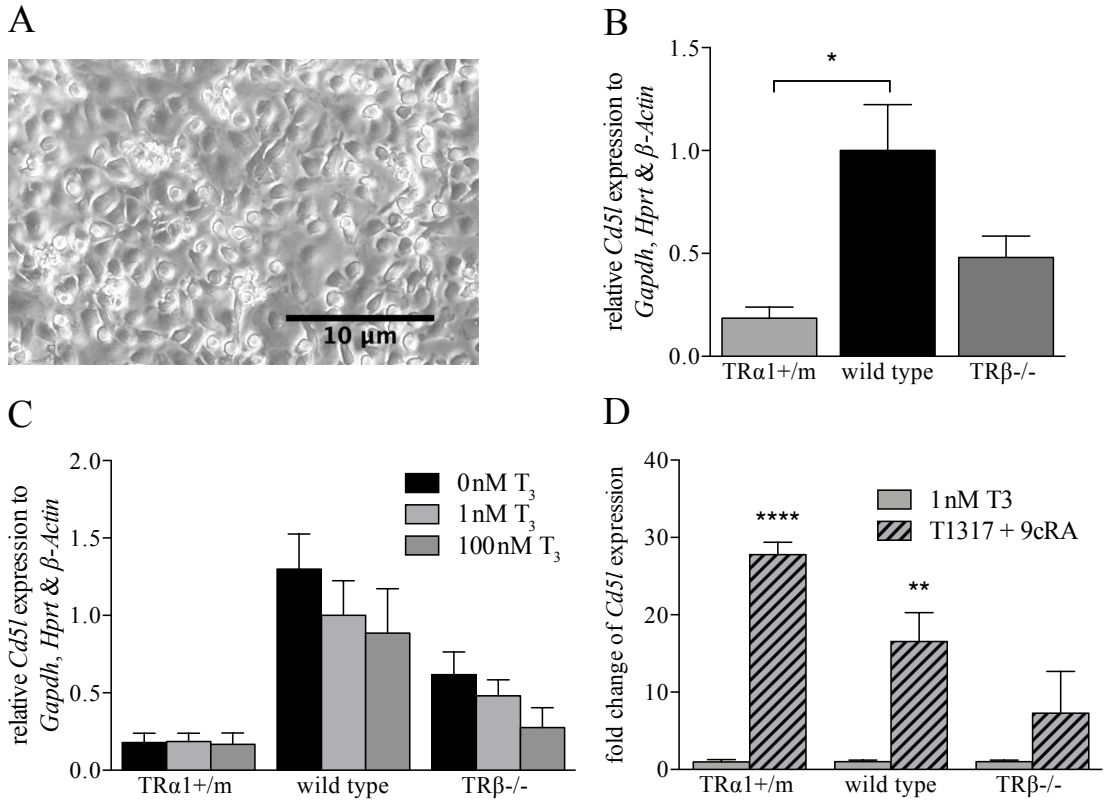

Figure 23 | Gene expression of primary bone marrow-derived macrophages. (A) Representative picture of M1 polarised BMDM after 24h of LPS & IFN-γ induced polarisation. (B) *Cd5l* expression in BMDM of wild type and TRα1+/m and TRβ-/- mutant mice. (C) *Cd5l* expression in BMDM upon hypo-, eu- or hyperthyroid conditions of wild type and TRα1+/m and TRβ-/- mutant mice. (D) Fold change of induction of *Cd5l* expression upon T1317+9cRA treatment compared to euthyroid condition in BMDM of wild type and TRα1+/m and TRβ-/- mutant mice. Statistically significant differences between groups were determined by an unpaired two-tailed Student's t-test with Welch's correction and were regarded and illustrated as statistically significant when $p < 0.05$ (*). Relative expression values are represented as mean ± SEM of n=3-6.

To elucidate whether changes in Cd5l expression were due to changes in BMDM polarisation, M1 and M2 marker genes were determined by qPCR. No changes were observed in M1 marker gene expression of *Nos2*, *Tnfa* or *Il1b*, but also the M2 marker gene expression of *Argi1* was not altered. However, M2 marker gene expression of *Il10* was highly significantly increased in BMDMs from TRα1+/m mice compared to wild type or TRβ-/- mice, indicating so changes towards a M2-like phenotype, as shown in **Figure 24A**. Moreover, the gene expression of the scavenger receptor and transporter for LXRα-ligands *Cd36* and of the LXRα receptor *Nr1h3* was measured to identify putative change that could influence *Cd5l* expression. No changes could be determined for Cd36 in any TR mutant mice, but *Nr1h3* was significantly increased in TRβ-/- mice, while no changes could be observed in TRα1+/m mice, as shown in **Figure 24B**.

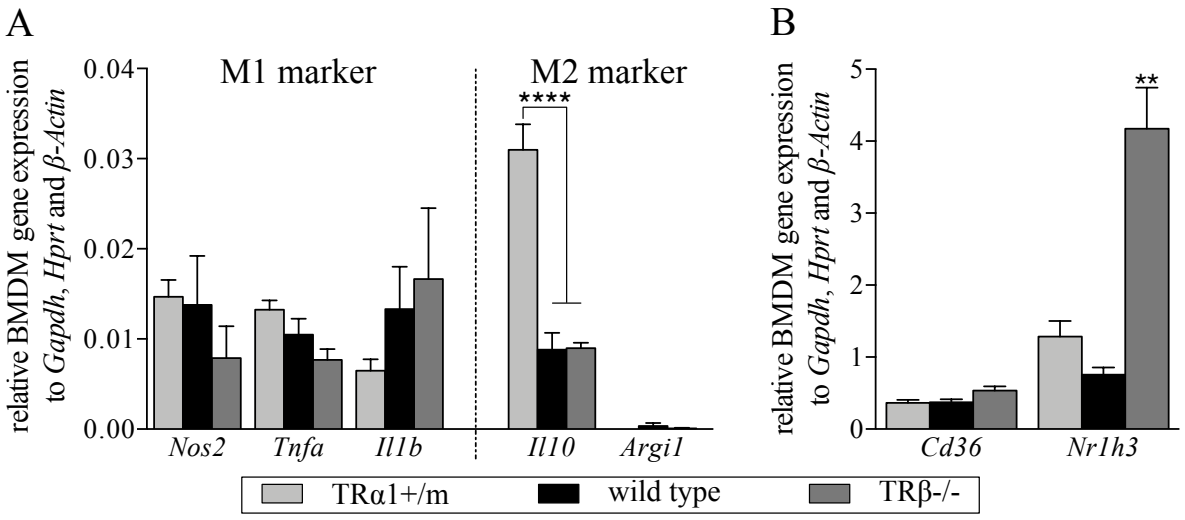

Figure 24 | Characterisation of bone marrow-derived macrophages from different TR mutant mice. (A) Determination of gene expression of M1 and M2 marker genes in BMDMs of wild type, TRα1+/m and TRβ-/- mice after 24 h incubation with LX-2 conditioned medium with 1 nM T_3 by qPCR. (B) Determination of gene expression in BMDMs of wild type, TRα1+/m and TRβ-/- mice after 24 h incubation with LX-2 conditioned medium with 1 nM T_3 by qPCR. Statistically significant differences between groups were determined by an unpaired two-tailed Student's t-test with Welch's correction and were regarded and illustrated as statistically significant when $p < 0.01$ (**) and $p < 0.0001$ (****). Relative expression values are represented as mean ± SEM of n=3-6.

The response of CD5L abundance in plasma proteome, liver mRNA levels and BMDM mRNA levels in mice carrying a mutation in *Thra* highlighted the importance of TRα1 on CD5L expression. Missing *Cd5l* expression alterations under different TH concentrations posed the question of an indirect effect induced by other tissue residing cells. Since hepatocytes are responsible for the expression of a variety of TH responsive genes, it was hypothesised that hepatocytes secrete a TH responsive factor which influences *Cd5l* expression in Kupffer cells or BMDMs. Therefore, HepG2 cells were incubated for 24 h with euthyroid medium (1 nM T_3). The HepG2 medium was then considered as HepG2-conditioned medium and directly transferred onto BMDM. After incubation for 24 h with HepG2-conditioned medium, mRNA of BMDMs was isolated and results of the subsequent qPCR analyses are shown in **Figure 25A**. As described before, the hepatocellular carcinoma cell line HepG2 is prone to induce experimentally artefacts due to dedifferentiation processes. Hence, this experiment was repeated with primary mouse hepatocytes and the human stellate cell line LX-2 as a control for putative consumption effects. Hepatocyte-conditioned medium induced *Cd5l* expression across different TH concentrations and also statistically significant in BMDMs of TRα1+/m mutant mice und euthyroid conditions, while in wild type mice it tended to be increased **Figure 25B+C**. Surprisingly, the hepatocyte-induced increase of *Cd5l* expression was abolished in BMDMs of TRβ-/- mice across all investigated TH concentrations, as shown in **Figure 25D**. The results of *Cd5l* expression in BMDM of different TR genotypes under euthyroid (1 nM T_3) conditions are depicted in **Figure 25E** for a more comprehensible summary of the determined effects in BMDMs.

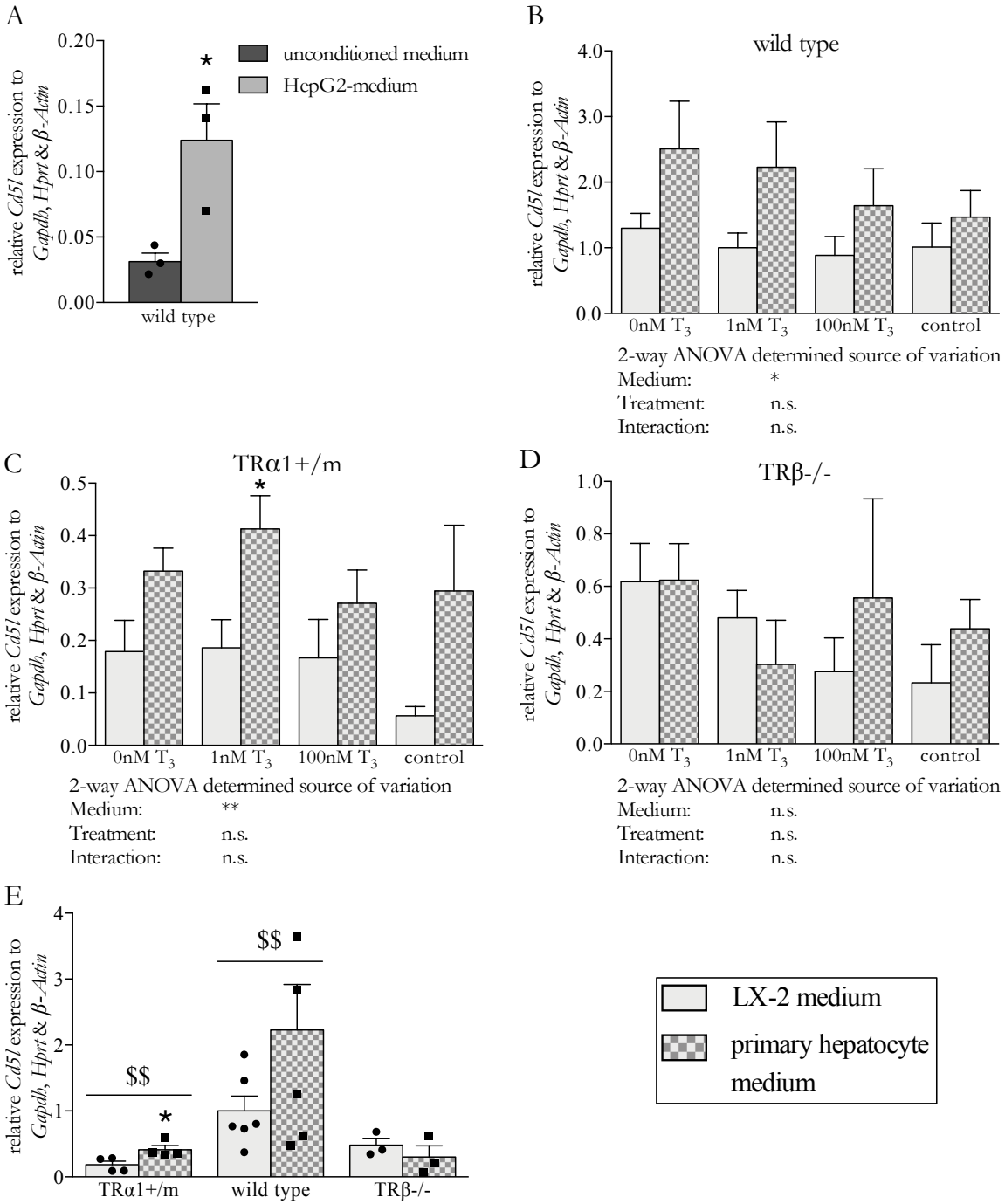

Figure 25 | *Cd5l* expression in bone marrow-derived macrophages with hepatocyte-primed medium. (A) *Cd5l* expression in BMDMs of wild type mice after 24 h incubation with unconditioned or HepG2-conditioned medium under euthyroid conditions. (B) Determination of *Cd5l* expression in BMDM after 48 h incubation with LX-2- or primary hepatocyte-conditioned medium of wild type mice. (C) Determination of *Cd5l* expression in BMDM after 48 h incubation with LX-2- or primary hepatocyte-conditioned medium of TRα1+/m mice. (D) Determination of *Cd5l* expression in BMDM after 48 h incubation with LX-2- or primary hepatocyte-conditioned medium of TRβ-/- mice. (E) Comparative overview of *Cd5l* expression in BMDMs under euthyroid conditions from (B-D). Determination of statistically significant source of variation on *Cd5l* expression of conditioned medium across different T_3 concentrations (B-D) was performed by a two-way ANOVA and is indicated for the medium by \$ for $p<0.05$, \$\$ for $p<0.01$ and \$\$\$\$ for $p<0.0001$. Statistically significant differences between groups were determined by an unpaired two-tailed Student's t-test with Welch's correction and were regarded and illustrated as statistically significant when $p < 0.05$ (*). Relative expression values are represented as mean ± SEM of n=3-6.

4 Discussion

4.1 Precision medicine and biomarker identification

Biomedical research has always been used to develop and improve new or existing treatments to cure patients from diseases and prolong and improve their lives. In the recent decade [182], the term precision medicine evolved to describe the usage and combination of innovative and sophisticated techniques on different biological information levels, e.g. genomic, epigenomic, transcriptomic, proteomic, metabolomic and microbiomic level [183]. The huge amounts of data that are obtained with the OMICs techniques can be subsequently used to calculate a unique biochemical fingerprint of a patient. The final aim of precision medicine is then to provide the optimal pharmacological treatment for every individual patient by identifying specific properties of therapeutic targets and metabolising and interfering factors [184]. Since the complete fingerprint of all biological levels for all individual patients is, so far, impossible to realise due to enormous costs and technical efforts, OMICs techniques are used to identify single prognostic markers, e.g. single nucleotide polymorphisms (SNPs) in tumour marker genes like *BRCA1* and *BRCA2* or *BRAF*V600E, to estimate individual pharmacokinetics, treatment strategies and cure rates [185]. These prognostic markers develop their highest potential in the context of inherited as well as acquired monogenic diseases, e.g. Chronic myeloid leukaemia (BCR-ABL), Cystic fibrosis (G551D), Thrombosis (Factor V Leiden) or Multiple endocrine neoplasia type 2 (RET), where these and other markers are solely sufficient to indicate distinct diseases and allow for direct medication [186]. In contrast, polygenic diseases require multiple and solely inconspicuous inherited or acquired genomic or non-genomic modifications to result in a specific phenotype. These forms of diseases change the whole transcriptomic and proteomic network across different cell types in an indirect manner and therefore their detection is more unambiguous on the mRNA, protein or metabolite level as compared to the genomic level [183, 187]. Hence, the combination of different OMICs techniques allows for the identification of new sets of single biomarkers which in turn enable for improved diagnostic and monitoring tools [188]. For that reason, the human and mouse plasma proteome data sets from the experimentally induced thyrotoxicosis studies were combined with associated mouse liver transcriptome data sets to discover TH-regulated and more specifically liver-secreted plasma proteins, as this organ has been identified almost 20 years ago as strongly dependent on peripheral TH concentration [169, 170, 189]. Another important factor in interpreting OMICs data sets is the compliance to stringent sample collection and analysis routines, as inaccuracy in these points result either in a loss of information or false positive hits [190]. As a consequence of this routine, the resulting target gene list is slightly different from published data

set of the human plasma proteome [128] where the statistical "Random Forest" analysis was used which differed from the more conservative ANOVA method employed here to for the analysis of the mouse plasma proteome and mouse liver transcriptome data sets. To receive a straightforward comparability between the different data sets, only the conservative ANOVA analyses were considered for target gene identification. Previous studies focused either on hypo- or hyperthyroidism in human or mouse samples and identified putatively regulated species-specific genes. Unfortunately, the results, obtained from these studies, display enormous differences, due to different sample handling and analysis methods, as mentioned above [60, 169, 170, 189, 191-194]. The major advantage of the comparative approach between human and mouse data within this study was to identify new TH target genes and validate them in well-established mouse models. Surprisingly, of 32 regulated and TH-dependent plasma proteins in human and mouse, only 16 were concordantly regulated. Of note, all 32 proteins can be regarded as putative biomarkers for human TH disorders, but for a better characterisation of these targets and for the opportunity to decipher underlying mechanisms by using animal models for acute or chronic TH disorders and employ molecular biology techniques, only the 16 concordantly expressed targets were further investigated. The massive differences between human und mice occurred even in well-described and highly conserved biological networks. One of these networks is the complement system and four of its proteins (CO3, CO8A, CO8B and CO8G) have been identified as being regulated by TH concentrations. In contrast to previous studies which show high similarity between the complement system in mouse and human [195], we found complement factors increased in thyrotoxic humans and decreased in thyrotoxic mice. Moreover, other groups found complement factors increased after long-term hypothyroidism and no effect of acute exogenous thyrotoxicosis [196-198], indicating an unspecific adaptation of the complement system under chronic pathophysiological TH concentrations, which would thus constitute a poor biomarker candidate.
As another well-described and highly conserved biological network, five proteins (CFAH, CFAI, FA9, IC1 and MASP2) of the coagulation system were upregulated upon thyrotoxicosis in human and downregulated in mice. For decades it is known, that hypothyroidism leads to decreased coagulation factors FA8, FA9 and FA11 [199], which can be corrected by exogenous L-thyroxine administration until reaching euthyroid range [200]. Thyroid hormones also effect fibronectin, von Willebrand factor, plasminogen activator I and others [197], resulting in an increased risk of developing venous thromboembolisms and deep vein thrombosis in hyperthyroidism and reversely decreased clotting time and clot density with an increased bleeding time in hypothyroidisms [201]. In humans, these effects were detectable even under minor TH pathologies, e.g. subclinical hypo- or hyperthyroidism [202, 203]. Despite this clear correlation of the coagulation system and TH concentrations, in line with previously conducted studies, a discordant regulation between humans

and rodents could be detected and excluded coagulation proteins from further biomarker validation [194, 204].

4.2 Identified target genes and their relation to thyroid hormone

The remaining 16 proteins, as revealed by a gene ontology analysis, are mainly involved in regulatory extracellular processes, as described in more detail in the following sections.

4.2.1 Apolipoproteins

Apolipoproteins are responsible for structure maintenance of plasma lipoprotein particles which are classified by their respective size and range from small high-density lipoproteins (HDL) to intermediate low- or very low-density lipoproteins (LDL and VLDL) and finally to large chylomicrons. The size and biological function of lipoprotein particle is defined by their apolipoprotein and cholesterol load [205]. Several apolipoproteins were found to be regulated by TH concentrations which has been shown by previous studies but will be explained in further detail within the next paragraphs.

Apolipoprotein a1 (APOA1) contributes to the formation of high-density lipoproteins and is mainly secreted by the liver [206]. It is essential for the reverse cholesterol transport from the periphery back to the liver [207]. The effects of TH on apolipoprotein a1 is still under debate, due to conflicting results, which range from direct [208] to indirect [209-211] correlations and also no effects [206, 212-214] were concluded. These conflicting results might be due to positive and negative regulating TR response elements in the promoter region of *APOA1* that could dominate the expression differently in specific populations [215]. Despite decreased levels of APOA1 in the here presented plasma proteome, no changes could be detected on the mRNA level in hyperthyroid mouse livers. Moreover, decreased *Apoa1* expression in MMI/ClO_4-treated animals support a direct correlation between TH and *Apoa1*, which would not be in line with the majority of previous findings. Interestingly, *Apoa1* expression was increased in liver and spleen with a mutation in *Thra* but the knock-out of *Thrb* did induce alteration, although treatment of hypercholesterolaemic patients with TRβ-specific agonist eprotirome results in reduced lipoprotein(a) concentrations, which depends also on *Apoa1* expression and highlight the influence of TRβ on *Apoa1* expression [216]. In contrast to patients carrying a heterozygous mutation in *THRA* (RTHα) who show decreased HDL cholesterol values, *Apoa1* expression was increased in liver and spleen of TRα1+/m mice, indicating increased degradation processes on the protein level [217, 218]. Another recent study identified that DIO1 regulates *Apoa1* expression in a TH-independent manner [219]. Since *Dio1* expression itself depends on TH concentration, the direct connection of

TH concentration and *Apoa1* expression suggests an explanation for the identification of TH levels and the progression of Parkinson's disease, which depends among other factors on the abundance of apolipoproteins [220, 221].

The apolipoprotein B (APOB) contributes to the formation of very low- and low-density lipoproteins (VLDL and LDL) and is mainly secreted by the liver [222]. The connection between TH and APOB is well-described and was first detected in patients with overt hypothyroidism who suffer from hypercholesterolaemia and increased VLDL and LDL particles [223-225] and in contrast to HDL particles, there is no conflicting data about this connection. The beneficial effect of hyperthyroidism on lipid disorders is also a well-described phenomenon [222] and was tried to be mimiced by several TRβ- and liver-specific compounds, so called thyromimetics. These drugs, e.g. Sobetirome or GC-1 (QuatRx), Eprotirome (KaroBio), VK2809 (Viking Therapeutics) and MGL-3196 (Madrigal Pharmaceuticals), all lowered LDL-cholesterol and triglycerides and MGL-3196 lowered also APOB [226], but none of these compounds reached the final marketability. In the studies presented here, *Apob* expression was not directly correlated to TH concentrations neither under acute nor under chronic pathological conditions.

Apolipoprotein c3 (APOC3) contributes to the formation of chylomicrons and LDL particles and is mainly secreted by the liver. It is known to induce pro-inflammatory cytokines and promotes cholesterol uptake of arterial macrophages with their subsequent transformation into foam cells and is therefore regarded as atherosclerosis marker [227, 228]. In a recent study, the influence of increased APOC3 levels on type 1diabetes mellitus was revealed by inducing voltage-gated L-type Ca^{2+} channels in pancreatic β cells, which increase intracellular Ca^{2+} levels and ultimately lead to their apoptosis [229]. This is in line with previous observations, which emphasise the higher incidence of type 1 diabetes mellitus of patients with thyroid disorders [230]. This connection between *Apoc3* and TH is also detectable in the here presented plasma OMICs and liver gene expression data after an experimentally induced thyrotoxicosis for two weeks. The plasma abundance of APOC3 strongly decreased, as already described in previous studies [231], which emphasises the beneficial effects of TH on blood lipids. The counterintuitive increase of *Apoc3* expression upon thyrotoxicosis and the reverse effect upon hypothyroxinemia, indicate a compensatory reaction of hepatocytes to counteract the decreased or increased plasma LDL and VLDL concentration. This was not detectable upon short-term treatment already shown in a previous study in rats, where TH exert only minimal effects on total *Apoc3* mRNA content [232]. Patients with RTHα show increased levels of LDL cholesterol in line with an increased *Apoc3* expression in TRα1+/m mutant mice [217, 218]. In these patients and mice, the TH disorder seem to induce a different adaptation pattern, as this was seen upon acute thyrotoxicosis. This effect is, so far not described in the literature and requires further studies.

Apolipoprotein c4 (APOC4) is a liver-secreted plasma protein, which belongs to the APOE/C1/C2/C4 locus and therefore contributes to the formation of chylomicrons and VLDL, but also HDL particles in the context of the reverse cholesterol transport (RCT) [222, 233-235]. The particular action of APOC4 in lipoprotein formation has not been investigated so far, and hence a distinct correlation with TH remains also elusive. However, in the here presented plasma proteome and liver gene expression data after a two-week thyrotoxicosis, decreased plasma protein levels and increased liver mRNA levels indicate a similar regulation as for *Apoc3*.

Apolipoprotein d (APOD) differs from other apolipoproteins, as it is smaller (29 kDa) than the other apolipoproteins and belongs structurally to the lipocalin family instead of the apolipoproteins, therefore it was termed as atypical apolipoprotein. In rodents, it is dominantly secreted by the central nervous system, but other sources from most peripheral tissues contribute at a lower level [236, 237]. The vast majority of plasma APOD contributes to the formation of HDL particles, which supply neuronal cells and other peripheral tissues with a variety of lipophilic molecules, since APOD has a high affinity to retinoic acid, sphingomyelin, progesterone, arachidonic acid, cholesterol, bilirubin and others [238]. It has a neuroprotective function, since a global knock-out in mice lead to increased peroxidation and decreased resistance to oxidative stress in the brains, while overexpressing *Apod* induced reverse effects together with a prolonged lifespan [239, 240]. So far there is no comparable study which supports the here presented finding of reduced APOD abundance upon acute thyrotoxicosis, but since TH did not alter *Apod* expression in any treated tissue, a consumption effect due to a higher HDL demanding RCT could explain the effect [128]. However, increased *Apod* expression in bones of TRα1+/m mice suggests also a negative TRE in the *APOD* promoter, since TRα is the predominantly expressed TR isoform in bones, but further studies would be required to answer that question.

4.2.2 Proteins of the extracellular matrix

The extracellular matrix protein (ECM) Fibulin 1 (FBLN1) is widely expressed in mammals with no main origin and exists in humans in 4 isoforms which all belong to a subclass termed as long fibulins, but differ in size and biological function [241]. Within the ECM it is associated with cell adhesion and mobility and matrix remodelling [242], and therefore occurs abundantly in the plasma, since it is also involved in clot formation and platelet adhesion [243]. The influence of THs on ECM modulation is long known, since patients with severe untreated hypothyroidism suffering from fibrosis and myxoedema caused by increased production of glycosaminoglycans [244, 245]. Increased concentration of TH on the other hand decrease the production of ECM-forming proteins [246]. These findings were confirmed in our studies, as *Fbln1* was upregulated in the spleen of TRα1+/m mice, which is, like the heart or lymphatic cells, predominantly regulated by TRα.

This is also true for bone tissue, but here no Fbln1 expression could be detected. Despite these well-characterised effects, plasma concentrations of FBLN1 have not yet been determined under pathological TH conditions in previous studies. Gene expression of *Fbln1* was found decreased after short term thyrotoxicosis for seven days of intra peritoneal or four days of enteral T_4 administration in heart and aorta tissue of wild type BL6 mice [64, 247], whereas in liver *Fbln1* expression was increased after short term thyrotoxicosis and no changes could be detected after a two-week administration of MMI/ClO_4, T_3 or T_4. The fact that *Fbln1* expression could not be detected in spleens of wild type BL6 mice after the two-week administration period, can be explained by low and putatively highly volatile expression levels, which in sum exclude FBLN1 as a TH biomarker.

The extracellular matrix protein lumican (LUM) belongs to the family of small leucine rich proteoglycans (SLRPs) and is involved in matrix organisation and regulation of cell growth and signalling [248]. It is, due to its function as a part of the physiological ECM composition, ubiquitously expressed [249] and it has already been demonstrated that increased levels of LUM can be found in various tumours and correlates with their potential in growth and metastatic potential [250, 251]. Noteworthy, also contradictory results have been found in prostate, breast and pancreas cancer, where LUM had tumour-suppressive potential, emphasising its multifaceted action [252-254]. Besides its contribution to cancer biology, LUM has also been described as a mediator of inflammatory signals for pathogen associated molecular patterns by interacting with toll-like receptors, and here especially LPS induced TLR-4 signalling [255, 256]. The influence of LUM expression in response to thyrotoxicosis has been demonstrated in the embryonal chicken eyes, which express both TR isoforms, where *Lum* was dose-dependently downregulated upon T_4-administration [257]. This TH-dependent regulation presents itself complex in the context of the results of this work, where LUM was upregulated in the plasma proteome and on mRNA level after a two-week T_3 administration. In contrast, short-term thyrotoxicosis induced a reduction of *Lum* expression in bones of T_3-treated mice, which was also detectable in bones of mice carrying a mutation in *THRA*. The dissection of these effects by determining the *Lum* expression in primary OBs and OCs from TRα1+/m and TRβ-/- mice, revealed an induction of *Lum* expression upon chronic hypothyroid conditions in OBs and OCs of TRα1+/m mice, since bones predominantly express the TRα isoform. The chronic hyperthyroid state occurring in TRβ-/- mice lowers *Lum* expression in OBs, while it tends to increase it in OCs. In contrast to the results in eyes, no response to different TH concentrations could be detected in primary bone cell culture [257], indicating a variable regulation which depends on the duration of the pathophysiologic condition, but also the cellular prerequisites, including receptors, transporters and metabolising enzymes. Despite of these controversial results, plasma LUM concentration should not totally be excluded from the list of

putative TH biomarkers, but its strong involvement in tumour progression or suppression would require a careful assessment of the physiological LUM range in the plasma and external influencing factors should be considered as well.

The vascular cell adhesion molecule 1 (VCAM1) belongs to the immunoglobulin superfamily, is mainly expressed by endothelial cells and mediates the adhesion at and transendothelial migration through blood vessels for the recruitment of leukocytes at inflammation sites [258, 259]. Further investigations on the role of endothelial adhesion molecules revealed also an important role in the invasion and formation of metastasis [260, 261]. These processes mainly depend on the migration and proliferation of endothelial cells which was already demonstrated to depend on TH concentration [262, 263]. However, the circulating concentrations of VCAM1, although increased in common autoimmune thyroid diseases, like HT and GD, depends on the occurrence of anti-TPO or anti-TG antibodies instead of alteration of TH concentrations [264-266]. Since there are well-established immunoassays available to detect changes in these autoantibodies, there is a reduced need for an additional biomarker for these common TH disorders compared to rare disorders. Nevertheless, acute thyrotoxicosis increased VCAM1 concentrations in human and mouse plasma samples, which was also confirmed in T_3-treated animals on mRNA level in mouse liver tissue. In contrast to the two-week thyrotoxicosis, neither short term TH administration nor chronic TH disorders in TR mutant mice changed *Vcam1* expression significantly, which indicates an adaptation process that is accompanied by increased body weight and length in T_3-treated animals, which is not or not yet existing in TR mutant mice or upon short-term treatment [267]. Since VCAM1 is not robustly changed by different TH concentrations, it cannot be regarded as a new putative TH biomarker.

4.2.3 Proteins of the immune system

The cathelicidin-related antimicrobial peptide CAMP also known as human cationic antimicrobial peptide hCAP18 encoded by *CAMP* leads to a pre-proprotein from the class of antimicrobial peptides [268]. In humans, the sole discovered antimicrobial peptide is LL-37 which is produced by an enzymatically cleavage of the 37 C-terminally located amino acids of the CAMP pro-protein [269]. This peptide has an amphipathic α-helical structure with a net charge of +6 at neutral pH and is therefore capable to bind to the negatively charged plasma membrane of bacteria and accumulate there to form pores and hence perforate the outer cell membrane which leads to the lysis of microbes [270]. Cholesterol containing membranes are protected from this mechanism, therefore mammalian cell membranes are not destroyed by LL-37 [271]. Besides its bacteriolytical properties, LL-37 is capable to bind to transmembrane receptors, e.g. toll-like receptor 4, of host leukocytes and modulate or enhance their immunological status, depending on the context, towards

a pro- or anti-inflammatory activation or deactivation [270]. In turn, pro- and anti-inflammatory factors, which are not necessarily pathogen-associated, alter *Camp* expression and LL-37 abundance for instance under acute myocardial infarction or liver disease [272, 273]. The effect of THs on *Camp* expression has been described in only one previous publication, where supraphysiological concentrations of both T_3 and T_4 increased *Camp* expression in the human colonic adenocarcinoma cell line HT-29 [274]. In contrast, CAMP was less abundant in thyrotoxic human and mouse plasma samples in the here presented studies, while THs had no effect on *Camp* expression in liver, spleen or bone in mice, indicating a more complex regulation, depending on the tissue specific biological context which is integrated in the altered peripheral protein concentrations. The importance of context-dependent and tissue specific differences in *Camp* expression is even more pronounced in TR mutant mice. Here, the absence of the tissue-specific predominantly expressed TR isoform (TRβ in liver, TRα in spleen and bone) lead to upregulated *Camp* expression, while an inactivating mutation in the subordinate TR isoform had no detectable effect. Further research would be required to dissect whether these findings could be explained by the chronic hypothyroid condition in the respective tissues and if this integrates in increased systemic LL-37 levels in patients carrying a mutation in *THRA* or *THRB*.

The interleukin 1 receptor accessory protein 1 (IL1RAP) is known as an extracellular membrane protein, which dimerises with interleukin 1 receptor (IL-1R) and is essential for IL-1 induced signal transduction [275]. It is mainly expressed by $CD34^+$ and/or $CD38^+$ positive cells, which comprises hematopoietic stem and progenitor cells, endothelial (progenitor) cells, but also $CD4^+$, $CD8^+$ and B cells [276]. It is described as strongly associated with various forms of chronic myeloid leukaemia and acute myeloid leukaemia, which all share increased expression levels of IL1RAP [277, 278]. The connection between cytokine signalling and TH metabolism was shown in mice which received inactivating antibodies against pro-inflammatory cytokines (IL-1, TNFα and IL-6), which were previously shown to decrease serum T_3 levels and induce a disease termed as "non-thyroidal illness syndrome" (NTIS), and these antibodies abolished the described effects [279, 280]. On the other hand, it was already demonstrated that increased concentrations of T_3 increase the activity of innate immune cells, but decrease pro-inflammatory cytokine release [281]. The decreased levels of IL1RAP in human and mouse plasma samples, which were confirmed in the mouse liver transcriptome fit into the frame of an immunological activated organism, while acute pro-inflammatory cytokine responses were downregulated. Surprisingly, neither the effect of acute or short-term thyrotoxicosis, nor chronic TH disorders in TR mutant mice, had an influence on *Il1rap* expression in any of the investigated tissues and therefore indispose this target as a putative TH biomarker.

Peptidoglycan-recognition protein 2 (*Pgrp2*) is the largest member of the peptidoglycan-recognition protein (PGRPs) family, which act as microbial recognition and antimicrobial effector proteins by binding to the peptidoglycan content of bacterial cell wall, which results in the microbial lysis. PGRPs are highly conserved in all mammals, insects and several invertebrates and occur in 4 isoforms in humans with an identical conserved sequence of 42%, but a similar functional structure [282, 283]. PGRP2 is mainly expressed in the liver and secreted into the bloodstream and strongly depends on pathogen-associated molecular pattern (PAMP)-induced NF-κB and Sp1 signalling [284, 285], but no direct effect of TH has yet been described. Since *Prgp2* expression depends on TLR4 signal transduction, which was also the case for *Camp*, *Fetua* and *Lum*, a present immunological active state in thyrotoxic humans and mice is corroborated, which explains increased PGRP2 concentration in the plasma proteome samples. Increased *Pgrp2* expression has only been found in livers of TRα1+/m mice. In these mice, the innate immune system, as the first line host defence, is chronically undersupplied with TH and could influence the hepatic secretion of host defence proteins, as an adaption process to maintain the host ability to control invading pathogens. Despite this hypothesis about innate immune response under chronically hypothyroid conditions, *Pgrp2* expression cannot be regarded as a putative TH biomarker due to its limited alteration upon different TH concentration, since only a downregulation in MMI/ClO_4^--treated mice could be detected.

4.2.4 Maintenance and transport proteins

As part on the renin-angiotensin-aldosterone system the prohormone angiotensinogen (ANGT) is involved in blood pressure regulation and salt and liquid homeostasis. Its main function is the provision of a substrate reservoir for the renal enzyme renin, which cleaves ANGT into angiotensin I, which in turn is cleaved by the angiotensin converting enzyme into the biologically active form angiotensin II. ANGT is mainly secreted by the liver, but also by the kidney, lung and adrenal gland. Studies with rats indicated an increased *Angt* expression during hyperthyroidism in liver, but also a decrease of plasma ANGT upon chronic hypothyroid conditions [286, 287]. Cells of the rat hepatoma cell line H35 did also respond to increasing T_3 concentrations by increased mRNA levels of *Angt* and secretion of ANGT protein into the medium [287]. In contrast, *Angt* expression in cells of the human hepatocellular carcinoma cell line HepG2 did not respond to T_3 concentrations, but previous studies showed that TRα1 overexpressing HepG2 cells increased *Angt* expression upon T_3 stimulation [189]. Transient TRβ overexpression did not change HepG2 responsiveness to T_3, indicating a TRα dominated expression pattern. This TRα-mediated effect, whereas an absent TRβ effect has also been measured in vascular smooth muscle cells and aorta cells and these are predominantly TRα-expressing tissues in contrast to TRβ dominated liver tissue,

could not be confirmed in the here presented studies [288]. Despite missing TH-dependent alterations in hepatic *Angt* expression after the two-week treatment, it was decreased upon short-term T_4 treatment and tend to be decreased in TRα1+/m mice, which fits to the observation of the previous studies of fast responding *Angt* alteration upon T_3 stimulation, but this effect does not seem to be long lasting, as it was abolished after two weeks of treatment [289]. Even though *Angt* appeared to be a promising candidate as a TH biomarker, its highly fluctuating plasma concentrations due to environmental and pathological conditions (e.g. acute kidney injury), the short duration of expression alterations upon TH treatment and conflicting results with previous studies, excludes this highly abundant protein as a TH biomarker [290].

Abnormal spindle-like microcephaly-associated protein (*Aspm*), with its role in mitosis through microtubule minus-end regulation, was mainly described in the context of primary autosomal recessive microcephaly [291], where mutations in *ASPM* reduce the cortical volume in humans about 50% [292], but also malformation in testis and ovary accompanied by massive germ line cell loss have been described [293]. It has yet only been described in the context of THs when it was upregulated in anaplastic thyroid carcinoma [294]. In the present studies, it was upregulated only in bones of TRα1+/m mutant mice. However, this effect could not be validated in primary OBs or OCs and indicates an indirect effect whose function or mechanism remained enigmatic.

The glycoprotein α-2-Heremans-Schmid glycoprotein (AHSG), also termed as fetuin A (FETUA) is a highly abundant plasma protein and more than 95% of this protein are secreted by the liver [295, 296]. FETUA acts as an endogenous inhibitor of the insulin receptor tyrosine kinase and has adipogenic properties, which implies higher hepatic fat content upon FETUA accumulation or increased production [297]. More over FETUA stimulates the production of pro-inflammatory cytokines by acting as an endogenous ligand of the toll-like receptor 4 [298]. In addition, FETUA is altered under several diseases, like the metabolic syndrome (MetS), type 2 diabetes mellitus (T2DM) and non-alcoholic fatty liver disease (NAFLD) [299-302] and high FETUA concentrations are associated with a higher risk to develop cardiovascular disease [303]. Interestingly, one previous study has already linked FETUA concentrations with TH concentrations and found reduced FETUA levels in hypothyroid patients [304]. This is in line with the data presented here, where FETUA was increased in thyrotoxic human and mouse plasma samples, but also decreased on the mRNA level in livers of MMI/ClO_4^--treated mice. Surprisingly, the knock-out of TRβ, the predominantly expressed TR isoform in hepatocytes, did not affect *Fetua* expression, but mutation of TRα1 increased its expression. This finding supports the idea of an indirect regulatory mechanism, which could be mediated by a less active inflammatory status in TRα1+/m mutant mice, since it was shown that intracellular TH concentrations directly determine the activity of Neutrophils and Macrophages [305, 306]. A leukocyte-secreted mediation factor

could thus influence FETUA secretion. A putative role of FETUA as a biomarker of TH status therefore needs to be questioned not only because its regulatory mechanisms is unclear but particularly by the known strong impact of other disease entities such as T2DM, NAFLD and/or liver cirrhosis.

Transthyretin (TTR) is a highly abundant plasma and cerebrospinal fluid protein, mainly expressed by the liver and by the choroid plexus [307, 308]. It was then recognised, that TTR functions as a high-affinity TH transport protein in blood and as the major TH binding protein in the cerebrospinal fluid (CSF) [309, 310]. It was shown in previous studies, that *Ttr* expression depends on the hepatocyte nuclear factor-3 (HNF3), which interacts with the hepatocyte nuclear factor-4α (HNF4α) [311, 312]. In another study, it was shown that TH regulates SHBG expression via HNF4α [313]. This hypothetical regulatory mechanism has yet not been experimentally confirmed, but might be a reasonable explanation for the reduction in TTR abundance in plasma proteome data of thyrotoxic human and mice. A consumption effect, due to increased peripheral TH concentrations, can be excluded, since it was shown in a previous study, that TTR-null mice did not have alteration in plasma or CSF tT_4 or tT_3 concentrations, which implies a minor role of TTR for TH transport that can easily be absorbed by other TH transport proteins, like thyroxine-binding globulin [314]. These findings together with the fact, that *Ttr* was not altered in any other experimental setup, disqualifies transthyretin as a putative TH biomarker.

4.3 The functions of CD5L and its role under pathophysiological conditions

The protein apoptosis inhibitor of macrophages (AIM) was first described in 1997 as a new member of the class B scavenger receptor cysteine-rich (SRCR) family and termed as secreted protein α (SPα) [315]. Proteins of the SRCR family share the presence of one or more SRCR domains, which are involved in the recognition of PAMPs and play therefore an important role in the first line immune defence and homeostasis of epithelia. The SRCR family was introduced after the identification of many receptors which share high similarities to the type I class A scavenger receptor expressed by macrophages and they can occur either secreted or membrane bound [316]. When Gebe *et al.* determined the amino acid sequence of SPα, they found high similarities to the SRCR family members CD5 and CD6 like their three SRCR domains, but it lacks their transmembrane domain and was hence described as secreted protein. Since it was found expressed in many lymphoid tissue like liver, spleen, bone marrow and thymus, it was hypothesised, that SPα is important for the development and maintenance of lymphoid compartments [315]. This was proven two years later, when SPα, which was now termed as AIM, was characterised as a macrophage-secreted, active inhibitor of apoptosis in thymocytes [179]. Further research identified

SPα as IgM associated and invented the term CD5 antigen-like protein or CD5L, which was the official nomenclature henceforward, although AIM is synonymously still in use [317]. Despite the detection of SRCR family members across mammals and different vertebrates, analogues to human CD5L have only been described in mice, cats and, most recently, dogs [318-320]. The expression of *CD5L* directly depends on a Liver X receptor α (LXRα) responsive element (LXRE) at position -5404 in the *CD5L* promoter, activated by a LXRα/retinoid X receptor (RXR) dimer [181]. The regulation of *Cd5l* expression is even more complex, since a regulating SREBP-1 responsive element (SRE) with a corresponding E-box element at position -507 and a MafB response element at position -54 were detected [321]. After secretion, these analogues are mainly bound to IgM pentamers, where it is located in a 50° gap between two of the monomers which functions as a binding groove for one CD5L molecule [322, 323]. The identification of CD5L as a modulator of innate immune responses lead to investigations of its involvement in many chronic diseases where macrophages and other innate immune cells are typically implicated. First it was shown that *Cd5l* expression was increased in mice after induction of hepatitis and that CD5L-deficient mice develop more severe symptoms compared to wild type littermates [180]. The effect of increased CD5L concentrations was also detected in humans suffering from hepatic fibrosis due to a chronic hepatitis C infection, but also in patients with liver damage due to hepatocellular carcinomas [324, 325]. Further investigations revealed an active role of CD5L in the maintenance of tissue homeostasis and the control of the fibrotic progression [326]. In lung disease CD5L was increased in patients with chronic obstructive pulmonary disease (COPD) and lead to increased anti-apoptotic B cell lymphoma leukaemia (BcL-xL) which ultimately reduced the apoptotic capacity of alveolar macrophages and leads to lung tissue destruction and impaired efferocytosis due to inadequately active M1 macrophages [327-329]. In addition, the chronic myeloid-specific overexpression of CD5L lead to the formation of adenocarcinomas in the lung and links chronic lung diseases with the formation of cancer [330]. Conversely, CD5L shows a protective role against the formation of hepatocellular carcinoma by activating the complement system towards a necrotic cell death induction of tumour cells [331]. In the same study the authors mention that timing seems to be the important factor, as high CD5L concentrations prevent for tumour formation, but support the enlargement of existing tumours. This effect could be explained by the property of CD5L to drive unpolarised MΦ macrophages towards anti-inflammatory M2 macrophages, which are the main population of tumour associated macrophages that induce a microenvironment for facilitated tumour growth and protect against chemotherapeutic agents [332, 333], but further research on this topic is required to strengthen this hypothesis.

Recent studies showed that mice fed with high fat diet have increased CD5L serum concentrations and CD5L knock out mice gain more weight than wild type littermates, which can be rescued by

CD5L application, indicating a potential direct effect of CD5L on adipocytes [334]. The effect of CD5L on adipocytes is mediated by the scavenger receptor CD36 which is expressed on macrophages, but also on adipocytes and the interaction of CD5L with CD36 leads to the endocytosis of CD5L. Here, CD5L acts as an endogenous inhibitor of the fatty acid synthase (FAS), which leads to increased lipolysis, a strong promoter of macrophage infiltration into adipose tissue. Hence, CD5L contributes to obesity-mediated progression of the metabolic syndrome [335]. CD36 also mediates the uptake of oxidised low-density lipoproteins (oxLDL), an endogenous ligand of LXR and therefore a strong inducer of CD5L expression. At arterial sites of chronic inflammation, oxLDL-induced CD5L expression leads to reduced macrophage apoptosis, accompanied by increased cholesterol-laden macrophages, so called foam cells. The accumulation of foam cells constitutes to the formation of atherosclerotic plaques, which was demonstrated as being reduced in CD5L knock out mice [336-338]. Moreover, it was also demonstrated that mice, lacking CD5L, have less infiltration of pro-inflammatory M1 macrophages after myocardial infarct and have improved survival rates [339].

One additional function of pro-inflammatory macrophages is the host defence against invading pathogens and here CD5L also contributes as a broad range pathogen recognition receptor which is able to bind to lipopolysaccharides (LPS) of Gram-negative bacteria, lipoteichoic acid (LTA) of Gram-positive bacteria, but also some fungal species [340-342], which ultimately leads to pathogen lysis. By inhibiting apoptosis not only of macrophages but also of T cells and natural killer T cells, CD5L plays another role in host defence mechanisms [343]. In contrast to this, CD5L is a strong inhibitor of B cell proliferation, which highlights the ambiguity of this protein [344].

Since CD5L expression is tightly related to innate and adaptive host defence mechanisms, it was also found regulated in autoimmune diseases like Crohns' disease or systemic lupus erythematosus [345, 346]. The mechanism for correlation or regulation could not be elucidated, but the plausibility for these findings were supported by another study which identified CD5L as an essential switch for the Th17 cell pathogenicity or non-pathogenicity, which is a known factor for autoimmunity [177, 178].

The different described contexts of CD5L action highlight its important role as an immune-modulating protein that is involved in various pathologies. But this implies the limits for CD5L as a putative TH biomarker as well. CD5L levels should be always considered together with liver marker to exclude false positive reports due to liver cirrhosis, steatosis or cancer. Additionally, autoimmune, chronic and infectious diseases bear the risk of false interpretations. Therefore, CD5L could be recommended as an additional but not sole marker for difficult thyroid disorders.

4.4 CD5L as a biomarker for thyroid hormone pathologies and hepatic crosstalk

Despite the numerous functions of CD5L that have been identified by previous studies, no connection between CD5L and TH has been described so far. However, in the experiments presented here a clear link and also statistically significant correlation between peripheral TH concentrations *in vivo* and CD5L abundance in plasma and *Cd5l* expression in the liver was detectable. In addition, the correlation of CD5L expression with TH concentrations has a quick response and was already statistically significant after 24 h of experimental thyrotoxicosis. This is comparable to the alterations in gene expression of the well-established hepatic TH target genes *Spot14* and *Dio1*, which are suggested as robust marker genes, but only for research purposes, as these are no secreted proteins and would require liver biopsies [21]. This correlation was no longer detectable upon chronic pathological TH conditions that occur in TR mutant mice, although CD5L expression tended to be decreased in livers of TRα1+/m mice. Surprisingly, neither HepG2 cells nor primary hepatocytes showed a *Cd5l* expression, thus indicating a peripheral origin of expression due to a similar expression pattern in spleen and bone with a moderate increase upon T_4 treatment but a clear increase upon T_3 treatment. This is in line with early publications on this topic that identified numerous lymphatic tissues, like liver, thymus and spleen, as sources for CD5L expression and also Th17 cells [177-179]. The cell sorting approach did not confirm *Cd5l* expression in any of the isolated leukocyte populations. Since *Cd5l* expression was neither described by previous studies in any B cell or circulating monocyte population nor did the T cell population contain inflammation site-specific Th17 cells, the main source for *Cd5l* expression remains as tissue-resident cells.

Tissue-resident macrophages were early identified as main source for CD5L secretion. Two main populations of macrophages occur in liver. The first main population of liver-resident macrophages are Kupffer cells (KCs), which constitute a locally proliferating, self-sustaining and tolerogenic macrophage population that derive from fetal liver-derived erythro-myeloid progenitors in humans and yolk sac-derived erythro-myeloid progenitors in mice [347-350]. The second main population of macrophages are monocyte-derived macrophages, often referred to as MoMFs, which are classically divided into pro-inflammatory M1 macrophages or anti-inflammatory M2 macrophages, but recent studies identified rather a macrophage spectrum than distinct classes [351]. KCs are statically located along the sinusoid endothelial cells and are hence able to sense and phagocyte potentially harmful antigens from the blood circulation and tissue site [352]. Here they are responsible to maintain liver homeostasis by degrading aged or damaged erythrocytes, digestive products and microbial antigens from the small and large intestine, but also invading pathogens and cellular debris after cell death or injury. Under physiological conditions, KCs are the greatest

macrophage population in the liver and occur in a ratio of 20-40 KCs per 100 hepatocytes [353]. After recognising danger- or pathogen-associated molecular patterns (DAMPs or PAMPs), they attract other innate immune cells, like neutrophils or monocytes, by secreting pro-inflammatory cytokines [354]. Depending on the spatial microenvironment, invading monocytes polarise into macrophages with pro- or anti-inflammatory phenotype and support KCs with tissue clearance or at later stages also with tissue restoration [355, 356]. In contrast to KCs, MoMFs have a relatively short half-life of about 20 h to two days depending on their function [357]. However, in murine models for chronic liver disorders, MoMFs account for the majority of liver-resident macrophages with overlapping surface marker patterns and it was also observed that, in KCs depleted mouse models, MoMFs were able to replenish liver-resident macrophages within two to four weeks [349, 358, 359]. Since the stimulation of monocytes with typical extracellular stimuli results in a spectrum of activated states and not defined M1 or M2 polarisation states, a clear discrimination between KCs and MoMFs is still challenging and requires sophisticated cell-tracking tools [349, 360]. Since the main population for CD5L expression was not totally clear, *Cd5l* expression upon different TH concentrations should be determined in pro-inflammatory BMDMs, as they were already described as a CD5L secreting population [336]. It could also be shown that isolated liver-residing macrophages change their expression pattern quickly, leading to a total loss of CD5L expression after 16 h in cell culture and excludes them for further investigation [179]. Interestingly, in primary OB and OC culture, *Cd5l* expression could also be determined and was significantly altered in TRβ-/- mice, but in opposed direction, indicating either different BMDM populations that developed due to different cytokine supply in the media or that BMDMs from TRβ-/- mice underwent phenotypic changes due to the hyperthyroid microenvironment in the bone marrow. To ensure most reliable results, BMDMs were generated by differentiating HSPCs into unpolarised MΦ, which were polarised by a combined treatment with interferon-γ and LPS, the gold standard method to produce M1 BMDMs [351, 360]. The binding of the ligand bound LXR to a LXRE in *Cd5l* promoter represents an essential factor for *Cd5l* expression [181]. LXREs and TREs share the same DNA recognising consensus sequence, which are direct repeating variations of AGGTCA with a 4 bp linker nucleotides sequence in between (DR4 motif). Moreover, overlapping actions for both the receptors and the ligands have been described in previous studies for other LXR target genes, for example *Chrebp*, *Cyp7a1* and *Srebp-1c* [361-363] and the LXRα expression itself is regulated by TRs [364]. The treatment of M1 polarised BMDMs with the LXR agonist T1317 raised *Cd5l* expression drastically, while different concentrations of T_3 over the same stimulation period had no effect, despite existing TRs [365, 366]. The expression of *Cd5l* in TRα1+/m mice was about 50% reduced compared to wild type littermates and this ratio stayed constant even after treatment with T1317. TRα is the predominantly expressed TR isoform in macrophages, therefore BMDMs

from TRα1+/m mice exhibit a chronically hypothyroid status. This chronic TH disorder results in impaired polarisation into M1 macrophages and less pro-inflammatory activity, which highlights the importance of TH signalling on *Cd5l* expression [366]. Most interestingly, *Cd5l* expression in BMDMs from TRβ-/- mice were unreceptive for T1317 treatment, which indicates two possible effects. Firstly, intracellular LXRα signalling in BMDMs depends on intact TRα mediated signalling, and secondly an extracellular mechanism depends on TRβ signalling, due to the fact that either the LXR agonist wasn't able to enter the BMDMs or a TRβ-dependent co-factor was not available. TRα is the predominantly expressed TR isoform in macrophages and therefore, increased peripheral TH concentrations that occur in TRβ-/- mice induce a chronic thyrotoxic microenvironment for mature macrophages and precursor cells in the bone marrow. Since the effect of TRβ knock out was detectable in BMDMs, differentiated from HSPCs, the thyrotoxic microenvironment in the bone marrow induced changes in stem cell physiology. Increased TH concentrations result in HSPCs in increased expression of TSHR to maintain TSH signalling, which appears to be essential for later proliferation and inhibition of premature differentiation steps [367, 368]. In TRβ-/- mice, increased TH concentrations are accompanied by increased TSH concentration leading to a massive overstimulation of the TSHR. Despite one study showed only slight changes in macrophage gene expression pattern after five days of recombinant TSH treatment, not much information are available about the effect of increased TSH signalling in HSPCs and its role on macrophage differentiation [369]. Further research on this topic is required to elucidate putative roles of chronically increased TSH signalling on macrophage function, but also other secondary signals that are not considered in this context so far could account for an indirect HSPC modification. One possibility could be the increased cyclic adenosine monophosphate (cAMP) production due to increased TSH signalling, which subsequently reduce CD36 expression and lead therefore to decreased oxLDL uptake, which could be one explanation for hampered *Cd5l* expression [370-372]. As described above, CD5L is mainly secreted by liver-resident macrophages which strongly relies on hepatocyte-derived signals, hence a hepatocyte-macrophage crosstalk that results in altered *Cd5l* expression appeared plausible. This was confirmed by the stimulation of M1 polarised BMDMs with HepG2- or primary hepatocyte-primed medium, which both increased *Cd5l* expression about 2-fold.

This study outlines the dependence of *Cd5l* expression in M1 macrophages on pathophysiological TH concentrations and a disturbed TH metabolism, but could not finally decipher the underlying mechanism. Since this correlation appears to be mediated by an indirect effect which depends on a hepatocyte/macrophage crosstalk, the involvement of cholesterol as one of the major interchangeable molecules requires a deeper consideration. The treatment of hypercholesterolaemia by induction of hyperthyroidism is a long-known effect which bases on the

finding that TH reduces serum triglyceride, cholesterol content and lipoprotein abundance by an increase in bile acid production in humans and mice [373, 374]. Despite these detailed information, there is conflicting data about the effects of TH on peripheral concentrations of oxidised LDL particles (oxLDL) [375-378]. However, increasing T_3 concentrations raise the intracellular oxidative stress in the liver, a major cause for oxLDL production [379]. Circulating oxLDL particles are mainly produced in the liver as intermediate particles in bile acid production, and are also incorporated into macrophages via CD36 transporters. They act as an endogenous ligand of LXR, thus driving the transcription of LXR target genes, e.g. *Cd5l*. However, increased oxLDL concentrations would be expected under hyperthyroid conditions but so far, any clear experimental proof remains elusive [380-383]. TRβ is the predominantly abundant TR isoform in the liver and consequently the whole cholesterol metabolism depends on TRβ as well and is therefore dysregulated in TRβ-/- mice. The missing responsiveness of BMDMs from TRβ-/- mice towards physiological hepatic signalling from hepatocyte-primed medium, suggests an unidentified TR target gene, called here *Gene X*, that is incorporated by liver-resident macrophages and could act in two different ways. First, it could directly influence the binding of LXR with its ligands (oxLDL or T1317) and is therefore an essential co-activator of the LXR/RXR dimer as an associated part of the transcription machinery. This would also explain the missing response to T1317, as the Gene X should be absent in BMDMs from TRβ-/- mice. Second, Gene X could be an essential co-activator of another *Cd5l*-regulating protein, called here Gene Y. The TRα-regulated Gene Y could constitute another co-activator for *Cd5l* expression, but might have a smaller interfering effect on the transcription machinery. Therefore, T1317 raised *Cd5l* expression in BMDMs from TRα1+/m mice with the same factor as in wild type BMDMs. One could now speculate that this could also be due to a reduced activity of BMDMs from TRα+/m mice, but gene expression of M1 marker genes were not altered compared to wild type. The increase of *Il10* in BMDMs from TRα1+/m mice suggests a more M2-like phenotype, while *Argi1*, another M2 marker was not altered and indicates an only slightly changed M1 phenotype compared to the other TR genotypes. Since gene expression analyses are not optimal to characterise cells and their putative functions, a flow cytometric determination of M1/M2 marker protein abundance would give a clearer answer to that question.

A regulation of the scavenger receptor and transmembrane transporter CD36 or the LXRα receptor could lead to altered *Cd5l* expression and were therefore determined in BMDMs from TR mutant mice. While the expression of *Cd36* appeared to be unaffected by mutations in *Thra* or *Thrb*, *Nr1h3* (LXRα) expression was highly increased in BMDMs from TRβ-/- mice. Surprisingly, no differences could be observed in TRα1+/m mice, indicating a TH-independent effect. It is also known from previous studies that the induction of LXR signalling leads to a more M2-like

phenotype, while a knock-out of LXR or its pharmacological downregulation has a pro-inflammatory effect [384-386]. Since the promoter region of *Nr1h3* has not yet been a target of intensive research, only one responsive element for the peroxisome proliferator-activated receptor α (PPARα) (PPRE) and one LXRE for LXRα have been identified. The main inducers for PPARα-mediated transcription has been identified as oxysterols, fatty acids and fatty acid-derived metabolites, suggesting a disturbed fatty acid metabolism in HSPCs and BMDMs from TRβ-/- mice. This finding is novel for TRβ knock out mice and requires further research [387, 388]. In human patients with RTH some cases were described with increased cholesterol and triglyceride content in serum, although this finding strongly depends on the specific mutation and is not shared by all patients [389]. There is conflicting data available for the promoter sequence of *Nr1h3*, which is described either with a LXRE at -2900 bp upstream of transcription starting site and no TRE or with one TRE between -1300 and -1240 bp upstream and no LXRE [364, 390]. A final conclusion about this discrepancy can't be made, but the absence of a TH-dependent *Nr1h3* expression (data not shown), suggests a regulation that depends more on PPARα and intracellular cholesterol and triglyceride content, since whole cholesterol metabolism depends TRβ that is hampered in TRβ-/- mice [391]. A summary of these findings is depicted in **Figure 26**.

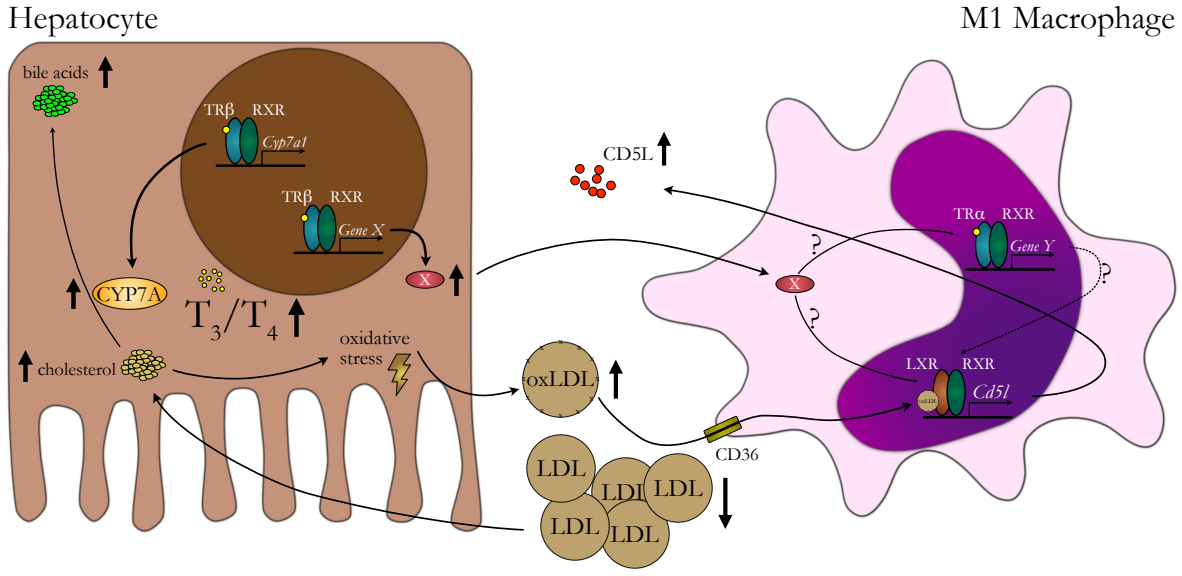

Figure 26 | Schematic overview of TH-dependent hepatocyte / macrophage cross-talk and *Cd5l* expression. Increased levels of intracellular THs lead to increased hepatic *Cyp7a1* expression that results in increased bile acid production accompanied by raised intracellular cholesterol concentrations due to enhanced LDL uptake from the blood stream. Higher rates of cholesterol catabolism generate higher levels of oxidative stress, due to intermediate reactive oxygen species, which oxidise LDL particles that are released into the periphery as oxLDL particles. These oxLDL particles are incorporated into macrophages and act as a ligand for LXR-regulated transcription of target genes, like *Cd5l*. TRβ-regulated gene expression in the liver of the unidentified gene X, could lead to increased X secretion and finally incorporation into macrophages. Here, X acts in two suspected ways. First, it interferes with oxLDL/LXR interaction via a not clear mechanism and mediates a TRβ-dependent effect on *Cd5l* expression. Second, it could regulate the TRα-dependent expression of an unidentified gene Y that constitutes another factor for *Cd5l* expression. CD36 – fatty acid translocase; *Cyp7a1* – cholesterol 7α-hydroxylase; LDL – low density lipoprotein; RXR – retinoid X receptor.

4.5 Outlook

Clinical endocrine conditions like resistance to TH, TSH-secreting pituitary adenoma or thyroidectomised patients share the problem of inconclusive or shallow results of routine parameters. The present study was designed in search for new tissue-specific TH-dependent biomarkers and was able to identify interesting candidates among them CAMP, FBLN1 or LUM and most promising the macrophage-derived serum protein CD5L. The constant and fast adaptation in gene expression of CD5L to comparable thyrotoxic states in independent, different studies, mark CD5L as a putative new TH biomarker. Currently the most important step for its characterisation as a clinical parameter is however missing as the development of an accurate and reliable bioassay to asses CD5L serum concentrations under various clinical conditions is outstanding. Available studies used *Cd5l* knock out mice and employed tissue-validated, but self-made, polyclonal anti-CD5L antibodies assays to determine serum or tissue concentration [326, 341, 392]. These assays already indicate high serum concentrations of CD5L in the range of 1-10 µg/ml with age and sex-specific alterations. Women appeared to have higher levels than men and serum concentrations decrease with age [321, 393]. Except for one, none of the utilised antibodies are commercially available, which is due to their small-scale and elaborative production. The one commercialised antibody did not support the data of increased CD5L under thyrotoxic conditions that were determined in the proteomics approach and raised questions about its specificity. This finding emphasises the need for robust and specific monoclonal antibodies to generate functional CD5L bioassays to determine its concentrations in cohorts of different thyroid pathologies. The verification of the treatment success was performed by using the established TH-dependent and liver-secreted protein ceruloplasmin, which showed the expected changes [171]. It could be possible that CD5L on the protein level behaves differently compared to *Cd5l* on the mRNA level, but inconsistent results across different western blots, as presented here, raised questions about the reliability of the antibody, which might be due batch problems, but highlights the demand for a professional and large-scale bioassay. It is problematic to translate findings made on the mRNA level, on the protein level, but preliminary data from serum relative CD5L concentrations in patients with overt hypo- or hyperthyroidism support the data from the mRNA level (Nock *et al.* (2020), under revision). Nonetheless, a constant increase of *Cd5l* expression about 2.5-fold upon T_4 treatment after 4 days would be sufficient for clinical practise where first measurements after initiation of the therapy are recommended after 4-12 weeks [109, 394].

To decipher the mechanism that drives *Cd5l* expression remains for further investigations and leaves the most important open question about how CD5L concentrations would change in chronic TH disorders. The tendency of decreased *Cd5l* expression in livers of TRα1+/m mice

could become significant on the protein level if the significance on the mRNA level got lost due to a dilution effect that occurred because the responsible M1 population appeared only to a minor extend in the liver. To estimate changes in CD5L abundance in patients with RTH it is important to find out, which of the identified effects on *Cd5l* expression plays the dominant role and result in increased or decreased CD5L concentrations or if they abolish themselves and CD5L would not be changed.

Taking all of these findings together, the optimisation of diagnosis and treatment of TH disorders have not yet come to an end and future research is still able to expedite the status quo and improve clinical outcomes. The here identified CD5L could therefore contribute to facilitate challenging differential diagnoses, e.g. differentiation between RTHβ and TSHoma, identification of patients with RTHα, optimisation of thyroxine supplementation. However, the validity and limitations of its use as a clinical biomarker still have to be determined in large independent cohort studies.

5 References

1. Yen PM, (2001) Physiological and molecular basis of thyroid hormone action. *Physiol Rev* 81: 1097-1142.
2. Oppenheimer JH, Schwartz HL, Surks MI, (1974) Tissue differences in the concentration of triiodothyronine nuclear binding sites in the rat: liver, kidney, pituitary, heart, brain, spleen, and testis. *Endocrinology* 95: 897-903.
3. Bernal J, Guadano-Ferraz A, Morte B, (2015) Thyroid hormone transporters--functions and clinical implications. *Nat Rev Endocrinol* 11: 406-417.
4. Rutigliano G, Zucchi R, (2017) Cardiac actions of thyroid hormone metabolites. *Mol Cell Endocrinol* 458: 76-81.
5. Williams GR, (2013) Thyroid hormone actions in cartilage and bone. *Eur Thyroid J* 2: 3-13.
6. Bloise FF, Cordeiro A, Ortiga-Carvalho TM, (2018) Role of thyroid hormone in skeletal muscle physiology. *J Endocrinol* 236: R57-R68.
7. Kline G, Sadrzadeh H (2017) Chapter 2 - Thyroid disorders. In: Sadrzadeh H, Kline G (eds) Endocrine Biomarkers. Elsevier, 41-93.
8. Baumann E, (1896) Der Jodgehalt der Schilddruessen von Menschen und Thieren. *Hoppe-Seyler's Zeitschrift für Physiologische Chemie* 22: 1-17.
9. Purtell K, Paroder-Belenitsky M, Reyna-Neyra A, Nicola JP, Koba W, Fine E, . . . Abbott GW, (2012) The KCNQ1-KCNE2 K(+) channel is required for adequate thyroid I(-) uptake. *FASEB J* 26: 3252-3259.
10. Wolff J, Chaikoff IL, (1948) Plasma inorganic iodide as a homeostatic regulator of thyroid function. *The Journal of biological chemistry* 174: 555-564.
11. Scott DA, Wang R, Kreman TM, Sheffield VC, Karniski LP, (1999) The Pendred syndrome gene encodes a chloride-iodide transport protein. *Nat Genet* 21: 440-443.
12. van den Hove MF, Croizet-Berger K, Jouret F, Guggino SE, Guggino WB, Devuyst O, Courtoy PJ, (2006) The loss of the chloride channel, ClC-5, delays apical iodide efflux and induces a euthyroid goiter in the mouse thyroid gland. *Endocrinology* 147: 1287-1296.
13. Iosco C, Cosentino C, Sirna L, Romano R, Cursano S, Mongia A, . . . Rhoden KJ, (2014) Anoctamin 1 is apically expressed on thyroid follicular cells and contributes to ATP- and calcium-activated iodide efflux. *Cell Physiol Biochem* 34: 966-980.
14. Taurog A, (1999) Molecular evolution of thyroid peroxidase. *Biochimie* 81: 557-562.
15. De Deken X, Corvilain B, Dumont JE, Miot F, (2014) Roles of DUOX-mediated hydrogen peroxide in metabolism, host defense, and signaling. *Antioxid Redox Signal* 20: 2776-2793.
16. Gavaret JM, Cahnmann HJ, Nunez J, (1981) Thyroid hormone synthesis in thyroglobulin. The mechanism of the coupling reaction. *J Biol Chem* 256: 9167-9173.
17. Ferreira AC, Lima LP, Araujo RL, Muller G, Rocha RP, Rosenthal D, Carvalho DP, (2005) Rapid regulation of thyroid sodium-iodide symporter activity by thyrotrophin and iodine. *J Endocrinol* 184: 69-76.
18. Targovnik HM, Citterio CE, Rivolta CM, (2017) Iodide handling disorders (NIS, TPO, TG, IYD). *Best Pract Res Clin Endocrinol Metab* 31: 195-212.
19. de Souza EC, Dias GR, Cardoso RC, Lima LP, Fortunato RS, Visser TJ, . . . Carvalho DP, (2015) MCT8 is Downregulated by Short Time Iodine Overload in the Thyroid Gland of Rats. *Horm Metab Res* 47: 910-915.
20. Bartalena L, (1990) Recent achievements in studies on thyroid hormone-binding proteins. *Endocr Rev* 11: 47-64.
21. Bianco AC, Anderson G, Forrest D, Galton VA, Gereben B, Kim BW, . . . Action, (2014) American Thyroid Association Guide to investigating thyroid hormone economy and action in rodent and cell models. *Thyroid* 24: 88-168.
22. Abe T, Kakyo M, Sakagami H, Tokui T, Nishio T, Tanemoto M, . . . Yawo H, (1998) Molecular characterization and tissue distribution of a new organic anion transporter subtype (oatp3) that transports thyroid hormones and taurocholate and comparison with oatp2. *J Biol Chem* 273: 22395-22401.
23. Friesema EC, Ganguly S, Abdalla A, Manning Fox JE, Halestrap AP, Visser TJ, (2003) Identification of monocarboxylate transporter 8 as a specific thyroid hormone transporter. *J Biol Chem* 278: 40128-40135.

24. Friesema EC, Jansen J, Jachtenberg JW, Visser WE, Kester MH, Visser TJ, (2008) Effective cellular uptake and efflux of thyroid hormone by human monocarboxylate transporter 10. *Mol Endocrinol* 22: 1357-1369.
25. Krause G, Hinz KM, (2017) Thyroid hormone transport across L-type amino acid transporters: What can molecular modelling tell us? *Mol Cell Endocrinol* 458: 68-75.
26. Pizzagalli F, Hagenbuch B, Stieger B, Klenk U, Folkers G, Meier PJ, (2002) Identification of a novel human organic anion transporting polypeptide as a high affinity thyroxine transporter. *Mol Endocrinol* 16: 2283-2296.
27. Escobar-Morreale HF, Obregon MJ, Escobar del Rey F, Morreale de Escobar G, (1995) Replacement therapy for hypothyroidism with thyroxine alone does not ensure euthyroidism in all tissues, as studied in thyroidectomized rats. *J Clin Invest* 96: 2828-2838.
28. Horst C, Rokos H, Seitz HJ, (1989) Rapid stimulation of hepatic oxygen consumption by 3,5-di-iodo-L-thyronine. *Biochem J* 261: 945-950.
29. Moreno M, Lanni A, Lombardi A, Goglia F, (1997) How the thyroid controls metabolism in the rat: different roles for triiodothyronine and diiodothyronines. *J Physiol* 505 (Pt 2): 529-538.
30. Moreno M, Giacco A, Di Munno C, Goglia F, (2017) Direct and rapid effects of 3,5-diiodo-L-thyronine (T2). *Mol Cell Endocrinol* 458: 121-126.
31. Bianco AC, Kim BW, (2006) Deiodinases: implications of the local control of thyroid hormone action. *J Clin Invest* 116: 2571-2579.
32. Bianco AC, Salvatore D, Gereben B, Berry MJ, Larsen PR, (2002) Biochemistry, cellular and molecular biology, and physiological roles of the iodothyronine selenodeiodinases. *Endocr Rev* 23: 38-89.
33. Bianco AC, Dumitrescu A, Gereben B, Ribeiro MO, Fonseca TL, Fernandes GW, Bocco B, (2019) Paradigms of Dynamic Control of Thyroid Hormone Signaling. *Endocr Rev* 40: 1000-1047.
34. Gogakos AI, Duncan Bassett JH, Williams GR, (2010) Thyroid and bone. *Arch Biochem Biophys* 503: 129-136.
35. Galton VA, de Waard E, Parlow AF, St Germain DL, Hernandez A, (2014) Life without the iodothyronine deiodinases. *Endocrinology* 155: 4081-4087.
36. Sap J, Munoz A, Damm K, Goldberg Y, Ghysdael J, Leutz A, . . . Vennstrom B, (1986) The c-erb-A protein is a high-affinity receptor for thyroid hormone. *Nature* 324: 635-640.
37. Hollenberg AN, Monden T, Wondisford FE, (1995) Ligand-independent and -dependent functions of thyroid hormone receptor isoforms depend upon their distinct amino termini. *J Biol Chem* 270: 14274-14280.
38. Mullur R, Liu YY, Brent GA, (2014) Thyroid hormone regulation of metabolism. *Physiol Rev* 94: 355-382.
39. Cheng SY, Leonard JL, Davis PJ, (2010) Molecular aspects of thyroid hormone actions. *Endocr Rev* 31: 139-170.
40. Chatonnet F, Guyot R, Benoit G, Flamant F, (2013) Genome-wide analysis of thyroid hormone receptors shared and specific functions in neural cells. *Proc Natl Acad Sci U S A* 110: E766-775.
41. Ramadoss P, Abraham BJ, Tsai L, Zhou Y, Costa-e-Sousa RH, Ye F, . . . Hollenberg AN, (2014) Novel mechanism of positive versus negative regulation by thyroid hormone receptor beta1 (TRbeta1) identified by genome-wide profiling of binding sites in mouse liver. *J Biol Chem* 289: 1313-1328.
42. Wagner RL, Apriletti JW, McGrath ME, West BL, Baxter JD, Fletterick RJ, (1995) A structural role for hormone in the thyroid hormone receptor. *Nature* 378: 690-697.
43. Feng W, Ribeiro RC, Wagner RL, Nguyen H, Apriletti JW, Fletterick RJ, . . . West BL, (1998) Hormone-dependent coactivator binding to a hydrophobic cleft on nuclear receptors. *Science* 280: 1747-1749.
44. Cohen RN, Brzostek S, Kim B, Chorev M, Wondisford FE, Hollenberg AN, (2001) The specificity of interactions between nuclear hormone receptors and corepressors is mediated by distinct amino acid sequences within the interacting domains. *Mol Endocrinol* 15: 1049-1061.
45. Yen PM, Ando S, Feng X, Liu Y, Maruvada P, Xia X, (2006) Thyroid hormone action at the cellular, genomic and target gene levels. *Mol Cell Endocrinol* 246: 121-127.
46. Schweizer U, Towell H, Vit A, Rodriguez-Ruiz A, Steegborn C, (2017) Structural aspects of thyroid hormone binding to proteins and competitive interactions with natural and synthetic compounds. *Mol Cell Endocrinol* 458: 57-67.

47. McKenna NJ, O'Malley BW, (2002) Minireview: nuclear receptor coactivators--an update. *Endocrinology* 143: 2461-2465.
48. Mendoza A, Astapova I, Shimizu H, Gallop MR, Al-Sowaimel L, MacGowan SMD, . . . Hollenberg AN, (2017) NCoR1-independent mechanism plays a role in the action of the unliganded thyroid hormone receptor. *Proc Natl Acad Sci U S A* 114: E8458-E8467.
49. Vujovic M, Nordstrom K, Gauthier K, Flamant F, Visser TJ, Vennstrom B, Mittag J, (2009) Interference of a mutant thyroid hormone receptor alpha1 with hepatic glucose metabolism. *Endocrinology* 150: 2940-2947.
50. Wrutniak-Cabello C, Casas F, Cabello G, (2017) Mitochondrial T3 receptor and targets. *Mol Cell Endocrinol* 458: 112-120.
51. Cook CB, Koenig RJ, (1990) Expression of erbA alpha and beta mRNAs in regions of adult rat brain. *Mol Cell Endocrinol* 70: 13-20.
52. Bradley DJ, Towle HC, Young WS, 3rd, (1992) Spatial and temporal expression of alpha- and beta-thyroid hormone receptor mRNAs, including the beta 2-subtype, in the developing mammalian nervous system. *J Neurosci* 12: 2288-2302.
53. Bradley DJ, Towle HC, Young WS, 3rd, (1994) Alpha and beta thyroid hormone receptor (TR) gene expression during auditory neurogenesis: evidence for TR isoform-specific transcriptional regulation in vivo. *Proc Natl Acad Sci U S A* 91: 439-443.
54. Lin JZ, Sieglaff DH, Yuan C, Su J, Arumanayagam AS, Firouzbakht S, . . . Webb P, (2013) Gene specific actions of thyroid hormone receptor subtypes. *PLoS One* 8: e52407.
55. Forrest D, (2002) THE THYROID HORMONE RECEPTOR FAMILY: INSIGHTS FROM KNOCKOUTS. *Hot Thyroidology* 3.
56. Flamant F, Gauthier K, (2013) Thyroid hormone receptors: the challenge of elucidating isotype-specific functions and cell-specific response. *Biochim Biophys Acta* 1830: 3900-3907.
57. De Vito P, Balducci V, Leone S, Percario Z, Mangino G, Davis PJ, . . . Incerpi S, (2012) Nongenomic effects of thyroid hormones on the immune system cells: New targets, old players. *Steroids* 77: 988-995.
58. Davis PJ, Goglia F, Leonard JL, (2016) Nongenomic actions of thyroid hormone. *Nat Rev Endocrinol* 12: 111-121.
59. Flamant F, Cheng SY, Hollenberg AN, Moeller LC, Samarut J, Wondisford FE, . . . Refetoff S, (2017) Thyroid Hormone Signaling Pathways: Time for a More Precise Nomenclature. *Endocrinology* 158: 2052-2057.
60. Hones GS, Rakov H, Logan J, Liao XH, Werbenko E, Pollard AS, . . . Moeller LC, (2017) Noncanonical thyroid hormone signaling mediates cardiometabolic effects in vivo. *Proc Natl Acad Sci U S A* 114: E11323-E11332.
61. Anyetei-Anum CS, Roggero VR, Allison LA, (2018) Thyroid hormone receptor localization in target tissues. *Journal of Endocrinology* 237: R19-R34.
62. Hynes RO, (1992) Integrins: versatility, modulation, and signaling in cell adhesion. *Cell* 69: 11-25.
63. Barja-Fidalgo C, Coelho AL, Saldanha-Gama R, Helal-Neto E, Mariano-Oliveira A, Freitas MS, (2005) Disintegrins: integrin selective ligands which activate integrin-coupled signaling and modulate leukocyte functions. *Braz J Med Biol Res* 38: 1513-1520.
64. Gachkar S, Nock S, Geissler C, Oelkrug R, Johann K, Resch J, . . . Mittag J, (2019) Aortic effects of thyroid hormone in male mice. *J Mol Endocrinol* 62: 91-99.
65. Vanderpump MP, (2011) The epidemiology of thyroid disease. *Br Med Bull* 99: 39-51.
66. De Leo S, Lee SY, Braverman LE, (2016) Hyperthyroidism. *Lancet* 388: 906-918.
67. Marino M, Latrofa F, Menconi F, Chiovato L, Vitti P, (2015) Role of genetic and non-genetic factors in the etiology of Graves' disease. *J Endocrinol Invest* 38: 283-294.
68. Pearce SH, Brabant G, Duntas LH, Monzani F, Peeters RP, Razvi S, Wemeau JL, (2013) 2013 ETA Guideline: Management of Subclinical Hypothyroidism. *Eur Thyroid J* 2: 215-228.
69. Laurberg P, Cerqueira C, Ovesen L, Rasmussen LB, Perrild H, Andersen S, . . . Carle A, (2010) Iodine intake as a determinant of thyroid disorders in populations. *Best Pract Res Clin Endocrinol Metab* 24: 13-27.
70. Laurberg P, Pedersen KM, Vestergaard H, Sigurdsson G, (1991) High incidence of multinodular toxic goitre in the elderly population in a low iodine intake area vs. high incidence of Graves' disease in the young in a high iodine intake area: comparative surveys of thyrotoxicosis epidemiology in East-Jutland Denmark and Iceland. *J Intern Med* 229: 415-420.

71. Schwartz F, Bergmann N, Zerahn B, Faber J, (2013) Incidence rate of symptomatic painless thyroiditis presenting with thyrotoxicosis in Denmark as evaluated by consecutive thyroid scintigraphies. *Scand J Clin Lab Invest* 73: 240-244.
72. Pearce EN, Farwell AP, Braverman LE, (2003) Thyroiditis. *N Engl J Med* 348: 2646-2655.
73. Alexander EK, Pearce EN, Brent GA, Brown RS, Chen H, Dosiou C, . . . Sullivan S, (2017) 2017 Guidelines of the American Thyroid Association for the Diagnosis and Management of Thyroid Disease During Pregnancy and the Postpartum. *Thyroid* 27: 315-389.
74. Clarke MJ, Erickson D, Castro MR, Atkinson JL, (2008) Thyroid-stimulating hormone pituitary adenomas. *J Neurosurg* 109: 17-22.
75. Yamada S, Fukuhara N, Horiguchi K, Yamaguchi-Okada M, Nishioka H, Takeshita A, . . . Inoshita N, (2014) Clinicopathological characteristics and therapeutic outcomes in thyrotropin-secreting pituitary adenomas: a single-center study of 90 cases. *J Neurosurg* 121: 1462-1473.
76. Taylor PN, Albrecht D, Scholz A, Gutierrez-Buey G, Lazarus JH, Dayan CM, Okosieme OE, (2018) Global epidemiology of hyperthyroidism and hypothyroidism. *Nat Rev Endocrinol* 14: 301-316.
77. Aoki Y, Belin RM, Clickner R, Jeffries R, Phillips L, Mahaffey KR, (2007) Serum TSH and total T4 in the United States population and their association with participant characteristics: National Health and Nutrition Examination Survey (NHANES 1999-2002). *Thyroid* 17: 1211-1223.
78. Hiromatsu Y, Satoh H, Amino N, (2013) Hashimoto's thyroiditis: history and future outlook. *Hormones (Athens)* 12: 12-18.
79. Hollowell JG, Staehling NW, Flanders WD, Hannon WH, Gunter EW, Spencer CA, Braverman LE, (2002) Serum TSH, T(4), and thyroid antibodies in the United States population (1988 to 1994): National Health and Nutrition Examination Survey (NHANES III). *J Clin Endocrinol Metab* 87: 489-499.
80. Medici M, Porcu E, Pistis G, Teumer A, Brown SJ, Jensen RA, . . . Peeters RP, (2014) Identification of novel genetic Loci associated with thyroid peroxidase antibodies and clinical thyroid disease. *PLoS Genet* 10: e1004123.
81. Schultheiss UT, Teumer A, Medici M, Li Y, Daya N, Chaker L, . . . Kottgen A, (2015) A genetic risk score for thyroid peroxidase antibodies associates with clinical thyroid disease in community-based populations. *J Clin Endocrinol Metab* 100: E799-807.
82. Kahraman D, Keller C, Schneider C, Eschner W, Sudbrock F, Schmidt M, . . . Kobe C, (2012) Development of hypothyroidism during long-term follow-up of patients with toxic nodular goitre after radioiodine therapy. *Clin Endocrinol (Oxf)* 76: 297-303.
83. Verloop H, Louwerens M, Schoones JW, Kievit J, Smit JW, Dekkers OM, (2012) Risk of hypothyroidism following hemithyroidectomy: systematic review and meta-analysis of prognostic studies. *J Clin Endocrinol Metab* 97: 2243-2255.
84. Gittoes NJ, Franklyn JA, (1995) Drug-induced thyroid disorders. *Drug Saf* 13: 46-55.
85. Danzi S, Klein I, (2015) Amiodarone-induced thyroid dysfunction. *J Intensive Care Med* 30: 179-185.
86. Cukier P, Santini FC, Scaranti M, Hoff AO, (2017) Endocrine side effects of cancer immunotherapy. *Endocr Relat Cancer* 24: T331-T347.
87. Wassner AJ, (2018) Congenital Hypothyroidism. *Clinics in Perinatology* 45: 1-18.
88. Nebesio TD, McKenna MP, Nabhan ZM, Eugster EA, (2010) Newborn screening results in children with central hypothyroidism. *J Pediatr* 156: 990-993.
89. Schoenmakers N, Alatzoglou KS, Chatterjee VK, Dattani MT, (2015) Recent advances in central congenital hypothyroidism. *J Endocrinol* 227: R51-71.
90. Beck-Peccoz P, Rodari G, Giavoli C, Lania A, (2017) Central hypothyroidism - a neglected thyroid disorder. *Nat Rev Endocrinol* 13: 588-598.
91. Asakura Y, Tachibana K, Adachi M, Suwa S, Yamagami Y, (2002) Hypothalamo-pituitary hypothyroidism detected by neonatal screening for congenital hypothyroidism using measurement of thyroid-stimulating hormone and thyroxine. *Acta Paediatr* 91: 172-177.
92. Bonomi M, Proverbio MC, Weber G, Chiumello G, Beck-Peccoz P, Persani L, (2001) Hyperplastic pituitary gland, high serum glycoprotein hormone alpha-subunit, and variable circulating thyrotropin (TSH) levels as hallmark of central hypothyroidism due to mutations of the TSH beta gene. *J Clin Endocrinol Metab* 86: 1600-1604.

93. Koulouri O, Nicholas AK, Schoenmakers E, Mokrosinski J, Lane F, Cole T, . . . Schoenmakers N, (2016) A Novel Thyrotropin-Releasing Hormone Receptor Missense Mutation (P81R) in Central Congenital Hypothyroidism. *J Clin Endocrinol Metab* 101: 847-851.
94. Persani L, Bonomi M, (2017) The multiple genetic causes of central hypothyroidism. *Best Pract Res Clin Endocrinol Metab* 31: 255-263.
95. Sun Y, Bak B, Schoenmakers N, van Trotsenburg AS, Oostdijk W, Voshol P, . . . Bernard DJ, (2012) Loss-of-function mutations in IGSF1 cause an X-linked syndrome of central hypothyroidism and testicular enlargement. *Nat Genet* 44: 1375-1381.
96. Heinen CA, Losekoot M, Sun Y, Watson PJ, Fairall L, Joustra SD, . . . van Trotsenburg AS, (2016) Mutations in TBL1X Are Associated With Central Hypothyroidism. *J Clin Endocrinol Metab* 101: 4564-4573.
97. Adeniran I, Whittaker DG, El Harchi A, Hancox JC, Zhang H, (2017) In silico investigation of a KCNQ1 mutation associated with short QT syndrome. *Sci Rep* 7: 8469.
98. Di Jeso B, Arvan P, (2016) Thyroglobulin From Molecular and Cellular Biology to Clinical Endocrinology. *Endocr Rev* 37: 2-36.
99. Ravera S, Reyna-Neyra A, Ferrandino G, Amzel LM, Carrasco N, (2017) The Sodium/Iodide Symporter (NIS): Molecular Physiology and Preclinical and Clinical Applications. *Annu Rev Physiol* 79: 261-289.
100. Grasberger H, Refetoff S, (2017) Resistance to thyrotropin. *Best Pract Res Clin Endocrinol Metab* 31: 183-194.
101. Briet C, Suteau-Courant V, Munier M, Rodien P, (2018) Thyrotropin receptor, still much to be learned from the patients. *Best Pract Res Clin Endocrinol Metab* 32: 155-164.
102. Armour CM, Kersseboom S, Yoon G, Visser TJ, (2015) Further Insights into the Allan-Herndon-Dudley Syndrome: Clinical and Functional Characterization of a Novel MCT8 Mutation. *PLoS One* 10: e0139343.
103. Roef GL, Rietzschel ER, De Meyer T, Bekaert S, De Buyzere ML, Van daele C, . . . Taes YE, (2013) Associations between single nucleotide polymorphisms in thyroid hormone transporter genes (MCT8, MCT10 and OATP1C1) and circulating thyroid hormones. *Clin Chim Acta* 425: 227-232.
104. Trajkovic-Arsic M, Visser TJ, Darras VM, Friesema EC, Schlott B, Mittag J, . . . Heuer H, (2010) Consequences of monocarboxylate transporter 8 deficiency for renal transport and metabolism of thyroid hormones in mice. *Endocrinology* 151: 802-809.
105. Heuer H, Visser TJ, (2013) The pathophysiological consequences of thyroid hormone transporter deficiencies: Insights from mouse models. *Biochim Biophys Acta* 1830: 3974-3978.
106. Nielsen TR, Appel EV, Svendstrup M, Ohrt JD, Dahl M, Fonvig CE, . . . Grarup N, (2017) A genome-wide association study of thyroid stimulating hormone and free thyroxine in Danish children and adolescents. *PLoS One* 12: e0174204.
107. Liu Y, Qu K, Hai Y, Li X, Zhao L, Zhao C, (2018) SNP mutations occurring in thyroid hormone receptor influenced individual susceptibility to triiodothyronine: Molecular dynamics and site-directed mutagenesis approaches. *J Cell Biochem* 119: 2604-2616.
108. Castagna MG, Dentice M, Cantara S, Ambrosio R, Maino F, Porcelli T, . . . Salvatore D, (2017) DIO2 Thr92Ala Reduces Deiodinase-2 Activity and Serum-T3 Levels in Thyroid-Deficient Patients. *J Clin Endocrinol Metab* 102: 1623-1630.
109. Chaker L, Bianco AC, Jonklaas J, Peeters RP, (2017) Hypothyroidism. *Lancet* 390: 1550-1562.
110. Tajima T, Jo W, Fujikura K, Fukushi M, Fujieda K, (2009) Elevated free thyroxine levels detected by a neonatal screening system. *Pediatr Res* 66: 312-316.
111. Refetoff S, DeWind LT, DeGroot LJ, (1967) Familial syndrome combining deaf-mutism, stuppled epiphyses, goiter and abnormally high PBI: possible target organ refractoriness to thyroid hormone. *J Clin Endocrinol Metab* 27: 279-294.
112. Pappa T, Refetoff S, (2018) Human Genetics of Thyroid Hormone Receptor Beta: Resistance to Thyroid Hormone Beta (RTHbeta). *Methods Mol Biol* 1801: 225-240.
113. Kahaly GJ, Matthews CH, Mohr-Kahaly S, Richards CA, Chatterjee VK, (2002) Cardiac involvement in thyroid hormone resistance. *J Clin Endocrinol Metab* 87: 204-212.
114. Refetoff S, Weiss RE, Usala SJ, (1993) The syndromes of resistance to thyroid hormone. *Endocr Rev* 14: 348-399.
115. Parrilla R, Mixson AJ, McPherson JA, McClaskey JH, Weintraub BD, (1991) Characterization of seven novel mutations of the c-erbA beta gene in unrelated kindreds with generalized thyroid

hormone resistance. Evidence for two "hot spot" regions of the ligand binding domain. *J Clin Invest* 88: 2123-2130.
116. Adams M, Matthews C, Collingwood TN, Tone Y, Beck-Peccoz P, Chatterjee KK, (1994) Genetic analysis of 29 kindreds with generalized and pituitary resistance to thyroid hormone. Identification of thirteen novel mutations in the thyroid hormone receptor beta gene. *J Clin Invest* 94: 506-515.
117. Mamanasiri S, Yesil S, Dumitrescu AM, Liao XH, Demir T, Weiss RE, Refetoff S, (2006) Mosaicism of a thyroid hormone receptor-beta gene mutation in resistance to thyroid hormone. *J Clin Endocrinol Metab* 91: 3471-3477.
118. Mittag J, Wallis K, Vennstrom B, (2010) Physiological consequences of the TRalpha1 aporeceptor state. *Heart Fail Rev* 15: 111-115.
119. Bochukova E, Schoenmakers N, Agostini M, Schoenmakers E, Rajanayagam O, Keogh JM, . . . Chatterjee K, (2012) A mutation in the thyroid hormone receptor alpha gene. *N Engl J Med* 366: 243-249.
120. van Mullem A, van Heerebeek R, Chrysis D, Visser E, Medici M, Andrikoula M, . . . Visser TJ, (2012) Clinical phenotype and mutant TRalpha1. *N Engl J Med* 366: 1451-1453.
121. Tylki-Szymanska A, Acuna-Hidalgo R, Krajewska-Walasek M, Lecka-Ambroziak A, Steehouwer M, Gilissen C, . . . Chrzanowska KH, (2015) Thyroid hormone resistance syndrome due to mutations in the thyroid hormone receptor alpha gene (THRA). *J Med Genet* 52: 312-316.
122. Briet C, Bouhours-Nouet N, Illouz F, Prunier-Mirebeau D, Rodien P, (2018) TRalpha Mutations in Human. *Methods Mol Biol* 1801: 241-245.
123. Korkmaz O, Ozen S, Ozdemir TR, Goksen D, Darcan S, (2019) A novel thyroid hormone receptor alpha gene mutation, clinic characteristics, and follow-up findings in a patient with thyroid hormone resistance. *Hormones (Athens)*.
124. Moran C, Agostini M, Visser WE, Schoenmakers E, Schoenmakers N, Offiah AC, . . . Chatterjee KK, (2014) Resistance to thyroid hormone caused by a mutation in thyroid hormone receptor (TR)α1 and TRα2: clinical, biochemical, and genetic analyses of three related patients. *The Lancet Diabetes & Endocrinology* 2: 619-626.
125. Kahaly GJ, Bartalena L, Hegedus L, Leenhardt L, Poppe K, Pearce SH, (2018) 2018 European Thyroid Association Guideline for the Management of Graves' Hyperthyroidism. *Eur Thyroid J* 7: 167-186.
126. Ross DS, Burch HB, Cooper DS, Greenlee MC, Laurberg P, Maia AL, . . . Walter MA, (2016) 2016 American Thyroid Association Guidelines for Diagnosis and Management of Hyperthyroidism and Other Causes of Thyrotoxicosis. *Thyroid* 26: 1343-1421.
127. Lambert EH, Underdahl LO, Beckett S, Mederos LO, (1951) A study of the ankle jerk in myxedema. *J Clin Endocrinol Metab* 11: 1186-1205.
128. Pietzner M, Engelmann B, Kacprowski T, Golchert J, Dirk AL, Hammer E, . . . Brabant G, (2017) Plasma proteome and metabolome characterization of an experimental human thyrotoxicosis model. *BMC Med* 15: 6.
129. Spencer CA, LoPresti JS, Patel A, Guttler RB, Eigen A, Shen D, . . . Nicoloff JT, (1990) Applications of a new chemiluminometric thyrotropin assay to subnormal measurement. *J Clin Endocrinol Metab* 70: 453-460.
130. Koulouri O, Gurnell M, (2013) How to interpret thyroid function tests. *Clinical Medicine* 13: 282-286.
131. Koulouri O, Moran C, Halsall D, Chatterjee K, Gurnell M, (2013) Pitfalls in the measurement and interpretation of thyroid function tests. *Best Pract Res Clin Endocrinol Metab* 27: 745-762.
132. Saravanan P, Chau WF, Roberts N, Vedhara K, Greenwood R, Dayan CM, (2002) Psychological well-being in patients on 'adequate' doses of l-thyroxine: results of a large, controlled community-based questionnaire study. *Clin Endocrinol (Oxf)* 57: 577-585.
133. Bell GM, Todd WT, Forfar JC, Martyn C, Wathen CG, Gow S, . . . Toft AD, (1985) End-organ responses to thyroxine therapy in subclinical hypothyroidism. *Clin Endocrinol (Oxf)* 22: 83-89.
134. Caron PJ, Nieman LK, Rose SR, Nisula BC, (1986) Deficient nocturnal surge of thyrotropin in central hypothyroidism. *J Clin Endocrinol Metab* 62: 960-964.
135. Gullo D, Latina A, Frasca F, Squatrito S, Belfiore A, Vigneri R, (2017) Seasonal variations in TSH serum levels in athyreotic patients under L-thyroxine replacement monotherapy. *Clin Endocrinol (Oxf)* 87: 207-215.

136. Hoermann R, Midgley JEM, Larisch R, Dietrich JWC, (2017) Advances in applied homeostatic modelling of the relationship between thyrotropin and free thyroxine. *PLoS One* 12: e0187232.
137. Hoermann R, Midgley JE, Larisch R, Dietrich JW, (2015) Homeostatic Control of the Thyroid-Pituitary Axis: Perspectives for Diagnosis and Treatment. *Front Endocrinol (Lausanne)* 6: 177.
138. Gullo D, Latina A, Frasca F, Le Moli R, Pellegriti G, Vigneri R, (2011) Levothyroxine monotherapy cannot guarantee euthyroidism in all athyreotic patients. *PLoS One* 6: e22552.
139. Slawik M, Klawitter B, Meiser E, Schories M, Zwermann O, Borm K, . . . Reincke M, (2007) Thyroid hormone replacement for central hypothyroidism: a randomized controlled trial comparing two doses of thyroxine (T4) with a combination of T4 and triiodothyronine. *J Clin Endocrinol Metab* 92: 4115-4122.
140. Akalin A, Colak O, Alatas O, Efe B, (2002) Bone remodelling markers and serum cytokines in patients with hyperthyroidism. *Clin Endocrinol (Oxf)* 57: 125-129.
141. Garnero P, Vassy V, Bertholin A, Riou JP, Delmas PD, (1994) Markers of bone turnover in hyperthyroidism and the effects of treatment. *J Clin Endocrinol Metab* 78: 955-959.
142. Refetoff S, Dumitrescu AM, (2007) Syndromes of reduced sensitivity to thyroid hormone: genetic defects in hormone receptors, cell transporters and deiodination. *Best Pract Res Clin Endocrinol Metab* 21: 277-305.
143. Brucker-Davis F, Skarulis MC, Grace MB, Benichou J, Hauser P, Wiggs E, Weintraub BD, (1995) Genetic and clinical features of 42 kindreds with resistance to thyroid hormone. The National Institutes of Health Prospective Study. *Ann Intern Med* 123: 572-583.
144. Li Y, Chen H, Tan J, Wang X, Liang H, Sun X, (1998) Impaired release of tissue plasminogen activator from the endothelium in Graves' disease - indicator of endothelial dysfunction and reduced fibrinolytic capacity. *Eur J Clin Invest* 28: 1050-1054.
145. Smallridge RC, Rogers J, Verma PS, (1983) Serum angiotensin-converting enzyme. Alterations in hyperthyroidism, hypothyroidism, and subacute thyroiditis. *JAMA* 250: 2489-2493.
146. Miksicek RJ, Towle HC, (1982) Changes in the rates of synthesis and messenger RNA levels of hepatic glucose-6-phosphate and 6-phosphogluconate dehydrogenases following induction by diet or thyroid hormone. *J Biol Chem* 257: 11829-11835.
147. Jonklaas J, Bianco AC, Bauer AJ, Burman KD, Cappola AR, Celi FS, . . . American Thyroid Association Task Force on Thyroid Hormone R, (2014) Guidelines for the treatment of hypothyroidism: prepared by the american thyroid association task force on thyroid hormone replacement. *Thyroid* 24: 1670-1751.
148. Ito M, Miyauchi A, Hisakado M, Yoshioka W, Ide A, Kudo T, . . . Amino N, (2017) Biochemical Markers Reflecting Thyroid Function in Athyreotic Patients on Levothyroxine Monotherapy. *Thyroid* 27: 484-490.
149. McAninch EA, Rajan KB, Miller CH, Bianco AC, (2018) Systemic Thyroid Hormone Status During Levothyroxine Therapy In Hypothyroidism: A Systematic Review and Meta-Analysis. *J Clin Endocrinol Metab* 103: 4533–4542.
150. Thaler MA, Seifert-Klauss V, Luppa PB, (2015) The biomarker sex hormone-binding globulin - from established applications to emerging trends in clinical medicine. *Best Pract Res Clin Endocrinol Metab* 29: 749-760.
151. Forrest D, Hanebuth E, Smeyne RJ, Everds N, Stewart CL, Wehner JM, Curran T, (1996) Recessive resistance to thyroid hormone in mice lacking thyroid hormone receptor beta: evidence for tissue-specific modulation of receptor function. *The EMBO journal* 15: 3006-3015.
152. Tinnikov A, Nordstrom K, Thoren P, Kindblom JM, Malin S, Rozell B, . . . Vennstrom B, (2002) Retardation of post-natal development caused by a negatively acting thyroid hormone receptor alpha1. *The EMBO journal* 21: 5079-5087.
153. Lietzow J, Golchert J, Homuth G, Volker U, Jonas W, Kohrle J, (2016) 3,5-T2 alters murine genes relevant for xenobiotic, steroid, and thyroid hormone metabolism. *J Mol Endocrinol* 56: 311-323.
154. Courtneidge SA, Dhand R, Pilat D, Twamley GM, Waterfield MD, Roussel MF, (1993) Activation of Src family kinases by colony stimulating factor-1, and their association with its receptor. *The EMBO journal* 12: 943-950.
155. Clark G, Stockinger H, Balderas R, van Zelm MC, Zola H, Hart D, Engel P, (2016) Nomenclature of CD molecules from the Tenth Human Leucocyte Differentiation Antigen Workshop. *Clin Transl Immunology* 5: e57.

156. Saunders AE, Johnson P, (2010) Modulation of immune cell signalling by the leukocyte common tyrosine phosphatase, CD45. *Cell Signal* 22: 339-348.
157. Tanaka K, Matsumoto Y, Mochizuki M, Takezawa M, Yoshimura M, Motomura T, . . . Nakao K, (1996) Thyroid hormone-free albumin: charcoal treatment or resin treatment. *Ann Nucl Med* 10: 357-359.
158. Xu L, Hui AY, Albanis E, Arthur MJ, O'Byrne SM, Blaner WS, . . . Eng FJ, (2005) Human hepatic stellate cell lines, LX-1 and LX-2: new tools for analysis of hepatic fibrosis. *Gut* 54: 142-151.
159. Aden DP, Fogel A, Plotkin S, Damjanov I, Knowles BB, (1979) Controlled synthesis of HBsAg in a differentiated human liver carcinoma-derived cell line. *Nature* 282: 615-616.
160. Takahashi N, Yamana H, Yoshiki S, Roodman GD, Mundy GR, Jones SJ, . . . Suda T, (1988) Osteoclast-like cell formation and its regulation by osteotropic hormones in mouse bone marrow cultures. *Endocrinology* 122: 1373-1382.
161. Martin TJ, Ingleton PM, Underwood JC, Michelangeli VP, Hunt NH, Melick RA, (1976) Parathyroid hormone-responsive adenylate cyclase in induced transplantable osteogenic rat sarcoma. *Nature* 260: 436-438.
162. Galli SJ, Borregaard N, Wynn TA, (2011) Phenotypic and functional plasticity of cells of innate immunity: macrophages, mast cells and neutrophils. *Nat Immunol* 12: 1035-1044.
163. Birnboim HC, Doly J, (1979) A rapid alkaline extraction procedure for screening recombinant plasmid DNA. *Nucleic Acids Res* 7: 1513-1523.
164. Konstantinou GN, (2017) Enzyme-Linked Immunosorbent Assay (ELISA). *Methods Mol Biol* 1592: 79-94.
165. Smith PK, Krohn RI, Hermanson GT, Mallia AK, Gartner FH, Provenzano MD, . . . Klenk DC, (1985) Measurement of Protein Using Bicinchoninic Acid. *Analytical Biochemistry* 150: 76-85.
166. Laemmli UK, (1970) Cleavage of structural proteins during the assembly of the head of bacteriophage T4. *Nature* 227: 680-685.
167. Short R, Posch A, (2011) Stain-Free Approach for Western Blotting. *Genetic Engineering & Biotechnology News* 31: 22-23.
168. Hoefig CS, Harder L, Oelkrug R, Meusel M, Vennstrom B, Brabant G, Mittag J, (2016) Thermoregulatory and Cardiovascular Consequences of a Transient Thyrotoxicosis and Recovery in Male Mice. *Endocrinology* 157: 2957-2967.
169. Flores-Morales A, Gullberg H, Fernandez L, Stahlberg N, Lee NH, Vennstrom B, Norstedt G, (2002) Patterns of liver gene expression governed by TR beta. *Molecular Endocrinology* 16: 1257-1268.
170. Feng X, Jiang Y, Meltzer P, Yen PM, (2000) Thyroid hormone regulation of hepatic genes in vivo detected by complementary DNA microarray. *Mol Endocrinol* 14: 947-955.
171. Mittag J, Behrends T, Nordstrom K, Anselmo J, Vennstrom B, Schomburg L, (2012) Serum copper as a novel biomarker for resistance to thyroid hormone. *Biochem J* 443: 103-109.
172. Maia AL, Kieffer JD, Harney JW, Larsen PR, (1995) Effect of 3,5,3'-Triiodothyronine (T3) administration on dio1 gene expression and T3 metabolism in normal and type 1 deiodinase-deficient mice. *Endocrinology* 136: 4842-4849.
173. Zavacki AM, Ying H, Christoffolete MA, Aerts G, So E, Harney JW, . . . Bianco AC, (2005) Type 1 iodothyronine deiodinase is a sensitive marker of peripheral thyroid status in the mouse. *Endocrinology* 146: 1568-1575.
174. Gerets HH, Tilmant K, Gerin B, Chanteux H, Depelchin BO, Dhalluin S, Atienzar FA, (2012) Characterization of primary human hepatocytes, HepG2 cells, and HepaRG cells at the mRNA level and CYP activity in response to inducers and their predictivity for the detection of human hepatotoxins. *Cell Biol Toxicol* 28: 69-87.
175. Wilkening S, Stahl F, Bader A, (2003) Comparison of primary human hepatocytes and hepatoma cell line Hepg2 with regard to their biotransformation properties. *Drug Metab Dispos* 31: 1035-1042.
176. Meyer Zu Schwabedissen HE, Ferreira C, Schaefer AM, Oufir M, Seibert I, Hamburger M, Tirona RG, (2018) Thyroid Hormones Are Transport Substrates and Transcriptional Regulators of Organic Anion Transporting Polypeptide 2B1. *Mol Pharmacol* 94: 700-712.
177. Wang C, Yosef N, Gaublomme J, Wu C, Lee Y, Clish CB, . . . Kuchroo VK, (2015) CD5L/AIM Regulates Lipid Biosynthesis and Restrains Th17 Cell Pathogenicity. *Cell* 163: 1413-1427.
178. Gaublomme JT, Yosef N, Lee Y, Gertner RS, Yang LV, Wu C, . . . Regev A, (2015) Single-Cell Genomics Unveils Critical Regulators of Th17 Cell Pathogenicity. *Cell* 163: 1400-1412.

179. Miyazaki T, Hirokami Y, Matsuhashi N, Takatsuka H, Naito M, (1999) Increased susceptibility of thymocytes to apoptosis in mice lacking AIM, a novel murine macrophage-derived soluble factor belonging to the scavenger receptor cysteine-rich domain superfamily. *J Exp Med* 189: 413-422.
180. Haruta I, Kato Y, Hashimoto E, Minjares C, Kennedy S, Uto H, . . . Miyazaki T, (2001) Association of AIM, a novel apoptosis inhibitory factor, with hepatitis via supporting macrophage survival and enhancing phagocytotic function of macrophages. *J Biol Chem* 276: 22910-22914.
181. Joseph SB, Bradley MN, Castrillo A, Bruhn KW, Mak PA, Pei L, . . . Tontonoz P, (2004) LXR-dependent gene expression is important for macrophage survival and the innate immune response. *Cell* 119: 299-309.
182. Jaccard E, Cornuz J, Waeber G, Guessous I, (2018) Evidence-Based Precision Medicine is Needed to Move Toward General Internal Precision Medicine. *J Gen Intern Med* 33: 11-12.
183. Hasin Y, Seldin M, Lusis A, (2017) Multi-omics approaches to disease. *Genome Biol* 18: 83.
184. Kotze MJ, Luckhoff HK, Peeters AV, Baatjes K, Schoeman M, van der Merwe L, . . . Schneider JW, (2015) Genomic medicine and risk prediction across the disease spectrum. *Crit Rev Clin Lab Sci* 52: 120-137.
185. Brittain HK, Scott R, Thomas E, (2017) The rise of the genome and personalised medicine. *Clin Med (Lond)* 17: 545-551.
186. Jameson JL, Longo DL, (2015) Precision medicine--personalized, problematic, and promising. *N Engl J Med* 372: 2229-2234.
187. Boyle EA, Li YI, Pritchard JK, (2017) An Expanded View of Complex Traits: From Polygenic to Omnigenic. *Cell* 169: 1177-1186.
188. Silvestri E, Lombardi A, de Lange P, Glinni D, Senese R, Cioffi F, . . . Moreno M, (2011) Studies of complex biological systems with applications to molecular medicine: the need to integrate transcriptomic and proteomic approaches. *J Biomed Biotechnol* 2011: 810242.
189. Lin KH, Lee HY, Shih CH, Yen CC, Chen SL, Yang RC, Wang CS, (2003) Plasma protein regulation by thyroid hormone. *J Endocrinol* 179: 367-377.
190. Konig IR, Fuchs O, Hansen G, von Mutius E, Kopp MV, (2017) What is precision medicine? *Eur Respir J* 50.
191. Engelmann B, Bischof J, Dirk AL, Friedrich N, Hammer E, Thiele T, . . . Volker U, (2015) Effect of Experimental Thyrotoxicosis onto Blood Coagulation: A Proteomics Study. *Eur Thyroid J* 4: 119-124.
192. Massolt ET, Meima ME, Swagemakers SMA, Leeuwenburgh S, van den Hout-van Vroonhoven M, Brigante G, . . . Visser WE, (2018) Thyroid State Regulates Gene Expression in Human Whole Blood. *J Clin Endocrinol Metab* 103: 169-178.
193. Alfadda AA, Benabdelkamel H, Masood A, Jammah AA, Ekhzaimy AA, (2018) Differences in the Plasma Proteome of Patients with Hypothyroidism before and after Thyroid Hormone Replacement: A Proteomic Analysis. *Int J Mol Sci* 19.
194. Shih CH, Chen SL, Yen CC, Huang YH, Chen CD, Lee YS, Lin KH, (2004) Thyroid hormone receptor-dependent transcriptional regulation of fibrinogen and coagulation proteins. *Endocrinology* 145: 2804-2814.
195. Pouw RB, Vredevoogd DW, Kuijpers TW, Wouters D, (2015) Of mice and men: The factor H protein family and complement regulation. *Mol Immunol* 67: 12-20.
196. Jafarzadeh A, Poorgholami M, Izadi N, Nemati M, Rezayati M, (2010) Immunological and hematological changes in patients with hyperthyroidism or hypothyroidism. *Clin Invest Med* 33: E271-279.
197. Hooper JM, Stuijver DJ, Orme SM, van Zaane B, Hess K, Gerdes VE, . . . Ajjan RA, (2012) Thyroid dysfunction and fibrin network structure: a mechanism for increased thrombotic risk in hyperthyroid individuals. *J Clin Endocrinol Metab* 97: 1463-1473.
198. Potlukova E, Jiskra J, Freiberger T, Limanova Z, Zivorova D, Malickova K, . . . Trendelenburg M, (2010) The production of mannan-binding lectin is dependent upon thyroid hormones regardless of the genotype: a cohort study of 95 patients with autoimmune thyroid disorders. *Clin Immunol* 136: 123-129.
199. Simone JV, Abildgaard CF, Schulman I, (1965) Blood coagulation in thyroid dysfunction. *N Engl J Med* 273: 1057-1061.

200. Stuijver DJ, Hooper JM, Orme SM, Van Zaane B, Squizzato A, Piantanida E, . . . Ajjan RA, (2012) Fibrin clot structure and fibrinolysis in hypothyroid individuals: the effects of normalising thyroid hormone levels. *J Thromb Haemost* 10: 1708-1710.
201. Elbers LPB, Fliers E, Cannegieter SC, (2018) The influence of thyroid function on the coagulation system and its clinical consequences. *J Thromb Haemost* 16: 634-645.
202. Elbers LP, Boon HA, Moes MI, van Zaane B, Brandjes DP, Fliers E, . . . Gerdes VE, (2016) Plasma Levels of Free Thyroxine and Risk of Major Bleeding in Bariatric Surgery. *Eur Thyroid J* 5: 139-144.
203. Coban E, Aydemir M, Yazicioglu G, Ozdogan M, (2006) Endothelial dysfunction in subjects with subclinical hyperthyroidism. *J Endocrinol Invest* 29: 197-200.
204. Salloum-Asfar S, Boelen A, Reitsma PH, van Vlijmen BJ, (2015) The immediate and late effects of thyroid hormone (triiodothyronine) on murine coagulation gene transcription. *PLoS One* 10: e0127469.
205. Mahley RW, Innerarity TL, Rall SC, Jr., Weisgraber KH, (1984) Plasma lipoproteins: apolipoprotein structure and function. *J Lipid Res* 25: 1277-1294.
206. Pazos F, Alvarez JJ, Rubies-Prat J, Varela C, Lasuncion MA, (1995) Long-term thyroid replacement therapy and levels of lipoprotein(a) and other lipoproteins. *J Clin Endocrinol Metab* 80: 562-566.
207. Zhou L, Li C, Gao L, Wang A, (2015) High-density lipoprotein synthesis and metabolism (Review). *Mol Med Rep* 12: 4015-4021.
208. Wilcox HG, Frank RA, Heimberg M, (1991) Effects of thyroid status and fasting on hepatic metabolism of apolipoprotein A-I. *J Lipid Res* 32: 395-405.
209. Liu XQ, Rahman A, Bagdade JD, Alaupovic P, Kannan CR, (1998) Effect of thyroid hormone on plasma apolipoproteins and apoA- and apoB-containing lipoprotein particles. *Eur J Clin Invest* 28: 266-270.
210. Beukhof CM, Massolt ET, Visser TJ, Korevaar TIM, Medici M, de Herder WW, . . . Peeters RP, (2018) Effects of Thyrotropin on Peripheral Thyroid Hormone Metabolism and Serum Lipids. *Thyroid* 28: 168-174.
211. Jung KY, Ahn HY, Han SK, Park YJ, Cho BY, Moon MK, (2017) Association between thyroid function and lipid profiles, apolipoproteins, and high-density lipoprotein function. *J Clin Lipidol* 11: 1347-1353.
212. Ito M, Arishima T, Kudo T, Nishihara E, Ohye H, Kubota S, . . . Miyauchi A, (2007) Effect of levo-thyroxine replacement on non-high-density lipoprotein cholesterol in hypothyroid patients. *J Clin Endocrinol Metab* 92: 608-611.
213. Lee WY, Suh JY, Rhee EJ, Park JS, Sung KC, Kim SW, (2004) Plasma CRP, apolipoprotein A-1, apolipoprotein B and Lpa levels according to thyroid function status. *Arch Med Res* 35: 540-545.
214. Langen VL, Niiranen TJ, Puukka P, Sundvall J, Jula AM, (2017) Association of thyroid-stimulating hormone with lipid concentrations: an 11-year longitudinal study. *Clin Endocrinol (Oxf)* 86: 120-127.
215. Taylor AH, Wishart P, Lawless DE, Raymond J, Wong NC, (1996) Identification of functional positive and negative thyroid hormone-responsive elements in the rat apolipoprotein AI promoter. *Biochemistry* 35: 8281-8288.
216. Angelin B, Kristensen JD, Eriksson M, Carlsson B, Klein I, Olsson AG, . . . Ladenson PW, (2015) Reductions in serum levels of LDL cholesterol, apolipoprotein B, triglycerides and lipoprotein(a) in hypercholesterolaemic patients treated with the liver-selective thyroid hormone receptor agonist eprotirome. *J Intern Med* 277: 331-342.
217. van Mullem AA, Chrysis D, Eythimiadou A, Chroni E, Tsatsoulis A, de Rijke YB, . . . Peeters RP, (2013) Clinical phenotype of a new type of thyroid hormone resistance caused by a mutation of the TRalpha1 receptor: consequences of LT4 treatment. *J Clin Endocrinol Metab* 98: 3029-3038.
218. Tang Y, Yu M, Lian X, (2016) Resistance to thyroid hormone alpha, revelation of basic study to clinical consequences. *J Pediatr Endocrinol Metab* 29: 511-522.
219. Liu J, Hernandez-Ono A, Graham MJ, Galton VA, Ginsberg HN, (2016) Type 1 Deiodinase Regulates ApoA-I Gene Expression and ApoA-I Synthesis Independent of Thyroid Hormone Signaling. *Arterioscler Thromb Vasc Biol* 36: 1356-1366.
220. Umehara T, Matsuno H, Toyoda C, Oka H, (2015) Thyroid hormone level is associated with motor symptoms in de novo Parkinson's disease. *J Neurol* 262: 1762-1768.
221. Li L, Liu MS, Li GQ, Tang J, Liao Y, Zheng Y, . . . Yuan MT, (2017) Relationship between Apolipoprotein Superfamily and Parkinson's Disease. *Chin Med J (Engl)* 130: 2616-2623.
222. Duntas LH, (2002) Thyroid disease and lipids. *Thyroid* 12: 287-293.

223. Kutty KM, Bryant DG, Farid NR, (1978) Serum lipids in hypothyroidism--a re-evaluation. *J Clin Endocrinol Metab* 46: 55-56.
224. Chen Y, Wu X, Wu R, Sun X, Yang B, Wang Y, Xu Y, (2016) Changes in profile of lipids and adipokines in patients with newly diagnosed hypothyroidism and hyperthyroidism. *Sci Rep* 6: 26174.
225. Duntas LH, Brenta G, (2018) A Renewed Focus on the Association Between Thyroid Hormones and Lipid Metabolism. *Front Endocrinol (Lausanne)* 9: 511.
226. Jakobsson T, Vedin LL, Parini P, (2017) Potential Role of Thyroid Receptor beta Agonists in the Treatment of Hyperlipidemia. *Drugs* 77: 1613-1621.
227. Reiner Z, (2017) Hypertriglyceridaemia and risk of coronary artery disease. *Nat Rev Cardiol* 14: 401-411.
228. Alaupovic P, Mack WJ, Knight-Gibson C, Hodis HN, (1997) The role of triglyceride-rich lipoprotein families in the progression of atherosclerotic lesions as determined by sequential coronary angiography from a controlled clinical trial. *Arterioscler Thromb Vasc Biol* 17: 715-722.
229. Juntti-Berggren L, Refai E, Appelskog I, Andersson M, Imreh G, Dekki N, . . . Berggren PO, (2004) Apolipoprotein CIII promotes Ca2+-dependent beta cell death in type 1 diabetes. *Proc Natl Acad Sci U S A* 101: 10090-10094.
230. Biondi B, Kahaly GJ, Robertson RP, (2019) Thyroid Dysfunction and Diabetes Mellitus : Two Closely Associated Disorders. *Endocr Rev*.
231. Chng CL, Lim AY, Tan HC, Kovalik JP, Tham KW, Bee YM, . . . Yen PM, (2016) Physiological and Metabolic Changes During the Transition from Hyperthyroidism to Euthyroidism in Graves' Disease. *Thyroid* 26: 1422-1430.
232. Lin-Lee YC, Strobl W, Soyal S, Radosavljevic M, Song M, Gotto AM, Jr., Patsch W, (1993) Role of thyroid hormone in the expression of apolipoprotein A-IV and C-III genes in rat liver. *J Lipid Res* 34: 249-259.
233. Rosenson RS, Brewer HB, Jr., Ansell BJ, Barter P, Chapman MJ, Heinecke JW, . . . Webb NR, (2016) Dysfunctional HDL and atherosclerotic cardiovascular disease. *Nat Rev Cardiol* 13: 48-60.
234. Pirim D, Radwan ZH, Wang X, Niemsiri V, Hokanson JE, Hamman RF, . . . Kamboh MI, (2019) Apolipoprotein E-C1-C4-C2 gene cluster region and inter-individual variation in plasma lipoprotein levels: a comprehensive genetic association study in two ethnic groups. *PLoS One* 14: e0214060.
235. Low-Kam C, Rhainds D, Lo KS, Barhdadi A, Boule M, Alem S, . . . Tardif JC, (2018) Variants at the APOE /C1/C2/C4 Locus Modulate Cholesterol Efflux Capacity Independently of High-Density Lipoprotein Cholesterol. *J Am Heart Assoc* 7: e009545.
236. Rassart E, Bedirian A, Do Carmo S, Guinard O, Sirois J, Terrisse L, Milne R, (2000) Apolipoprotein D. *Biochimica et Biophysica Acta (BBA) - Protein Structure and Molecular Enzymology* 1482: 185-198.
237. Weech PK, Provost P, Tremblay NM, Camato RN, Milne RW, Marcel YL, Rassart E, (1991) Apolipoprotein D--an atypical apolipoprotein. *Prog Lipid Res* 30: 259-266.
238. Dassati S, Waldner A, Schweigreiter R, (2014) Apolipoprotein D takes center stage in the stress response of the aging and degenerative brain. *Neurobiol Aging* 35: 1632-1642.
239. Ganfornina MD, Do Carmo S, Lora JM, Torres-Schumann S, Vogel M, Allhorn M, . . . Sanchez D, (2008) Apolipoprotein D is involved in the mechanisms regulating protection from oxidative stress. *Aging Cell* 7: 506-515.
240. Johnson AA, Stolzing A, (2019) The role of lipid metabolism in aging, lifespan regulation, and age-related disease. *Aging Cell*: e13048.
241. Cangemi C, Hansen ML, Argraves WS, Rasmussen LM, (2014) Fibulins and their role in cardiovascular biology and disease. *Adv Clin Chem* 67: 245-265.
242. Zheng P, Wang Q, Teng J, Chen J, (2015) Calumenin and fibulin-1 on tumor metastasis: Implications for pharmacology. *Pharmacol Res* 99: 11-15.
243. Godyna S, Diaz-Ricart M, Argraves WS, (1996) Fibulin-1 mediates platelet adhesion via a bridge of fibrinogen. *Blood* 88: 2569-2577.
244. Smith TJ, Murata Y, Horwitz AL, Philipson L, Refetoff S, (1982) Regulation of glycosaminoglycan synthesis by thyroid hormone in vitro. *J Clin Invest* 70: 1066-1073.
245. Parving HH, Hansen JM, Nielsen SL, Rossing N, Munck O, Lassen NA, (1979) Mechanisms of edema formation in myxedema--increased protein extravasation and relatively slow lymphatic drainage. *N Engl J Med* 301: 460-465.
246. de Rycker C, Vandalem JL, Hennen G, (1984) Effects of 3,5,3'-triiodothyronine on collagen synthesis by cultured human skin fibroblasts. *FEBS Lett* 174: 34-37.

247. Miller LD, McPhie P, Suzuki H, Kato Y, Liu ET, Cheng SY, (2004) Multi-tissue gene-expression analysis in a mouse model of thyroid hormone resistance. *Genome Biol* 5: R31.
248. Nikitovic D, Aggelidakis J, Young MF, Iozzo RV, Karamanos NK, Tzanakakis GN, (2012) The biology of small leucine-rich proteoglycans in bone pathophysiology. *J Biol Chem* 287: 33926-33933.
249. Wang X, Zhou Q, Yu Z, Wu X, Chen X, Li J, . . . Su L, (2017) Cancer-associated fibroblast-derived Lumican promotes gastric cancer progression via the integrin beta1-FAK signaling pathway. *Int J Cancer* 141: 998-1010.
250. Engebretsen KV, Lunde IG, Strand ME, Waehre A, Sjaastad I, Marstein HS, . . . Tonnessen T, (2013) Lumican is increased in experimental and clinical heart failure, and its production by cardiac fibroblasts is induced by mechanical and proinflammatory stimuli. *FEBS J* 280: 2382-2398.
251. Nikitovic D, Papoutsidakis A, Karamanos NK, Tzanakakis GN, (2014) Lumican affects tumor cell functions, tumor-ECM interactions, angiogenesis and inflammatory response. *Matrix Biol* 35: 206-214.
252. Karamanou K, Franchi M, Piperigkou Z, Perreau C, Maquart FX, Vynios DH, Brezillon S, (2017) Lumican effectively regulates the estrogen receptors-associated functional properties of breast cancer cells, expression of matrix effectors and epithelial-to-mesenchymal transition. *Sci Rep* 7: 45138.
253. Coulson-Thomas VJ, Coulson-Thomas YM, Gesteira TF, Andrade de Paula CA, Carneiro CR, Ortiz V, . . . Nader HB, (2013) Lumican expression, localization and antitumor activity in prostate cancer. *Exp Cell Res* 319: 967-981.
254. Li X, Kang Y, Roife D, Lee Y, Pratt M, Perez MR, . . . Fleming JB, (2017) Prolonged exposure to extracellular lumican restrains pancreatic adenocarcinoma growth. *Oncogene* 36: 5432-5438.
255. Beutler B, (2004) Inferences, questions and possibilities in Toll-like receptor signalling. *Nature* 430: 257-263.
256. Lee S, Bowrin K, Hamad AR, Chakravarti S, (2009) Extracellular matrix lumican deposited on the surface of neutrophils promotes migration by binding to beta2 integrin. *J Biol Chem* 284: 23662-23669.
257. Conrad AH, Zhang Y, Walker AR, Olberding LA, Hanzlick A, Zimmer AJ, . . . Conrad GW, (2006) Thyroxine affects expression of KSPG-related genes, the carbonic anhydrase II gene, and KS sulfation in the embryonic chicken cornea. *Invest Ophthalmol Vis Sci* 47: 120-132.
258. Ley K, Laudanna C, Cybulsky MI, Nourshargh S, (2007) Getting to the site of inflammation: the leukocyte adhesion cascade updated. *Nat Rev Immunol* 7: 678-689.
259. Marchese ME, Berdnikovs S, Cook-Mills JM, (2012) Distinct sites within the vascular cell adhesion molecule-1 (VCAM-1) cytoplasmic domain regulate VCAM-1 activation of calcium fluxes versus Rac1 during leukocyte transendothelial migration. *Biochemistry* 51: 8235-8246.
260. Schlesinger M, Bendas G, (2015) Vascular cell adhesion molecule-1 (VCAM-1)--an increasing insight into its role in tumorigenicity and metastasis. *Int J Cancer* 136: 2504-2514.
261. Kong DH, Kim YK, Kim MR, Jang JH, Lee S, (2018) Emerging Roles of Vascular Cell Adhesion Molecule-1 (VCAM-1) in Immunological Disorders and Cancer. *Int J Mol Sci* 19.
262. Liu X, Zheng N, Shi YN, Yuan J, Li L, (2014) Thyroid hormone induced angiogenesis through the integrin alphavbeta3/protein kinase D/histone deacetylase 5 signaling pathway. *J Mol Endocrinol* 52: 245-254.
263. Jungheim K, Caspar G, Usadel KH, Schumm-Draeger PM, (2001) Expression of intracellular adhesion molecule-1 and vascular cell adhesion molecule-1 and homing factor CD44 after engraftment of Graves' lymphocytes in xenotransplanted human thyroid tissue in athymic nude mice. *Thyroid* 11: 831-837.
264. Ozderya A, Aydin K, Temizkan S, Dogru Abbasoglu S, Vural P, Altuntas Y, (2016) High circulating levels of sICAM-1 and sVCAM-1 in the patients with Hashimoto's thyroiditis. *Endocrine Research* 42: 110-116.
265. Marazuela M, Postigo AA, Acevedo A, Diaz-Gonzalez F, Sanchez-Madrid F, de Landazuri MO, (1994) Adhesion molecules from the LFA-1/ICAM-1,3 and VLA-4/VCAM-1 pathways on T lymphocytes and vascular endothelium in Graves' and Hashimoto's thyroid glands. *Eur J Immunol* 24: 2483-2490.
266. Beumer W, Effraimidis G, Drexhage RC, Wiersinga WM, Drexhage HA, (2013) Changes in serum adhesion molecules, chemokines, cytokines, and tissue remodeling factors in euthyroid women

without thyroid antibodies who are at risk for autoimmune thyroid disease: a hypothesis on the early phases of the endocrine autoimmune reaction. *J Clin Endocrinol Metab* 98: 2460-2468.
267. Johann K, Cremer AL, Fischer AW, Heine M, Pensado ER, Resch J, . . . Mittag J, (2019) Thyroid-Hormone-Induced Browning of White Adipose Tissue Does Not Contribute to Thermogenesis and Glucose Consumption. *Cell Rep* 27: 3385-3400 e3383.
268. Kahlenberg JM, Kaplan MJ, (2013) Little peptide, big effects: the role of LL-37 in inflammation and autoimmune disease. *J Immunol* 191: 4895-4901.
269. Oren Z, Lerman JC, Gudmundsson GH, Agerberth B, Shai Y, (1999) Structure and organization of the human antimicrobial peptide LL-37 in phospholipid membranes: relevance to the molecular basis for its non-cell-selective activity. *Biochem J* 341 (Pt 3): 501-513.
270. Fabisiak A, Murawska N, Fichna J, (2016) LL-37: Cathelicidin-related antimicrobial peptide with pleiotropic activity. *Pharmacological Reports* 68: 802-808.
271. Ding B, Soblosky L, Nguyen K, Geng J, Yu X, Ramamoorthy A, Chen Z, (2013) Physiologically-relevant modes of membrane interactions by the human antimicrobial peptide, LL-37, revealed by SFG experiments. *Sci Rep* 3: 1854.
272. Wertenbruch S, Drescher H, Grossarth V, Kroy D, Giebeler A, Erschfeld S, . . . Streetz K, (2015) The Anti-Microbial Peptide LL-37/CRAMP Is Elevated in Patients with Liver Diseases and Acts as a Protective Factor during Mouse Liver Injury. *Digestion* 91: 307-317.
273. Bei Y, Pan LL, Zhou Q, Zhao C, Xie Y, Wu C, . . . Xiao J, (2019) Cathelicidin-related antimicrobial peptide protects against myocardial ischemia/reperfusion injury. *BMC Med* 17: 42.
274. Cederlund A, Nylen F, Miraglia E, Bergman P, Gudmundsson GH, Agerberth B, (2014) Label-free quantitative mass spectrometry reveals novel pathways involved in LL-37 expression. *J Innate Immun* 6: 365-376.
275. Cullinan EB, Kwee L, Nunes P, Shuster DJ, Ju G, McIntyre KW, . . . Labow MA, (1998) IL-1 receptor accessory protein is an essential component of the IL-1 receptor. *J Immunol* 161: 5614-5620.
276. Zhao K, Yin LL, Zhao DM, Pan B, Chen W, Cao J, . . . Xu KL, (2014) IL1RAP as a surface marker for leukemia stem cells is related to clinical phase of chronic myeloid leukemia patients. *International Journal of Clinical and Experimental Medicine* 7: 4787-U1376.
277. Jaras M, Johnels P, Hansen N, Agerstam H, Tsapogas P, Rissler M, . . . Fioretos T, (2010) Isolation and killing of candidate chronic myeloid leukemia stem cells by antibody targeting of IL-1 receptor accessory protein. *Proc Natl Acad Sci U S A* 107: 16280-16285.
278. Mitchell K, Barreyro L, Todorova TI, Taylor SJ, Antony-Debre I, Narayanagari SR, . . . Steidl U, (2018) IL1RAP potentiates multiple oncogenic signaling pathways in AML. *J Exp Med* 215: 1709-1727.
279. Boelen A, PlatvoetterSchiphorst MC, Wiersinga WM, (1997) Immunoneutralization of interleukin-1, tumor necrosis factor, interleukin-6 or interferon does not prevent the LPS-induced sick euthyroid syndrome in mice. *Journal of Endocrinology* 153: 115-122.
280. de Vries EM, Fliers E, Boelen A, (2015) The molecular basis of the non-thyroidal illness syndrome. *J Endocrinol* 225: R67-81.
281. De Vito P, Incerpi S, Pedersen JZ, Luly P, Davis FB, Davis PJ, (2011) Thyroid hormones as modulators of immune activities at the cellular level. *Thyroid* 21: 879-890.
282. Royet J, Dziarski R, (2007) Peptidoglycan recognition proteins: pleiotropic sensors and effectors of antimicrobial defences. *Nat Rev Microbiol* 5: 264-277.
283. Jaillon S, Ponzetta A, Magrini E, Barajon I, Barbagallo M, Garlanda C, Mantovani A, (2016) Fluid phase recognition molecules in neutrophil-dependent immune responses. *Semin Immunol* 28: 109-118.
284. Uehara A, Sugawara Y, Kurata S, Fujimoto Y, Fukase K, Kusumoto S, . . . Takada H, (2005) Chemically synthesized pathogen-associated molecular patterns increase the expression of peptidoglycan recognition proteins via toll-like receptors, NOD1 and NOD2 in human oral epithelial cells. *Cell Microbiol* 7: 675-686.
285. Li X, Wang S, Wang H, Gupta D, (2006) Differential expression of peptidoglycan recognition protein 2 in the skin and liver requires different transcription factors. *J Biol Chem* 281: 20738-20748.
286. Ruiz M, Montiel M, Jimenez E, Morell M, (1987) Effect of thyroid hormones on angiotensinogen production in the rat in vivo and in vitro. *J Endocrinol* 115: 311-315.

287. Hong-Brown LQ, Deschepper CF, (1992) Effects of thyroid hormones on angiotensinogen gene expression in rat liver, brain, and cultured cells. *Endocrinology* 130: 1231-1237.
288. Neggazi S, Hamlat N, Canaple L, Gauthier K, Samarut J, Bricca G, . . . Beylot M, (2019) TRalpha inhibits arterial renin-angiotensin system expression and prevents cholesterol accumulation in vascular smooth muscle cells. *Ann Endocrinol (Paris)* 80: 89-95.
289. Kimura S, Iwao H, Fukui K, Abe Y, Tanaka S, (1990) Effects of thyroid hormone on angiotensinogen and renin messenger RNA levels in rats. *Jpn J Pharmacol* 52: 281-285.
290. Kashani K, Cheungpasitporn W, Ronco C, (2017) Biomarkers of acute kidney injury: the pathway from discovery to clinical adoption. *Clin Chem Lab Med* 55: 1074-1089.
291. Kaindl AM, Passemard S, Kumar P, Kraemer N, Issa L, Zwirner A, . . . Gressens P, (2010) Many roads lead to primary autosomal recessive microcephaly. *Prog Neurobiol* 90: 363-383.
292. Johnson MB, Sun X, Kodani A, Borges-Monroy R, Girskis KM, Ryu SC, . . . Bae BI, (2018) Aspm knockout ferret reveals an evolutionary mechanism governing cerebral cortical size. *Nature* 556: 370-375.
293. Pulvers JN, Bryk J, Fish JL, Wilsch-Brauninger M, Arai Y, Schreier D, . . . Huttner WB, (2010) Mutations in mouse Aspm (abnormal spindle-like microcephaly associated) cause not only microcephaly but also major defects in the germline. *Proc Natl Acad Sci U S A* 107: 16595-16600.
294. Weinberger P, Ponny SR, Xu H, Bai S, Smallridge R, Copland J, Sharma A, (2017) Cell Cycle M-Phase Genes Are Highly Upregulated in Anaplastic Thyroid Carcinoma. *Thyroid* 27: 236-252.
295. Stefan N, Hennige AM, Staiger H, Machann J, Schick F, Krober SM, . . . Haring HU, (2006) Alpha2-Heremans-Schmid glycoprotein/fetuin-A is associated with insulin resistance and fat accumulation in the liver in humans. *Diabetes Care* 29: 853-857.
296. Kaushik SV, Plaisance EP, Kim T, Huang EY, Mahurin AJ, Grandjean PW, Mathews ST, (2009) Extended-release niacin decreases serum fetuin-A concentrations in individuals with metabolic syndrome. *Diabetes Metab Res Rev* 25: 427-434.
297. Singh M, Sharma PK, Garg VK, Mondal SC, Singh AK, Kumar N, (2012) Role of fetuin-A in atherosclerosis associated with diabetic patients. *J Pharm Pharmacol* 64: 1703-1708.
298. Mukhopadhyay S, Bhattacharya S, (2016) Plasma fetuin-A triggers inflammatory changes in macrophages and adipocytes by acting as an adaptor protein between NEFA and TLR-4. *Diabetologia* 59: 859-860.
299. Pal D, Dasgupta S, Kundu R, Maitra S, Das G, Mukhopadhyay S, . . . Bhattacharya S, (2012) Fetuin-A acts as an endogenous ligand of TLR4 to promote lipid-induced insulin resistance. *Nat Med* 18: 1279-1285.
300. Ix JH, Shlipak MG, Brandenburg VM, Ali S, Ketteler M, Whooley MA, (2006) Association between human fetuin-A and the metabolic syndrome: data from the Heart and Soul Study. *Circulation* 113: 1760-1767.
301. Peter A, Kovarova M, Staiger H, Machann J, Schick F, Konigsrainer A, . . . Stefan N, (2018) The hepatokines fetuin-A and fetuin-B are upregulated in the state of hepatic steatosis and may differently impact on glucose homeostasis in humans. *Am J Physiol Endocrinol Metab* 314: E266-E273.
302. Guo VY, Cao B, Cai C, Cheng KK, Cheung BMY, (2018) Fetuin-A levels and risk of type 2 diabetes mellitus: a systematic review and meta-analysis. *Acta Diabetol* 55: 87-98.
303. Weikert C, Stefan N, Schulze MB, Pischon T, Berger K, Joost HG, . . . Fritsche A, (2008) Plasma fetuin-a levels and the risk of myocardial infarction and ischemic stroke. *Circulation* 118: 2555-2562.
304. Bakiner O, Bozkirli E, Ertugrul D, Sezgin N, Ertorer E, (2014) Plasma fetuin-A levels are reduced in patients with hypothyroidism. *Eur J Endocrinol* 170: 411-418.
305. Kwakkel J, Surovtseva OV, de Vries EM, Stap J, Fliers E, Boelen A, (2014) A novel role for the thyroid hormone-activating enzyme type 2 deiodinase in the inflammatory response of macrophages. *Endocrinology* 155: 2725-2734.
306. van der Spek AH, Jim KK, Karaczyn A, van Beeren HC, Ackermans MT, Darras VM, . . . Boelen A, (2018) The Thyroid Hormone Inactivating Type 3 Deiodinase Is Essential for Optimal Neutrophil Function: Observations From Three Species. *Endocrinology* 159: 826-835.
307. Felding P, Fex G, (1982) Cellular origin of prealbumin in the rat. *Biochim Biophys Acta* 716: 446-449.
308. Aleshire SL, Bradley CA, Richardson LD, Parl FF, (1983) Localization of human prealbumin in choroid plexus epithelium. *J Histochem Cytochem* 31: 608-612.

309. Irace G, Edelhoch H, (1978) Thyroxine-induced conformational changes in prealbumin. *Biochemistry* 17: 5729-5733.
310. Richardson SJ, (2009) Evolutionary changes to transthyretin: evolution of transthyretin biosynthesis. *FEBS J* 276: 5342-5356.
311. Samadani U, Qian XB, Costa RH, (1996) Identification of a transthyretin enhancer site that selectively binds the hepatocyte nuclear factor-3 beta isoform. *Gene Expression* 6: 23-33.
312. Wang Z, Burke PA, (2010) Hepatocyte nuclear factor-4alpha interacts with other hepatocyte nuclear factors in regulating transthyretin gene expression. *FEBS J* 277: 4066-4075.
313. Selva DM, Hammond GL, (2009) Thyroid hormones act indirectly to increase sex hormone-binding globulin production by liver via hepatocyte nuclear factor-4alpha. *J Mol Endocrinol* 43: 19-27.
314. Palha JA, Episkopou V, Maeda S, Shimada K, Gottesman ME, Saraiva MJ, (1994) Thyroid hormone metabolism in a transthyretin-null mouse strain. *J Biol Chem* 269: 33135-33139.
315. Gebe JA, Kiener PA, Ring HJZ, Li X, Francke U, Aruffo A, (1997) Molecular cloning, mapping to human chromosome 1 q21-q23, and cell binding characteristics of Sp alpha, a new member of the scavenger receptor cysteine-rich (SRCR) family of proteins. *Journal of Biological Chemistry* 272: 6151-6158.
316. Martinez VG, Moestrup SK, Holmskov U, Mollenhauer J, Lozano F, (2011) The conserved scavenger receptor cysteine-rich superfamily in therapy and diagnosis. *Pharmacol Rev* 63: 967-1000.
317. Tissot JD, Sanchez JC, Vuadens F, Scherl A, Schifferli JA, Hochstrasser DF, . . . Duchosal MA, (2002) IgM are associated to Sp alpha (CD5 antigen-like). *Electrophoresis* 23: 1203-1206.
318. Gebe JA, Llewellyn M, Hoggatt H, Aruffo A, (2000) Molecular cloning, genomic organization and cell-binding characteristics of mouse Spalpha. *Immunology* 99: 78-86.
319. Sugisawa R, Hiramoto E, Matsuoka S, Iwai S, Takai R, Yamazaki T, . . . Miyazaki T, (2016) Impact of feline AIM on the susceptibility of cats to renal disease. *Sci Rep* 6: 35251.
320. Uchida M, Uchida K, Maeda S, Yonezawa T, (2019) Expression of apoptosis inhibitor of macrophages in tissue macrophages, leukocytes and vascular endothelial cells of dogs. *Tissue Cell* 58: 112-120.
321. Sanjurjo L, Aran G, Roher N, Valledor AF, Sarrias MR, (2015) AIM/CD5L: a key protein in the control of immune homeostasis and inflammatory disease. *J Leukoc Biol* 98: 173-184.
322. Kai T, Yamazaki T, Arai S, Miyazaki T, (2014) Stabilization and augmentation of circulating AIM in mice by synthesized IgM-Fc. *PLoS One* 9: e97037.
323. Hiramoto E, Tsutsumi A, Suzuki R, Matsuoka S, Arai S, Kikkawa M, Miyazaki T, (2018) The IgM pentamer is an asymmetric pentagon with an open groove that binds the AIM protein. *Science Advances* 4.
324. Mera K, Uto H, Mawatari S, Ido A, Yoshimine Y, Nosaki T, . . . Tsubouchi H, (2014) Serum levels of apoptosis inhibitor of macrophage are associated with hepatic fibrosis in patients with chronic hepatitis C. *BMC Gastroenterol* 14: 27.
325. Yamazaki T, Mori M, Arai S, Tateishi R, Abe M, Ban M, . . . Miyazaki T, (2014) Circulating AIM as an indicator of liver damage and hepatocellular carcinoma in humans. *PLoS One* 9: e109123.
326. Barcena C, Aran G, Perea L, Sanjurjo L, Tellez E, Oncins A, . . . Sarrias MR, (2019) CD5L is a pleiotropic player in liver fibrosis controlling damage, fibrosis and immune cell content. *EBioMedicine* 43: 513-524.
327. Kojima J, Araya J, Hara H, Ito S, Takasaka N, Kobayashi K, . . . Kuwano K, (2013) Apoptosis inhibitor of macrophage (AIM) expression in alveolar macrophages in COPD. *Respir Res* 14: 30.
328. Barnes PJ, (2009) The cytokine network in chronic obstructive pulmonary disease. *Am J Respir Cell Mol Biol* 41: 631-638.
329. Hodge S, Matthews G, Mukaro V, Ahern J, Shivam A, Hodge G, . . . Reynolds PN, (2011) Cigarette smoke-induced changes to alveolar macrophage phenotype and function are improved by treatment with procysteine. *Am J Respir Cell Mol Biol* 44: 673-681.
330. Qu P, Du H, Li Y, Yan C, (2009) Myeloid-specific expression of Api6/AIM/Sp alpha induces systemic inflammation and adenocarcinoma in the lung. *J Immunol* 182: 1648-1659.
331. Maehara N, Arai S, Mori M, Iwamura Y, Kurokawa J, Kai T, . . . Miyazaki T, (2014) Circulating AIM prevents hepatocellular carcinoma through complement activation. *Cell Rep* 9: 61-74.

332. Sanjurjo L, Aran G, Tellez E, Amezaga N, Armengol C, Lopez D, . . . Sarrias MR, (2018) CD5L Promotes M2 Macrophage Polarization through Autophagy-Mediated Upregulation of ID3. *Front Immunol* 9: 480.
333. De Palma M, Lewis CE, (2013) Macrophage regulation of tumor responses to anticancer therapies. *Cancer Cell* 23: 277-286.
334. Kurokawa J, Arai S, Nakashima K, Nagano H, Nishijima A, Miyata K, . . . Miyazaki T, (2010) Macrophage-derived AIM is endocytosed into adipocytes and decreases lipid droplets via inhibition of fatty acid synthase activity. *Cell Metab* 11: 479-492.
335. Miyazaki T, Kurokawa J, Arai S, (2011) AIMing at Metabolic Syndrome - Towards the Development of Novel Therapies for Metabolic Diseases via Apoptosis Inhibitor of Macrophage (AIM). *Circulation Journal* 75: 2522-2531.
336. Arai S, Shelton JM, Chen M, Bradley MN, Castrillo A, Bookout AL, . . . Miyazaki T, (2005) A role for the apoptosis inhibitory factor AIM/Spalpha/Api6 in atherosclerosis development. *Cell Metab* 1: 201-213.
337. Amezaga N, Sanjurjo L, Julve J, Aran G, Perez-Cabezas B, Bastos-Amador P, . . . Sarrias MR, (2014) Human scavenger protein AIM increases foam cell formation and CD36-mediated oxLDL uptake. *J Leukoc Biol* 95: 509-520.
338. Hamada M, Nakamura M, Tran MT, Moriguchi T, Hong C, Ohsumi T, . . . Takahashi S, (2014) MafB promotes atherosclerosis by inhibiting foam-cell apoptosis. *Nat Commun* 5: 3147.
339. Ishikawa S, Noma T, Fu HY, Matsuzaki T, Ishizawa M, Ishikawa K, . . . Minamino T, (2017) Apoptosis inhibitor of macrophage depletion decreased M1 macrophage accumulation and the incidence of cardiac rupture after myocardial infarction in mice. *PLoS One* 12: e0187894.
340. Sarrias MR, Rosello S, Sanchez-Barbero F, Sierra JM, Vila J, Yelamos J, . . . Lozano F, (2005) A role for human Sp alpha as a pattern recognition receptor. *J Biol Chem* 280: 35391-35398.
341. Martinez VG, Escoda-Ferran C, Tadeu Simoes I, Arai S, Orta Mascaro M, Carreras E, . . . Lozano F, (2014) The macrophage soluble receptor AIM/Api6/CD5L displays a broad pathogen recognition spectrum and is involved in early response to microbial aggression. *Cell Mol Immunol* 11: 343-354.
342. Tomita T, Arai S, Kitada K, Mizuno M, Suzuki Y, Sakata F, . . . Ito Y, (2017) Apoptosis inhibitor of macrophage ameliorates fungus-induced peritoneal injury model in mice. *Sci Rep* 7: 6450.
343. Kuwata K, Watanabe H, Jiang SY, Yamamoto T, Tomiyama-Miyaji C, Abo T, . . . Naito M, (2003) AIM inhibits apoptosis of T cells and NKT cells in Corynebacterium-induced granuloma formation in mice. *Am J Pathol* 162: 837-847.
344. Yusa S, Ohnishi S, Onodera T, Miyazaki T, (1999) AIM, a murine apoptosis inhibitory factor, induces strong and sustained growth inhibition of B lymphocytes in combination with TGF-beta1. *Eur J Immunol* 29: 1086-1093.
345. Ono Y, Kanmura S, Morinaga Y, Oda K, Kawabata K, Arima S, . . . Ido A, (2017) The utility of apoptosis inhibitor of macrophages as a possible diagnostic marker in patients with Crohn's disease. *BMC Gastroenterol* 17: 40.
346. Lai X, Xiang Y, Zou L, Li Y, Zhang L, (2018) Elevation of serum CD5L concentration is correlated with disease activity in patients with systemic lupus erythematosus. *Int Immunopharmacol* 63: 311-316.
347. Gomez Perdiguero E, Klapproth K, Schulz C, Busch K, Azzoni E, Crozet L, . . . Rodewald HR, (2015) Tissue-resident macrophages originate from yolk-sac-derived erythro-myeloid progenitors. *Nature* 518: 547-551.
348. Hoeffel G, Chen J, Lavin Y, Low D, Almeida FF, See P, . . . Ginhoux F, (2015) C-Myb(+) erythro-myeloid progenitor-derived fetal monocytes give rise to adult tissue-resident macrophages. *Immunity* 42: 665-678.
349. Scott CL, Zheng F, De Baetselier P, Martens L, Saeys Y, De Prijck S, . . . Guilliams M, (2016) Bone marrow-derived monocytes give rise to self-renewing and fully differentiated Kupffer cells. *Nat Commun* 7: 10321.
350. Schulz C, Gomez Perdiguero E, Chorro L, Szabo-Rogers H, Cagnard N, Kierdorf K, . . . Geissmann F, (2012) A lineage of myeloid cells independent of Myb and hematopoietic stem cells. *Science* 336: 86-90.
351. Murray PJ, Allen JE, Biswas SK, Fisher EA, Gilroy DW, Goerdt S, . . . Wynn TA, (2014) Macrophage activation and polarization: nomenclature and experimental guidelines. *Immunity* 41: 14-20.

352. Tacke F, Zimmermann HW, (2014) Macrophage heterogeneity in liver injury and fibrosis. *J Hepatol* 60: 1090-1096.
353. Lopez BG, Tsai MS, Baratta JL, Longmuir KJ, Robertson RT, (2011) Characterization of Kupffer cells in livers of developing mice. *Comp Hepatol* 10: 2.
354. Gordon S, Pluddemann A, (2017) Tissue macrophages: heterogeneity and functions. *BMC Biol* 15: 53.
355. You Q, Holt M, Yin H, Li G, Hu CJ, Ju C, (2013) Role of hepatic resident and infiltrating macrophages in liver repair after acute injury. *Biochem Pharmacol* 86: 836-843.
356. Dal-Secco D, Wang J, Zeng Z, Kolaczkowska E, Wong CH, Petri B, . . . Kubes P, (2015) A dynamic spectrum of monocytes arising from the in situ reprogramming of CCR2+ monocytes at a site of sterile injury. *J Exp Med* 212: 447-456.
357. Yona S, Kim KW, Wolf Y, Mildner A, Varol D, Breker M, . . . Jung S, (2013) Fate mapping reveals origins and dynamics of monocytes and tissue macrophages under homeostasis. *Immunity* 38: 79-91.
358. Devisscher L, Scott CL, Lefere S, Raevens S, Bogaerts E, Paridaens A, . . . Van Vlierberghe H, (2017) Non-alcoholic steatohepatitis induces transient changes within the liver macrophage pool. *Cell Immunol* 322: 74-83.
359. Karlmark KR, Weiskirchen R, Zimmermann HW, Gassler N, Ginhoux F, Weber C, . . . Tacke F, (2009) Hepatic recruitment of the inflammatory Gr1+ monocyte subset upon liver injury promotes hepatic fibrosis. *Hepatology* 50: 261-274.
360. Xue J, Schmidt SV, Sander J, Draffehn A, Krebs W, Quester I, . . . Schultze JL, (2014) Transcriptome-based network analysis reveals a spectrum model of human macrophage activation. *Immunity* 40: 274-288.
361. Gauthier K, Billon C, Bissler M, Beylot M, Lobaccaro JM, Vanacker JM, Samarut J, (2010) Thyroid hormone receptor beta (TRbeta) and liver X receptor (LXR) regulate carbohydrate-response element-binding protein (ChREBP) expression in a tissue-selective manner. *J Biol Chem* 285: 28156-28163.
362. Hashimoto K, Cohen RN, Yamada M, Markan KR, Monden T, Satoh T, . . . Wondisford FE, (2006) Cross-talk between thyroid hormone receptor and liver X receptor regulatory pathways is revealed in a thyroid hormone resistance mouse model. *J Biol Chem* 281: 295-302.
363. Kawai K, Sasaki S, Morita H, Ito T, Suzuki S, Misawa H, Nakamura H, (2004) Unliganded thyroid hormone receptor-beta1 represses liver X receptor alpha/oxysterol-dependent transactivation. *Endocrinology* 145: 5515-5524.
364. Hashimoto K, Matsumoto S, Yamada M, Satoh T, Mori M, (2007) Liver X receptor-alpha gene expression is positively regulated by thyroid hormone. *Endocrinology* 148: 4667-4675.
365. van der Spek AH, Fliers E, Boelen A, (2017) Thyroid hormone metabolism in innate immune cells. *J Endocrinol* 232: R67-R81.
366. van der Spek AH, Surovtseva OV, Jim KK, van Oudenaren A, Brouwer MC, Vandenbroucke-Grauls C, . . . Boelen A, (2018) Regulation of Intracellular Triiodothyronine Is Essential for Optimal Macrophage Function. *Endocrinology* 159: 2241-2252.
367. Bassett JH, Williams AJ, Murphy E, Boyde A, Howell PG, Swinhoe R, . . . Williams GR, (2008) A lack of thyroid hormones rather than excess thyrotropin causes abnormal skeletal development in hypothyroidism. *Mol Endocrinol* 22: 501-512.
368. Zhang W, Zhang Y, Liu Y, Wang J, Gao L, Yu C, . . . Xu J, (2014) Thyroid-stimulating hormone maintains bone mass and strength by suppressing osteoclast differentiation. *J Biomech* 47: 1307-1314.
369. Gagnon A, Lochnan HA, Tran CS, Sorisky A, (2016) Thyroid-stimulating hormone acutely increases monocyte gene expression in vivo. *Neuro Endocrinol Lett* 37: 121-123.
370. Zingg JM, Hasan ST, Nakagawa K, Canepa E, Ricciarelli R, Villacorta L, . . . Meydani M, (2017) Modulation of cAMP levels by high-fat diet and curcumin and regulatory effects on CD36/FAT scavenger receptor/fatty acids transporter gene expression. *Biofactors* 43: 42-53.
371. Kalveram L, Kleinau G, Szymanska K, Scheerer P, Rivero-Muller A, Gruters-Kieslich A, Biebermann H, (2019) The Pathogenic TSH beta-subunit Variant C105Vfs114X Causes a Modified Signaling Profile at TSHR. *Int J Mol Sci* 20.

372. Neumann S, Malik SS, Marcus-Samuels B, Eliseeva E, Jang D, Klubo-Gwiezdzinska J, . . . Gershengorn MC, (2020) Thyrotropin Causes Dose-dependent Biphasic Regulation of cAMP Production Mediated by Gs and Gi/o Proteins. *Mol Pharmacol* 97: 2-8.
373. Sinha RA, Singh BK, Yen PM, (2018) Direct effects of thyroid hormones on hepatic lipid metabolism. *Nat Rev Endocrinol* 14: 259-269.
374. Bonde Y, Plosch T, Kuipers F, Angelin B, Rudling M, (2012) Stimulation of murine biliary cholesterol secretion by thyroid hormone is dependent on a functional ABCG5/G8 complex. *Hepatology* 56: 1828-1837.
375. Zelzer S, Mangge H, Pailer S, Ainoedhofer H, Kieslinger P, Stojakovic T, . . . Gruber HJ, (2015) Oxidized LDL Is Strictly Limited to Hyperthyroidism Irrespective of Fat Feeding in Female Sprague Dawley Rats. *Int J Mol Sci* 16: 11689-11698.
376. Oge A, Sozmen E, Karaoglu AO, (2004) Effect of thyroid function on LDL oxidation in hypothyroidism and hyperthyroidism. *Endocr Res* 30: 481-489.
377. Vicinanza R, Coppotelli G, Malacrino C, Nardo T, Buchetti B, Lenti L, . . . Scarpa S, (2013) Oxidized low-density lipoproteins impair endothelial function by inhibiting non-genomic action of thyroid hormone-mediated nitric oxide production in human endothelial cells. *Thyroid* 23: 231-238.
378. Duntas LH, Mantzou E, Koutras DA, (2002) Circulating levels of oxidized low-density lipoprotein in overt and mild hypothyroidism. *Thyroid* 12: 1003-1007.
379. Varela P, Tapia G, Fernandez V, Videla LA, (2006) The role of thyroid hormone calorigenesis in the redox regulation of gene expression. *Biol Res* 39: 611-617.
380. Repa JJ, Berge KE, Pomajzl C, Richardson JA, Hobbs H, Mangelsdorf DJ, (2002) Regulation of ATP-binding cassette sterol transporters ABCG5 and ABCG8 by the liver X receptors alpha and beta. *J Biol Chem* 277: 18793-18800.
381. Yu L, York J, von Bergmann K, Lutjohann D, Cohen JC, Hobbs HH, (2003) Stimulation of cholesterol excretion by the liver X receptor agonist requires ATP-binding cassette transporters G5 and G8. *J Biol Chem* 278: 15565-15570.
382. Wilund KR, Yu L, Xu F, Hobbs HH, Cohen JC, (2004) High-level expression of ABCG5 and ABCG8 attenuates diet-induced hypercholesterolemia and atherosclerosis in Ldlr-/- mice. *J Lipid Res* 45: 1429-1436.
383. Yang C, McDonald JG, Patel A, Zhang Y, Umetani M, Xu F, . . . Hobbs HH, (2006) Sterol intermediates from cholesterol biosynthetic pathway as liver X receptor ligands. *J Biol Chem* 281: 27816-27826.
384. Higham A, Lea S, Plumb J, Maschera B, Simpson K, Ray D, Singh D, (2013) The role of the liver X receptor in chronic obstructive pulmonary disease. *Respir Res* 14: 106.
385. Tabraue C, Lara PC, De Mirecki-Garrido M, De La Rosa JV, Lopez-Blanco F, Fernandez-Perez L, . . . Castrillo A, (2019) LXR Signaling Regulates Macrophage Survival and Inflammation in Response to Ionizing Radiation. *Int J Radiat Oncol Biol Phys* 104: 913-923.
386. Han S, Zhuang H, Shumyak S, Wu J, Xie C, Li H, . . . Reeves WH, (2018) Liver X Receptor Agonist Therapy Prevents Diffuse Alveolar Hemorrhage in Murine Lupus by Repolarizing Macrophages. *Front Immunol* 9: 135.
387. Tobin KAR, Steineger HH, Alberti S, Spydevold O, Auwerx J, Gustafsson JA, Nebb HI, (2000) Cross-talk between fatty acid and cholesterol metabolism mediated by liver X receptor-alpha. *Molecular Endocrinology* 14: 741-752.
388. Parikh M, Patel K, Soni S, Gandhi T, (2014) Liver X receptor: a cardinal target for atherosclerosis and beyond. *J Atheroscler Thromb* 21: 519-531.
389. Refetoff S, Weiss RE, Usala SJ, (1993) The Syndromes of Resistance to Thyroid-Hormone. *Endocrine Reviews* 14: 348-399.
390. Whitney KD, Watson MA, Goodwin B, Galardi CM, Maglich JM, Wilson JG, . . . Kliewer SA, (2001) Liver X receptor (LXR) regulation of the LXRalpha gene in human macrophages. *J Biol Chem* 276: 43509-43515.
391. Gullberg H, Rudling M, Salto C, Forrest D, Angelin B, Vennstrom B, (2002) Requirement for thyroid hormone receptor beta in T3 regulation of cholesterol metabolism in mice. *Mol Endocrinol* 16: 1767-1777.
392. Arai S, Maehara N, Iwamura Y, Honda S, Nakashima K, Kai T, . . . Miyazaki T, (2013) Obesity-associated autoantibody production requires AIM to retain the immunoglobulin M immune complex on follicular dendritic cells. *Cell Rep* 3: 1187-1198.

393. Arai S, Miyazaki T, (2018) A scavenging system against internal pathogens promoted by the circulating protein apoptosis inhibitor of macrophage (AIM). *Semin Immunopathol* 40: 567-575.
394. Woeber KA (2005) Treatment of hypothyroidism. In: Wilkins PLW (ed) The Thyroid. 864-869.

6 Appendix

6.1 List of figures

6.2 List of tables

6.3 Non-standard abbreviations

9cRA	9-cis retinoic acid
ANOVA	Analysis of variance
BL6	Mice strain C57BL/6NCrl
BMDM	Bone marrow-derived macrophages
cAMP	Cyclic adenosine monophosphate
CD36	Fatty acid translocase
CD5L	CD5 antigen-like peptide
CeH	Central hypothyroidism
CH	Congenital hypothyroidism
ClO_4^-	Perchlorate ion
CP	Ceruloplasmin
DAMP	Danger-associated molecular pattern
DEHAL	Dehalogenase
DIO1/2/3	Deiodinase 1,2 or 3
DIT	Diiodotyrosine
DUOX2	Dual oxidase 2
DR4	Direct repeat 4 motif
ECM	Extracellular matrix
FACS	Fluorescence-activated cell scanning
FAS	Fatty acid synthase
GD	Graves' disease
HDL	High-density lipoproteins
HPT axis	Hypothalamus-pituitary-thyroid axis
HSPC	Hematopoietic stem & progenitor cell
HT	Hashimoto's thyroiditis
IFN-γ	Interferon γ
KC	Kupffer cell
L-T_4	Levothyroxine
LAT1/2	L-type amino acid transporter 1 or 2
LDL	Low-density lipoproteins
LPS	Lipopolysaccharide
LRE	LXR response element
LXRα/β	Liver X receptor α or β
M-CSF	Macrophage colony stimulating factor
MCT8/10	Monocarboxylate transporter 8 or 10
MIT	Monoiodotyrosine
MMI	Methimazole
NCoA	Nuclear receptor coactivator
NCoR1	Nuclear receptor corepressor 1
NIS	Sodium iodine symporter
NTIS	Non-thyroidal illness syndrome
OATP	Organic anion-transport polypeptide
OB	Osteoblast
OC	Osteoclast
oxLDL	Oxidised low-density lipoprotein
PAMP	Pathogen-associated molecular pattern
RANKL	Receptor activator of NF-κB ligand
RCT	Reverse cholesterol transport
rT3	3,3',5'-Triiodothyronine
RTHα/β	Resistance to Thyroid Hormone α or β
RXR	Retinoid X receptor
SEM	Standard error of the mean
SMRT	silencing mediator of retinoic acid receptor
SNP	Single nucleotide polymorphism
SRC	Steroid receptor coactivator
T1317	T0901317 LXR agonist
T_2	3,5-Diiodothyronine
(f/t)T_3	(free or total) 3,3',5-Triiodothyronine
(f/t)T_4	(free or total) 3,3',5,5'-Tetraiodothyronine
TBG	Thyroxine-binding globulin
TG	Thyroglobulin
TH	Thyroid Hormone
TPO	Thyroid peroxidase
TR	Thyroid hormone receptor
TRE	TR response element
TRH	Thyrotropin releasing hormone
TRα/β	Thyroid hormone receptor α or β
TSH	Thyroid-stimulating hormone
TSHoma	TSH-secreting pituitary adenoma
TSHR	TSH receptor
VLDL	Very low-density lipoprotein
WT	Wild type

6.4 MySQL source code for the identification of thyroid hormone target genes

Code used for the overlay between mouse plasma proteome and liver transcriptome:

```
INSERT INTO `FC 1.05 proteome overlay`(`SwissProt accession entry`,`Protein
      name`,`annotation`,`P-Value`,`Fold Change`)
SELECT `serum t4 vs co no fc`.`Swissprot accession entry`,`serum t4 vs co no
      fc`.`protein name`,` serum t4 vs co no fc `.`annotation`,`serum t4
      vs co no fc`.`P-Value`,` serum t4 vs co no fc`.`FC`
FROM `serum t4 vs co no fc`,`serum t4 vs rec no fc`
WHERE (`serum t4 vs co no fc`.`FC` >= 1.05 OR ` serum t4 vs co no
      fc`.`FC` <= (-1.05))
AND (`serum t4 vs rec no fc`.`FC` >= 1.05 OR ` serum t4 vs rec no
      fc`.`FC` <= (-1.05))
AND (`serum t4 vs co no fc`.`Swissprot accession entry` = `serum t4 vs rec no
      fc`.`Swissprot accession entry`);
```

Code used for the exclusion of proteins with p-value > 0.05:

```
INSERT INTO `p-cutoff proteome overlay`(`SwissProt accession entry`,`Protein
      name`,`annotation`,`P-Value`,`Fold Change`)
SELECT `FC 1.05 proteome overlay`.`SwissProt accession entry`,`FC 1.05 proteome
      overlay`.`Protein name`,`FC 1.05 proteome overlay`.`annotation`,`FC 1.05
      proteome overlay`.`P-Value`,`FC 1.05 proteome overlay`.`Fold Change`)
FROM `FC 1.05 proteome overlay`
WHERE `FC 1.05 proteome overlay`.`P-Value` > '0.05';
```

Code used for the combination of the human and the mouse target genes:

```
INSERT INTO `p-cutoff FC 1.05 human - serum overlay` (`SwissProt accession
      entry`,`Protein name mouse`,`Protein name human`,`annotation`, `P-Value
      serum`,`Fold Change serum`,`P-Value human`,`Fold Change human`)
SELECT `p-cutoff FC 1.05 serum overlay`.`SwissProt accession entry`, `p-cutoff FC
      1.05 serum overlay`.`Protein name mouse`, `p-cutoff human proteome`.`Protein
      name human`, `p-cutoff FC 1.05 serum overlay`.`annotation`, `p-cutoff FC 1.05
      serum overlay`.`P-Value serum`, `p-cutoff FC 1.05 serum overlay`.`Fold Change
      serum`, `p-cutoff human proteome`.`P-Value human`, `p-cutoff human
      proteome`.`Fold Change human`
FROM `p-cutoff human proteome`, `p-cutoff FC 1.05 serum overlay`
WHERE substring(lcase(`p-cutoff human proteome`.`Protein name human`),1,4) like
      substring(lcase(`p-cutoff FC 1.05 serum overlay`.`Protein name mouse`),1,4);
```

Code used for the exclusion of duplets:

```
DELETE FROM `FC 1.05 proteome - transcriptome overlay`
USING `FC 1.05 proteome - transcriptome overlay`, `dup FC 1.05 proteome –
      transcriptome overlay`
WHERE NOT `FC 1.05 proteome - transcriptome overlay`.`id`=`dup FC 1.05 proteome –
      transcriptome overlay`.`id`
AND `FC 1.05 proteome - transcriptome overlay`.`id` > `dup FC 1.05 proteome –
      transcriptome overlay`.`id`
AND `FC 1.05 proteome - transcriptome overlay`.`SwissProt accession entry`=`dup FC
      1.05 proteome - transcriptome overlay`.`SwissProt accession entry`;
```

Code used for the exclusion of incompletely annotated genes:

```
SELECT *
FROM biomarkers.`transkriptom liver everything`
WHERE `Primary Sequence Name` != ""
AND `Protein names` != "#NV"
ORDER BY `Primary Sequence Name`;
```

6.5 Maps of used plasmids

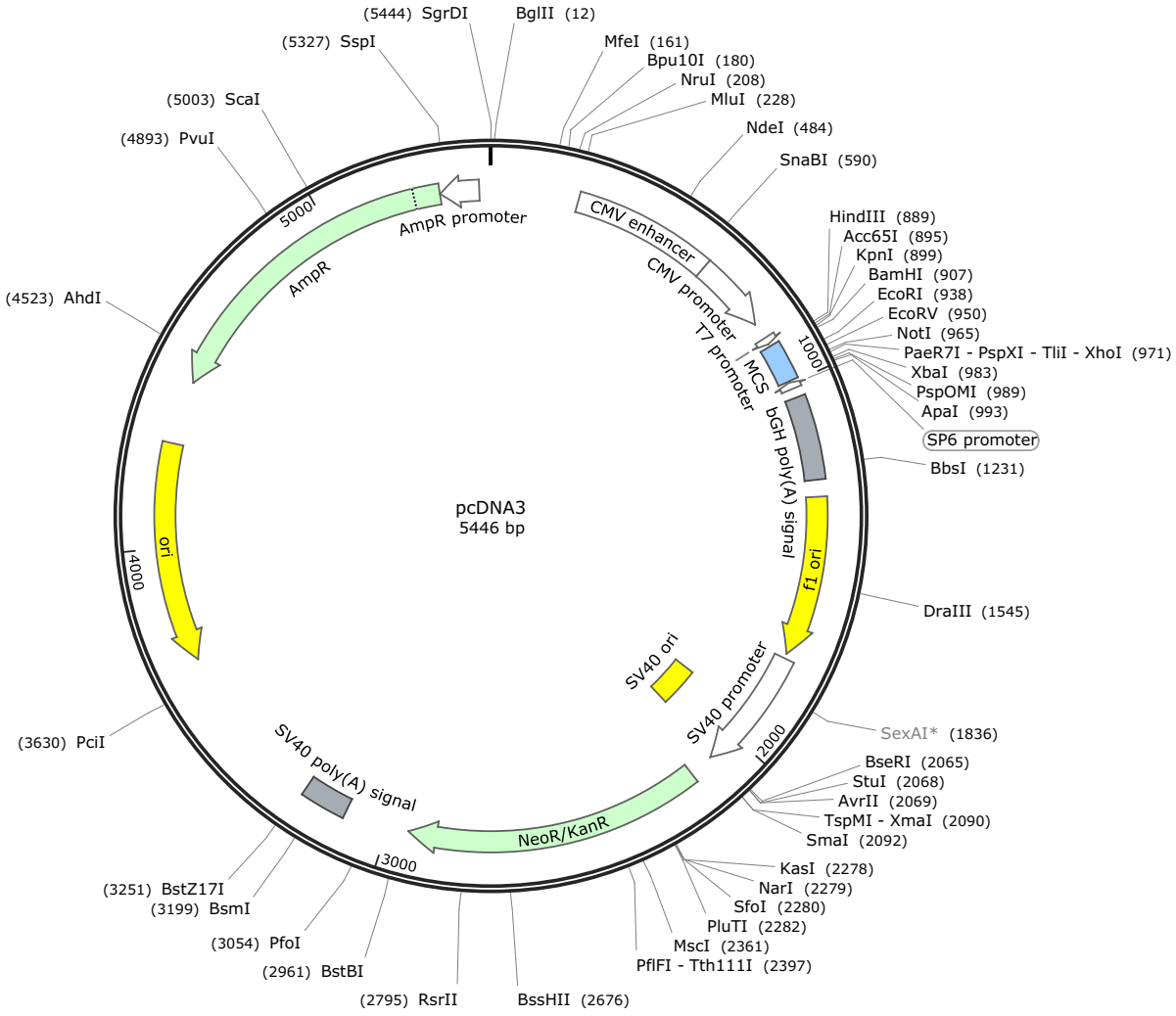

Figure 27 | Map of pcDNA3 transfection Plasmid.

6.6 Publications

Parts of this thesis were submitted to a peer-review journal for publication due to priority reasons.

Nock S, Hofig C, Harder L, Schomburg L, Brabant G, Mittag J, (2019) Unraveling the Molecular Basis for Successful Thyroid Hormone Replacement Therapy: The Need for New Thyroid Tissue- and Pathway-Specific Biomarkers. *Exp Clin Endocrinol Diabetes*.

Nock S, Johann K, Harder L, Wirth EK, Renko K, Hoefig CS, Kracke V, Hackler J, Engelmann B, Rauner M, Köhrle J, Schomburg L, Homuth G, Völker U, Brabant G, Mittag J (2020) CD5L constitutes a novel biomarker for integrated hepatic thyroid hormone action. *Thyroid*. in press

Publications that were not part of this thesis:

Gachkar S, Nock S, Geissler C, Oelkrug R, Johann K, Resch J, Rahman A, Arner A, Kirchner H, Mittag J, (2019) Aortic effects of thyroid hormone in male mice. *J Mol Endocrinol* 62: 91-99.

Johann K, Cremer AL, Fischer AW, Heine M, Pensado ER, Resch J, Nock S, Virtue S, Harder L, Oelkrug R, Astiz M, Brabant G, Warner A, Vidal-Puig A, Oster H, Boelen A, Lopez M, Heeren J, Dalley JW, Backes H, Mittag J, (2019) Thyroid-Hormone-Induced Browning of White Adipose Tissue Does Not Contribute to Thermogenesis and Glucose Consumption. *Cell Rep* 27: 3385-3400 e3383.

Danksagung

Ich möchte mich an dieser Stelle bei allen Personen bedanken die zur Erstellung dieser Arbeit beigetragen haben.
Besonderer Dank gilt dabei zunächst meinen Doktorvätern Prof. Jens Mittag und Prof. Georg Brabant für die Ausgabe des Themas und das damit verbundene Vertrauen in mich. Der ständige Austausch an Ideen und die experimentellen Freiheiten die mir eingeräumt wurden, haben die Entwicklung des Projekts in eine spannende und für alle unerwartete Richtung erst ermöglicht.
Weiterhin bedanke ich mich bei den Mitgliedern des Prüfungsausschusses für die Übernahme dieser Aufgabe.
Den Verantwortlichen des Graduiertenkollegs 1957 „Adipocyte brain crosstalk“ danke ich dafür, dass sie mich als assoziiertes Mitglied aufgenommen und so die Möglichkeit gegeben haben, an lehrreichen Workshops, Seminaren und summer schools teilnehmen zu können.
Ich danke den Mitgliedern des Instituts für funktionelle Genomforschung der Universität Greifswald um Prof. Uwe Völker und Georg Homuth für die Durchführung der OMICs-analysen und Maik und Janine zusätzlich für die zahlreichen spannenden und unterhaltsamen gemeinsamen Konferenzbesuche.
Prof. Martina Rauner, Prof. Lutz Schomburg, Eva Wirth und Kostja Renko danke ich für die Zeit, die ich in ihren Laboren verbringen dürfte um in ihre Geheimnisse der primären Zellkulturen eingeweiht zu werden und Anja und Maria für die nötigen praktischen Fertigkeiten.
Ganz besonderer Dank gilt Rebecca in ihren Funktionen als PostDoc, Problemlöserin, Kummerkasten, Motivationscoach, Dekorateurin und Kaffeepausengesellschaft.
Danke Julia, dass du, als gute Seele des Labors, in allen Lebenslagen helfen konntest und für alle Probleme eine praktische Lösung gefunden hast und ja, ich habe extra für dich besonders viele Kommas in diesen Satz eingefügt.
Auch den derzeitigen und ehemaligen Mitgliedern der AG Mittag, Alex, Beate, Cathy, Francesca, Kornelia, Maike, Mehdi, Natalie, Ricci, Sandro und Sogol möchte ich für die freundliche und kollegiale Arbeitsatmosphäre danken. Dieses motivierende und trotzdem nette Umfeld hat in besonderem Maße zum Gelingen dieser Arbeit beigetragen.
Vielen Dank allen derzeitigen und ehemaligen Mitarbeitern des 1. OG im CBBM für den meist reibungslosen Ablauf der Experimente und schnelle Hilfe, wenn mir mal wieder am Freitagnachmittag eine Idee gekommen ist, die ich unbedingt ausprobieren muss. Insbesondere danke ich Prof. Ungefroren, Ralf, Henriette, Nina, Heike, Sylvia, Steffi, Xenia, Jana, Isa, Christin und Martina und ganz besonders Rose und Lisa als geduldige und sympathische Bürokollegen.
Abseits des Labors gab es ebenfalls wichtige Menschen die mich maßgeblich beeinflusst und unterstützt haben und insbesondere möchte ich den Volleyballmännern der TG Rangenberg und meiner Reisegruppe „Unangenehm“ danken.
Ein ganz besonders großer Dank gilt meiner Familie die mich mein ganzes Leben durch Schule, Ausbildung, Studium und dann auch noch die Promotion begleitet habt und es wohl kaum erwarten kann, dass ich nun hoffentlich zur Abwechslung mal was Vernünftiges mache.
Zu guter Letzt möchte ich Lisbeth für ihren Zuspruch und ihre Unterstützung danken und dafür, dass du in all der Zeit immer für mich da warst; ohne dich wäre diese Arbeit nie entstanden.

Curriculum vitae